

Receptor-targeted viral vectors: Tracking of stem cells and side by side comparison of AAV and lentiviral vectors

Vom Fachbereich Biologie der Technischen Universität Darmstadt

zur Erlangung des akademischen Grades

eines Doctor rerum naturalium

genehmigte Dissertation von

Master of Science Sarah-Katharina Kays

aus Nürnberg

1. Referentin: Prof. Dr. Beatrix Süß

2. Referentin: Prof. Dr. Ulrike A. Nuber

3. Referent: Prof. Dr. Christian J. Buchholz

Tag der Einreichung: 9. Juni 2015

Tag der mündlichen Prüfung: 17. Juli 2015

Darmstadt 2015

Die vorliegende Arbeit wurde unter der Leitung von Prof. Dr. Christian J. Buchholz in der Arbeitsgruppe „Molekulare Biotechnologie und Gentherapie“ am Paul-Ehrlich-Institut in Langen angefertigt.

Die Betreuung seitens der Technischen Universität Darmstadt erfolgte durch Prof. Dr. Beatrix Süß vom Fachbereich Biologie.

Parts of this thesis have been published

Kays, S.K., Kaufmann, K.B., Abel, T., Brendel, C., Bonig, H., Grez, M., Buchholz, C.J., and Kneissl, S. (2015). CD105 is a Surface Marker for Receptor-targeted Gene Transfer into Human Long-Term Repopulating Hematopoietic Stem Cells. *Stem cells and development* 24, 714-723.

Presentations at international conferences

Kays, S.K., Kaufmann, K.B., Abel, T., Bonig, H., Grez, M., Buchholz, C.J., and Kneissl, S. CD105 as surface marker for targeted gene transfer into human hematopoietic stem cells.

17th Annual Meeting of the American Society of Gene- and Cell therapy, 2014, Washington D.C., USA. Oral presentation.

Kays, S.K., Kaufmann, K.B., Abel, T., Bonig, H., Grez, M., Buchholz, C.J., and Kneissl, S. CD105 as surface marker for targeted gene transfer into human hematopoietic stem cells.

20th Annual Meeting of the German Society for Gene Therapy, 2014, Ulm, Germany. Oral presentation.

Kays, S.K., Kaufmann, K.B., Abel, T., Brendel, C., Bonig, H., Grez, M., Buchholz, C.J., and Kneissl, S. CD105 - a surface marker for receptor-targeted gene transfer into human long-term repopulating hematopoietic stem cells.

2nd International Annual Conference of the German Stem Cell Network, 2014, Heidelberg, Germany. Poster presentation.

SUMMARY	1
ZUSAMMENFASSUNG	3
1. INTRODUCTION	5
1.1 Gene therapy	5
1.2. Milestones of viral vector-based gene therapy	5
1.3 Basics about lentiviral vectors	8
1.4 Basics about adeno-associated viral (AAV) vectors.....	10
1.5 Receptor targeting	11
1.5.1 Receptor-targeted lentiviral vectors	12
1.5.2 Receptor targeted AAV vectors	13
1.6 Cell surface markers	15
1.7 Objective	18
2. MATERIAL AND METHODS	19
2.1 Material.....	19
2.1.1 Equipment.....	19
2.1.2 Kits	20
2.1.3 Buffers and chemicals	21
2.1.4 Antibodies	22
2.1.5 Oligonucleotides	23
2.1.6 Plasmids	23
2.1.7 Bacterial strains and mammalian cells	25
2.1.8 Culture media.....	25
2.2 Methods of molecular biology.....	26
2.2.1 Transformation of chemically competent bacteria.....	26
2.2.2 Plasmid preparation.....	26
2.2.3 Restriction of DNA	27
2.2.4 Agarose gel electrophoresis	27
2.2.5 Isolation of DNA from agarose gels	28
2.2.6 Isolation of genomic DNA	28
2.2.7 Isolation of total RNA	28
2.2.8 Generation of RNA standard	28
2.2.9 Reverse transcription.....	29
2.2.10 Quantitative real-time PCR	29
2.2.11 Polymerase chain reaction	31
2.2.12 Enzyme-linked immunosorbent assay (ELISA)	32

2.3 Cell culture and virological methods.....	33
2.3.1 Cultivation of cell lines	33
2.3.2 Freezing and thawing of cultured cells	33
2.3.3 Production and purification of vector particles.....	33
2.3.4 Transduction of adherent cell lines and titration of vectors	34
2.3.5 Isolation of human CD34 ⁺ , respectively, CD105 ⁺ cells from mobilized peripheral blood	34
2.3.6 Cultivation and stimulation of HSPCs.....	35
2.3.7 Transduction of HSPCs	36
2.3.8 Colony forming assay	36
2.3.9 Analysis of cells by flow cytometry and fluorescence activated cell sorting.....	36
2.3.10 Annexin V/propidium iodide staining	37
2.3.11 Competition assay	37
2.3.12 Serum stability assay.....	38
2.3.13 Expression of soluble CD105 protein	38
2.3.14 Isolation of blood, BM and spleen cells from mice	38
2.4 Experimental mouse work.....	39
2.4.1 Repopulation of NSG mice with human CD34 ⁺ cells.....	39
2.4.2 Subcutaneous injection of SK-OV-3 cells.....	39
2.4.3 Administration of vector particles.....	40
2.4.4 <i>In vivo</i> imaging	40
3. RESULTS.....	41
3.1 Side by side comparison of receptor targeted lentiviral and AAV vector stocks 41	
3.1.1 Quantification of titers of lentiviral and AAV vector stocks	42
3.1.1.1 Genomic titers	42
3.1.1.2 Quantification of physical titers.....	46
3.1.1.3 Quantification of functional titers	46
3.1.1.4 Comparison of functional, genomic and physical titers.....	47
3.1.2 Transduction of Her2 ⁺ SK-OV-3 cells with Her2-AAV ^{GFP} and Her2-LV ^{GFP} <i>in vitro</i>	48
3.1.3 Biodistribution of Her2-LV and Her2-AAV in a subcutaneous tumor mouse model	50
3.1.3.1 Particle distribution at early time points after vector administration	50
3.1.3.2 Monitoring the biodistribution of Her2-LV and Her2-AAV by <i>in vivo</i> imaging.....	53
3.1.4 Serum stability	55
3.2 Targeted gene transfer into human hematopoietic stem cells	57
3.2.1 Expression of CD105 on human HSCs	57
3.2.2 Transduction of HSCs using CD105-LV	58
3.2.2.1 Transduction of CD34 ⁺ cells by CD105-LV ^{GFP}	58
3.2.2.2 Transduction of CD105 enriched cells by CD105-LV ^{GFP}	60
3.2.2.3 Specificity of CD105 dependent transduction	62
3.2.3 Stable transgene expression <i>in vitro</i>	63

3.2.4 Stable transduction of CD105-LV transduced cells in repopulated NSG mice	65
3.2.5 Competitive repopulation of CD105-LV or VSVG-LV transduced HSCs in NSG mice	68
3.2.6 Vector mediated toxicity on CD34 ⁺ cells.....	72
4. DISCUSSION	74
4.1 Side by side comparison of lentiviral and AAV vectors	74
4.2 Side by side comparison of Her2-LV and Her2-AAV.....	76
4.3 Hematopoietic stem cell-targeted lentiviral vectors	80
4.4 Potential of receptor-targeted lentiviral vectors.....	84
5. REFERENCES	88
6. ABBREVIATIONS.....	104
7. CURRICULUM VITAE.....	107
8. DANKSAGUNG	108
9. EHRENWÖRTLICHE ERKLÄRUNG.....	109

SUMMARY

In recent years, substantial progress in gene therapy has been made as proofed by several successful clinical trials providing substantial benefit to patients and the first marketing authorization of an adeno-associated virus (AAV) vector-based medical product. Especially lentiviral and AAV vectors represent promising tools for gene transfer. They have been further improved to ensure safety and efficiency. One strategy to customize these viral vectors is the generation of receptor-targeted vectors that restrict gene delivery to cells expressing the targeted receptor. The first part of this thesis compares lentiviral and AAV vectors targeted to the receptor Her2/neu which is overexpressed in various tumor cells. This is for the first time a true side by side comparison of this totally different vector types, since here, both use the same receptor for cell entry. The second part investigates the potential of receptor-targeted lentiviral gene transfer into human hematopoietic stem cells (HSCs) via the cell surface protein CD105 and evaluates if CD105 is a marker for human long-term repopulating HSCs.

The Her2-targeted lentiviral and AAV vector had been generated and characterized before (Münch et al., 2011; Münch et al., 2013). Both particles display a Her2/neu specific targeting ligand, the designed ankyrin repeat protein 9.29. First, functional, genomic and physical titers of Her2-LV and Her2-AAV vector stocks were determined side by side to allow precise normalization of both vector types. While the Her2-LV vector stocks showed higher genomic titers, Her2-AAV vectors comprised more functional particles per genome containing particles. Accordingly, about 10-fold more genome copies of Her2-LV than Her2-AAV had to be administered systemically in a subcutaneous tumor mouse model for detectable transgene expression. Analysis of the vector distribution short time after systemic administration *in vivo* revealed that the non-enveloped Her2-AAV vector circulated stably in the blood of mice for a prolonged time compared to Her2-LV. Accumulation of Her2-AAV within the target tissue occurred only after 24 hours.

Lentiviral vectors are currently the preferred vector type for the modification of HSCs due to their capability of integrating the transgene into the host cell's genome. Thereby the entire hematopoietic system can be reconstituted with cells carrying the corrected gene. True HSCs which are capable of self-renewal and differentiate into

all hematopoietic lineages can be identified by the expression of specific cell surface markers. In mice, CD105 was previously shown to be present on most immature, long-term repopulating HSCs. After confirming that human CD105 is expressed on 30-80% of human CD34⁺ cells, CD34⁺ cells were transduced with a lentiviral vector targeted to human CD105 (CD105-LV) and transplanted into NOD-scid IL2R $\gamma^{-/-}$ mice. Stable reporter gene expression in engrafted cells was detected long-term in all human hematopoietic lineages in bone marrow, spleen and blood. In addition, competitive repopulation experiments in mice showed a superior engraftment of CD105-LV transduced CD34⁺ cells in bone marrow and spleen compared to cells transduced with a conventional non-targeted lentiviral vector confirming CD105 as a marker for early HSCs with high repopulating capacity.

The data shown in this thesis highlight the potential of receptor-targeted vectors to trace cell subsets and identify new markers for specific cell populations. In addition, it demonstrates the potential of comparing vectors derived from different virus families once they have been targeted to the same entry receptor.

ZUSAMMENFASSUNG

Während der letzten Jahre wurden bedeutende Fortschritte im Bereich der Gentherapie erzielt, was durch mehrere erfolgreich durchgeführte klinische Studien, die zu therapeutischen Verbesserung für die Patienten führten, sowie durch die erste Markteinführung eines Adeno-assozierter Virus (AAV) Vektor basierten Therapeutikums bestätigt wurde. Vor allem lentivirale und AAV Vektoren stellen vielversprechende Hilfsmittel für den Gentransfer dar. Sie wurden stetig weiterentwickelt, um deren Sicherheit und Effizienz zu gewährleisten. Eine Strategie, die viralen Vektoren anzupassen, ist das sogenannte Rezeptortargeting, das den Gentransfer nur in Zellen, die einen definierten Rezeptor exprimieren, ermöglicht. Der erste Teil dieser Dissertation vergleicht lentivirale und AAV Targetingvektoren, die an den Zielrezeptor Her2/neu, ein Oberflächenprotein, das in vielen Tumorzelltypen überexprimiert ist, binden. Dieser direkte Vergleich zeigt Einblicke in Leistung, Verteilung und Anwendbarkeit von zielgerichteten lentiviralen und AAV Vektoren. Der zweite Teil dieser Arbeit untersucht das Potential eines zielgerichteten lentiviralen Vektors Gene in hämatopoetische Stammzellen (HSZ) einzuschleusen. Der Gentransfer erfolgt nach Bindung an das Oberflächenprotein CD105 und untersucht dabei gleichzeitig, ob CD105 ein Oberflächenmarker für humane lang-zeit repopulierende HSZ ist.

Lentivirale und AAV Vektoren, die über die Bindung an den Rezeptor Her2/neu Gentransfer vermitteln, waren vor Beginn dieser Arbeit generiert und charakterisiert worden (Münch et al., 2011; Münch et al., 2013). Durch die Präsentation des gleichen Targetingliganden auf der Vektoroberfläche binden beide Vektortypen an den gleichen Zielrezeptor, was einen direkten Vergleich beider Vektortypen *in vitro* und *in vivo* ermöglicht. Zunächst wurden funktionale, genomische und physische Titer von Her2-LV und Her2-AAV Vektorstocks nebeneinander bestimmt, sodass eine genaue Normalisierung beider Vektortypen ermöglicht wurde. Die Her2-LV Vektorstocks beinhalteten mehr Genomkopien, allerdings enthielten Her2-AAV Vektorstocks mehr funktionale Partikel pro Genomkopien. Daher waren etwa 10-fach mehr Genomkopien des Her2-LV als des Her2-AAV in einem subkutanen Tumormausmodell nötig, um eine effiziente Genexpression zu erreichen. Die Analyse der Vektorverteilung kurze Zeit nach intravenöser Vektorinjektion zeigte, dass der nicht behüllte Her2-AAV länger im Blut zirkulierte als Her2-LV. Während der ersten 24

Stunden nach Vektorgabe konnte keine Akkumulation von Her2-AAV Partikeln im Zielgewebe beobachtet werden.

Wegen ihrer Fähigkeit, das Transgen in das Genom der Zielzelle zu integrieren, sind lentivirale Vektoren der präferierte Vektortyp für die Modifikation von HSZ. So kann das gesamte hämatopoetische System mit Zellen rekonstituiert werden, die das korrigierte Gen tragen. Echte HSZ besitzen die Fähigkeit sich selbst zu erneuern und sind gleichzeitig in der Lage, in alle hämatopoetischen Zellen auszudifferenzieren. Diese Stammzellen können anhand von bestimmten Oberflächenproteinen identifiziert werden. In Mäusen konnte CD105 als ein Rezeptor bestimmt werden, der auf unreifen, lang-zeit repopulierenden HSZ zu finden ist. In dieser Arbeit wurde bestätigt, dass humanes CD105 auf 30-80% der humanen CD34⁺ Zellen exprimiert wird. Anschließend wurden CD34⁺ Zellen mit einem lentiviralen Vektor transduziert, der an den humanen CD105 Rezeptor (CD105-LV) der Zielzellen bindet, und in NOD-scid IL2R $\gamma^{-/-}$ Mäuse transplantiert. In allen humanen hämatopoetischen Linien im Knochenmark, Milz und Blut wurde eine langfristig stabile Expression des Reportergens nachgewiesen. In einem Kompetitionsexperiment konnte außerdem gezeigt werden, dass CD34⁺ Zellen, die mit CD105-LV transduziert wurden, in Knochenmark und Milz einen höheren Transplantationserfolg zeigten als Zellen, die mit einem konventionellen nicht ziel-gerichteten lentiviralen Vektor transduziert wurden. Dies bestätigt CD105 als Marker für primitive HSZ, die eine hohe Repopulationseigenschaft besitzen.

Die Daten, die in dieser Arbeit gezeigt werden, verdeutlichen das Potential von Vektoren, mittels Rezeptortargeting Zellsubpopulationen zu markieren und zu verfolgen, was eine Identifikation von neuen Markern auf spezifischen Zellpopulationen ermöglicht. Des Weiteren demonstriert diese Arbeit die Möglichkeit, verschiedene virale Vektortypen, die den gleichen Zelleintrittsrezeptor verwenden, zu vergleichen.

1. INTRODUCTION

1.1 Gene therapy

Gene therapy is expected to cure or prevent human diseases by delivery of a functional, therapeutic gene or by transfer of genes leading to the reduction or elimination of harmful gene products or cells. First clinical gene therapy studies were already conducted 25 years ago. Since then, the therapeutic approaches have been improved continuously. As vehicles for the delivery of transgenes, integrating and non-integrating viral and non-viral vectors have been used. The focus of the first gene therapy studies was on the treatment of primary immune deficiencies since in absence of a suitable bone marrow donor for these, gene therapy represents the only therapeutic option.

1.2. Milestones of viral vector-based gene therapy

Primary immune deficiencies (PID) are currently treated either by allogenic hematopoietic stem cell transplantation (HSCT) or by *ex vivo* gene modification. For HSCT, hematopoietic stem cells (HSCs) from a matching donor are infused into the patient early after detection of the disease. However, matching donors are not available for each patient. Therefore, genetic modification of autologous HSCs represents an alternative strategy. CD34⁺ cells from bone marrow (BM) or cells from granulocyte colony stimulating factor (GM-CSF) mobilized peripheral blood are harvested from the patients. Then, the cells are manipulated *ex vivo* and reinfused into the patients. The first clinical trial for PID gene therapy was conducted in 1990 treating two children suffering from adenosine deaminase (ADA) deficiency by autologous transplantation of *ex vivo* corrected T-lymphocytes using a gammaretroviral vector. Despite normalization of T-lymphocyte counts in the blood and improvement of ADA enzyme activity in one of the patients, both patients had to remain on enzyme replacement therapy (Blaese et al., 1995). In the approach to treat SCID-X1 patients by gammaretroviral vector mediated gene therapy, the T-cell immune functions were fully restored in 18 out of 20 patients. However, 5 of the patients developed acute T-cell lymphoblastic leukemia (T-ALL) 2-5.5 years after

therapy caused by insertional activation of the proto-oncogene *LMO2* (LIM domain only 2) (Hacein-Bey-Abina et al., 2003; Howe et al., 2008).

Due to the occurrence of additional cases of leukemia in other clinical trials treating patients with Wiskott-Aldrich syndrome (WAS) (Persons and Baum, 2011; Braun et al., 2014), the integration profile of retroviral vectors was investigated intensively. It was found that gammaretroviral vectors tend to integrate into or near to gene regulatory regions such as enhancer, promoter genes or locus control regions. By comparing the integration sites of the affected patients, integration hot spots (especially *LMO2*, *MDS-EVI1*) were identified (Hacein-Bey-Abina et al., 2003; Ott et al., 2006). Vector integration into these genes led to clonal dominance associated with leukemia. In contrast to gammaretroviral vectors (Wu et al., 2003; Palma et al., 2005; Deichmann et al., 2007), lentiviral vectors (LVs) preferentially integrate into active transcription units and are able to transduce non-dividing cells; (Schröder et al., 2002; Mitchell et al., 2004; Wang et al., 2009).

By the generation of self-inactivating lentiviral vectors (SIN-LV) (see chapter 1.3) the safety of these vectors was significantly improved. Therefore, SIN-LVs are the preferred tool for the manipulation of HSCs today. So far, several phase I/II clinical trials using SIN-LVs are ongoing including the treatment of WAS (Aiuti et al., 2013), ADA-SCID (NCT01380990), chronic granulomatous disease (CGD) (NCT02234934), X-linked adrenoleukodystrophy (X-ALD) (Cartier et al., 2009; Cartier et al., 2012), metachromatic leukodystrophy (MLD) (Biffi et al., 2013) and β -thalassemia (Cavazzana-Calvo et al., 2010). So far, 10 patients have been enrolled in the current WAS trial. Autologous HSCs were modified with a VSVG-pseudotyped SIN-LV *ex vivo*. The expression of WAS protein was restored, resulting in increased platelet counts, enhanced immune functions and improvement of clinical disease symptoms (Aiuti et al., 2013). Genetic modifications of HSCs to correct X-ALD (Cartier et al., 2009) and MLD (Biffi et al., 2013) have been resulting in therapeutic effects in two other gene therapy trials. In addition to the clinical benefits, in all of these studies no clonal outgrowth has been observed so far with one clinical trial treating β -thalassemia being the exception. In this study which was initiated in 2007 the LV integrated into the tumor suppressor gene high mobility group AT-hook 2 (HMGA2) leading to benign clonal expansion of cells within the myeloid lineage (Cavazzana-Clavo 2010).

Other promising tools for gene therapy are adeno-associated virus (AAV)-derived vectors. They are highly stable, producible in high titer vector stocks, show low immunogenicity and do not integrate into the host's genome but are predominantly present episomally (Philpott et al., 2002). Therefore, AAV vectors are used for gene correction of post-mitotic tissues such as the retina, liver, central nervous system, and skeletal and cardiac muscle. In the first gene therapy trials treating patients with inherited eye disease, Leber's congenital amaurosis (LCA), the retinal pigment epithelium-specific protein 65kDa (RPE65) was expressed after subretinal administration of a AAV2 vector leading to improvements in vision. In addition to the clinical benefit, the immune response against the vector itself or the transgene was very low and the therapy well tolerated (Bainbridge, James W B et al., 2008; Hauswirth et al., 2008; Maguire et al., 2008; Jacobson et al., 2012). Demonstrating proof-of-concept, these first three trials facilitated initiations of other clinical eye studies. Within the first clinical study to treat hemophilia B by AAV vector mediated gene therapy, therapeutic relevant levels of factor IX were not achieved but this trial demonstrated safety and possible application of intramuscular injection of AAV vectors for gene therapy (Kay et al., 2000). In subsequent clinical studies, the focus was on transduction of liver cells that are more prone to secrete factors to the circulating blood (Manno et al., 2006) and are thought to induce immune tolerance against transgenes following vector administration via the portal vein (Mays and Wilson, 2011). The expression of factor IX increased to therapeutic relevant levels, but also dropped in few patients several weeks after gene therapy. This fact was put down to memory T-cells that recognized AAV capsid proteins by some investigators (Mingozzi and High, 2011) and to induction of cytotoxic T-cell response against the transgene by others (Li et al., 2009). AAV vector mediated gene transfer has been shown a notable safety profile and efficacy record *in vivo*, leading to the granting of the first marketing authorization in the western world for an AAV-based therapeutic medicine in November 2012 by the European Commission. Previously, alipogen tiparvovec (also known as Glybera) was successfully tested in several clinical trials treating the ultra-rare familial lipoprotein lipase deficiency (LPLD). The naturally occurring gain of function mutated gene LPL^{S447X} was administered intramuscular by a serotype 1 AAV vector that demonstrates high muscular tropism (Mingozzi et al., 2009). Treated patients showed clinical improvement up to 2 years after

intramuscular vector administration (Gaudet et al., 2012) while sustained transgene expression was not impaired by immune response (Ferreira et al., 2014).

1.3 Basics about lentiviral vectors

Lentiviral vectors are derived from lentiviruses which belong to the *Retroviridae* family. Lentiviruses, such as the human immunodeficiency virus 1 (HIV-1), are enveloped viruses with a diploid, positive sense, single stranded RNA genome. The envelope consists of host cell membrane and viral envelope proteins (Env) and encloses the capsid which is composed of approximately 2000 p24 proteins (Wilk et al., 2001). Within the capsid, viral replication enzymes and the two linear RNA molecules surrounded by nucleocapsid proteins are located. The genome, which has a size of about 7 to 13 kb per monomer, encodes for the genes *gag/pol* and *env*. The *gag* gene provides all structural proteins such as matrix protein, capsid protein, nucleocapsid protein as well as SP1, SP2 and p6. The *pol* gene encodes for the reverse transcriptase, protease and integrase, *env* for the Env protein. The protein-encoding regions are flanked at both ends by long terminal repeats (LTR) which consist of 3' unique elements (U3), repeat elements (R) and 5' unique elements (U5). The LTRs contain promoter and enhancer sequences, the transactivation response element (TAR), the poly-adenylation signals and the *att* repeats that are necessary for viral integration into the host genome. The packaging signal psi is responsible for the packaging of genomic RNA into the viral particles (Xie et al., 2002; Freed and Martin, 2006; Pluta and Kacprzak, 2009).

Instead of the viral genome, lentiviral vectors contain a transgene. Therefore, LVs are replication deficient, but they can transfer and integrate a gene of interest into the genome of mammalian cells which is termed transduction. Most of the LVs are derived from HIV-1. Similar to lentiviruses which can not only infect mitotically active cells, LV can transduce non-dividing cells. This makes them a promising tool for gene therapy. However, several safety issues have to be considered using LVs. Long-term follow up studies of clinical trials revealed that the risk of abnormal clonal expansion of LVs transduced cells is rather low compared to gammaretroviral vector studies since LV tend to integrate not near promoters and regulatory elements, but into active transcription units (Mitchell et al., 2004). Another safety concern that needs to be

minimized is the potential of development of replication competent lentiviruses within vector preparations. Therefore, transfection protocols were established in which *gag/pol* and *env* genes are split onto two separate plasmids that both lack the packaging signal psi. In addition, accessory proteins that are not essential for the production of LVs, namely Vpr, Vif, Vpu, and Nef, are deleted from the packaging plasmid leaving *tat* and *rev* besides *gag/pol* (Zufferey et al., 1997). Only the transfer plasmid which encodes for the gene of interest contains a functional psi signal which is the reason that only the transgene is packaged into the generated vector particles.

Further improvement of vector safety was achieved by generation of self-inactivating (SIN) vectors. Here, the U3 region of the 5' LTR is replaced with a heterologous promoter, e.g. the cytomegalovirus (CMV) promoter, resulting in a Tat-independent transcription. In addition, the transcriptional unit is deleted from the LTRs by partially deletion of the U3 region of the 3' LTR (Miyoshi et al., 1998). LVs have a large cargo capacity which is in general 7-9 kb, but can be exhausted up to 18 kb, although this reduces the functional titers of the vector stocks (Kumar et al., 2001). LVs are produced by transient or stable transfection of packaging cell lines, usually HEK293T cells, since they are highly susceptible to transfection and express the SV40 T-large antigen which allows replication of plasmids containing the SV40 origin of replication (Soneoka et al., 1995). The vector particles bud from the cell membrane of the producer cells and then can be harvested from the cell supernatant. As a result of the budding process the vector envelope consists of the cellular lipid bilayer as well as viral envelope proteins that are expressed on the cell surface.

Therefore, the cell specificity of LV depends on the envelope protein used for transfection. By substitution of the natural Env protein with other viral surface proteins, the tropism of the LV can be altered – a procedure known as pseudotyping. The first reports about successful pseudotyping demonstrated incorporation of murine leukemia virus (MLV) or HTLV-1 Env into HIV-1-based LVs (Page et al., 1990; Landau et al., 1991). Since then, lots of glycoproteins from different viruses were used for pseudotyping (Cronin et al., 2005; Frecha et al., 2008). Nevertheless, the most common pseudotype is the glycoprotein of the vesicular stomatitis virus (VSVG). Its broad tropism enables VSVG pseudotyped LVs (VSVG-LV) to transduce all mammalian cells while maintaining high titers and excellent stability of virions. However, VSVG-LVs are not applicable for *in vivo* gene therapy, since complement-

and antibody mediated immune response against the glycoprotein will occur (DePolo et al., 2000; Higashikawa and Chang, 2001). In addition, despite the successful application of VSVG-LV in several hematopoietic stem cell-based therapeutic approaches, unstimulated human HSCs lack the entry receptor LDL-R (low-density lipid receptor) for VSV (Amirache et al., 2014). Therefore, the transduction of HSCs requires usually several days of *ex vivo* pre-stimulation, followed by 1 – 3 rounds of transduction at a very high multiplicity of infection (MOI) for efficient gene transfer (Aiuti et al., 2013; Biffi et al., 2013). This can be circumvented by transduction of the cells using a receptor-targeted LV (see chapter 1.5.1).

1.4 Basics about adeno-associated viral (AAV) vectors

Adeno-associated viruses belong to the family of *Paroviridae*. One characteristic of AAV is that successful replication is dependent on a helper virus such as vaccinia virus (Schlehofer et al., 1986), herpes simplex virus (Buller et al., 1981), human cytomegalovirus (McPherson et al., 1985) or adenovirus (Casto et al., 1967), leading to the classification to the genus of *Dependovirus*. Replication of AAV is initiated by transactivation of the AAV promoters by proteins of the helper virus. In the absence of a helper virus, AAV undergoes latent infection by integrating into the chromosome 19 of the host's genome (Kotin et al., 1990; Samulski et al., 1991) or persisting episomally until the presence of a helper virus initiates the replication cycle of AAV. The icosahedral formed capsid consists of 60 subunits that are composed of the three structural proteins VP1, VP2 and VP3 (Xie et al., 2002). The single-stranded DNA genome is flanked by two inverted terminal repeats (ITRs) forming hair-pin structures. The ITRs are involved in genome integration, packaging and regulation of gene expression. They also contain binding elements required for the initiation of replication. The three capsid proteins are translated from one mRNA by alternative splicing resulting in expression of different amounts of proteins (Berns and Parrish, 2006).

So far, several human and non-human primate AAV serotypes have been identified. Genome size and organization are identical among these serotypes, but the capsid protein homology and the target entry receptors differ leading to diverse tissue tropism (Wu et al., 2006). For AAV2, heparin sulfate proteoglycan (HSPG) has been

found to be the primary binding receptor. HSPG is mainly expressed in liver tissue, resulting in a strong liver tropism (Kern et al., 2003; Opie et al., 2003). For gene therapeutic approaches the gene of interest is integrated into the AAV genome. The size of the transgene is limited to approximately 4.4 kb.

In addition to the single-stranded AAV (ssAAV) vectors, self-complementary AAV (scAAV) vectors were developed (McCarty et al., 2001). In one of the ITRs the terminal resolution site is removed resulting in primarily dimeric inverted repeat forms of the AAV genome (McCarty et al., 2003). Thereby, the host cell-mediated synthesis of a double-stranded DNA from the single stranded AAV vector DNA is circumvented and the synthesis of the transgene occurs faster and transduction efficiency is enhanced (McCarty et al., 2003; Wang et al., 2003). Although, compared to ssAAV, the cargo capacity of scAAV is limited to about half the size, less vector particles are required for comparable transduction efficiencies (McCarty, 2008).

AAV vectors have been engineered to alter the natural tropism. On the one hand, this can be achieved by a rational design of the AAV capsid such as generation of mosaic (Hauck et al., 2003) or chimeric capsids (Hauck and Xiao, 2003). On the other hand, modifications of the capsid can be introduced in a library-based high throughput format. By error-prone PCR, DNA shuffling or insertion of random peptides with subsequent directed evolution, AAV vector mutants highly efficient for the cell type applied for selection were identified (Müller et al., 2003; Perabo et al., 2003; Maheshri et al., 2006; Perabo et al., 2006; Michelfelder et al., 2007; Grimm et al., 2008). Indeed, the tropism of the AAV vectors is altered by these methods, but gene delivery is not restricted to specific cell types, but usually expanded. Therefore, a flexible receptor targeted gene transfer approach was established by Münch et al. that will be described in chapter 1.5.2 in detail (Münch et al., 2013).

1.5 Receptor targeting

For therapeutic applications gene transfer into all cells is not desirable but should be restricted to cells affected by the dysfunctional gene. The expression of the transgene in healthy cells is especially of concern, if a suicide gene for example encoding the herpes simplex virus thymidine kinase (HSV-TK) is delivered. Therefore, viral vectors have been generated that allow directed gene delivery.

1.5.1 Receptor-targeted lentiviral vectors

The normal tropism of lentiviral vectors can be altered by pseudotyping of the vector particles. Here, the natural glycoprotein of HIV-1 is replaced with glycoproteins of another virus species (Cronin et al., 2005; Frecha et al., 2008). Thereby, the tropism can either be broadened as in the case for VSVG pseudotyped LV or restricted to the normal tropism of the expressed glycoprotein. Efficient incorporation of these glycoproteins into vector particles often requires modification of the cytoplasmatic tail such as truncations or construction of chimeric glycoproteins (Sandrin et al., 2002) The glycoproteins can be further engineered by mutation of the natural receptor recognition site or by presentation of a specific targeting ligand.

The principal of receptor targeted lentiviral vectors used in this thesis was established by Funke et al. HIV-1 particles were pseudotyped with the measles virus hemagglutinin (H) and fusion (F) proteins. The cytoplasmatic tail of the H protein was truncated by 18 amino acids and that of the F protein by 30 amino acids to allow efficient incorporation into the vector particle. In addition, the natural binding site was mutated preventing transduction of cells expressing the measles virus recognition receptors CD46, SLAM and nectin-4. Originally, a single-chain antibody against the surface protein CD20 was fused to the ectodomain of the H protein restricting gene transfer to CD20⁺ cells (Funke et al., 2008). The flexibility of this targeting system was demonstrated by exchanging the single-chain antibody against CD20 with further single-chain antibodies, but also with designed ankyrin repeat proteins (DARPins). Thereby, LVs targeted to a broad variety of cell surface receptors and the corresponding cell types including CD105⁺, CD4⁺, CD8⁺, CD30⁺ or Her2/neu⁺ cells were obtained (Anliker et al., 2010; Münch et al., 2011; Zhou et al., 2012; Abel et al., 2013; Friedel et al., 2015).

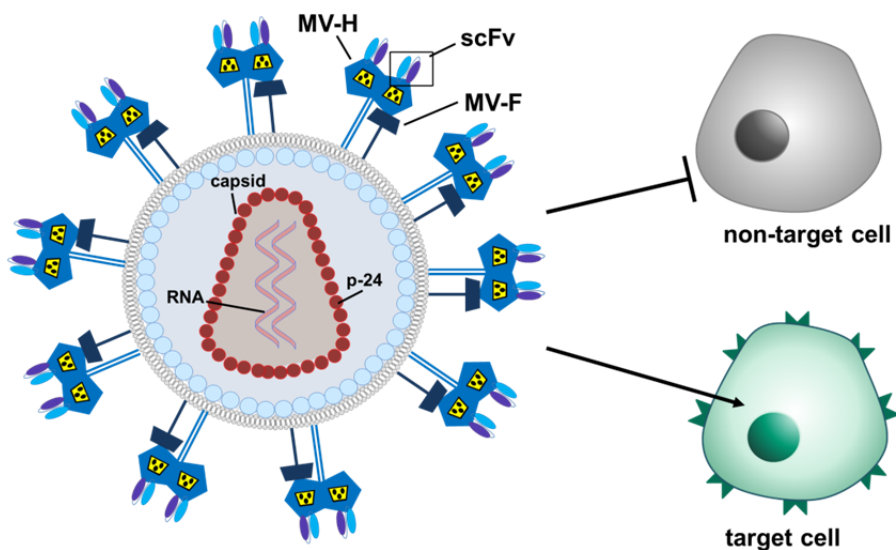


Figure 1: Receptor targeted LV. The cytoplasmatic domains of measles virus F and H proteins are truncated. The natural binding site within the H protein is mutated and blinded for the natural receptors of measles virus. In addition, a targeting ligand, here a single-chain antibody, is fused to the ectodomain of the H protein allowing transduction of receptor positive targeting cells only.

1.5.2 Receptor targeted AAV vectors

Incorporation of receptor ligands into the capsid of AAV vectors is not well-tolerated. Therefore, the identification of suitable ligands with respect to length and sequence are critical for proper capsid assembly. In addition, only the fusion of a targeting ligand to the N-terminus of the VP2 protein allows the production of functional vector particles (Yang et al., 1998; Wu et al., 2000). A universal targeting approach was investigated by Ried et al. They inserted a truncated immunoglobulin-binding domain into AAV2 particles that allows loading of the vector particle with various antibodies. These vectors transduced target cells specifically, but the titers remained very low (Ried et al., 2002). Therefore, retargeting of AAV2 vectors with small high binding affinity molecules, namely DARPins was established by Münch et al. A DARPin against Her2/neu was fused to the N-terminus of the AAV2 VP2 capsid protein resulting in successful incorporation of the receptor targeting domain into the vector particles. In addition, by mutation of the native binding site HSPG the generated AAV vector particles were blinded for the natural receptor leading to restricted gene transfer into Her2/neu⁺ cells. Furthermore, by de-targeting of the Her2-AAV vector from the natural liver tropism, severe liver damage was prevented compared to the

INTRODUCTION

AAV2 wild-type vector after systemical administration *in vivo*. The therapeutic relevance of the newly generated targeting vector was demonstrated by delivery of the HSV-TK gene into Her2/neu positive tumor tissue after i.v. injection. In combination with injection of the prodrug ganciclovir, growth of the tumor was reduced resulting in prolonged survival of the mice (Münch et al., 2013). This retargeting approach was further optimized by separation of DARPin containing AAV particles from DARPin-deficient particles by immobilized metal ion affinity chromatography resulting in tissue specific transgene expression without detectable off-targeting effects in a mouse model. The flexibility of the system was shown by generation of two other receptor targeted vectors, namely CD4-AAV and EpCAM-AAV (Münch et al., 2015).

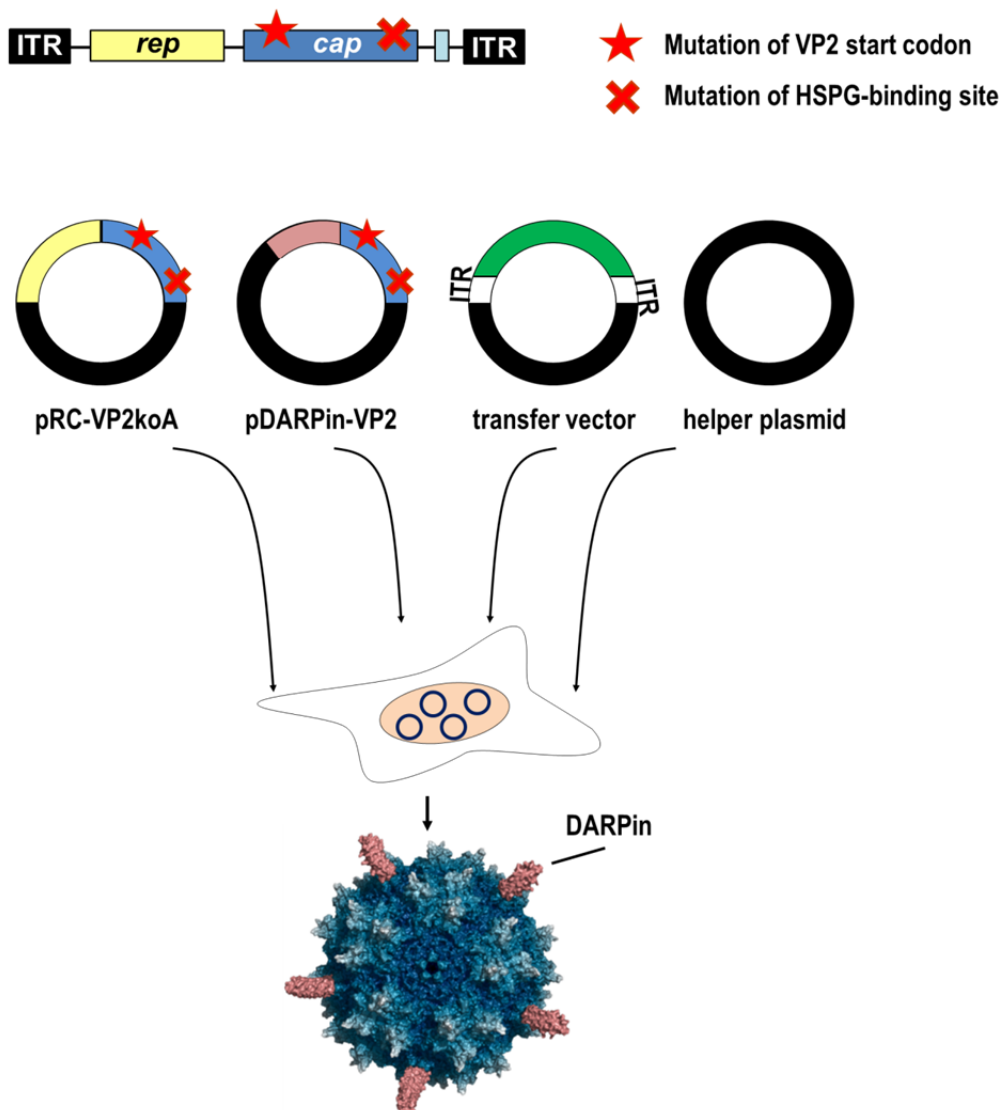


Figure 2: Generation of receptor targeted AAV vectors. By transient transfection of producer cells AAV particles are generated. The VP2 start codon as well as the HSPG-binding site of the AAV2 capsid gene were mutated resulting in expression of VP1 and VP2 proteins. The DARPin-VP2 capsid protein is expressed from a separate plasmid. The transfer vector contains ITRs, resulting in packaging of the transgene into the assembled particle.

1.6 Cell surface markers

Using receptor targeted viral vectors, transgenes can be delivered selectively into specific cell types *in vitro* as well as *in vivo*. Target cells can be defined by the expression of surface molecules and depending on the target cell population the receptor of choice can be selected. In tumor therapy, progression of tumor or response to treatment and risk of recurrence is often determined by monitoring of

established surface markers that are overexpressed in diverse tumor types. Among these markers is the human epidermal growth factor receptor 2 (Her2/neu) a type 1 receptor tyrosine kinase belonging to the epidermal growth factor family. It is over-expressed on varies cancer cells such as pancreatic, ovarian and breast cancer cells (Slamon et al., 1987; Slamon et al., 1989; Hall et al., 1990). Other common tumor markers include but are not limited to the epithelial cell adhesion molecule (EpCAM), the epidermal growth factor receptor (EGFR) or CD20.

As described in chapter 1.2 gene modification of HSPCs is often achieved by *ex vivo* transduction with lentiviral vectors pseudotyped with VSVG due to their broad tropism (Cartier et al., 2009; Aiuti et al., 2013; Biffi et al., 2013). A receptor targeted transduction approach would allow gene modification of specific subsets of HSPC including very primitive cells. In bone marrow, cord and mobilized peripheral blood the frequency of true HSCs capable of self-renewal is limited to estimated 0.01-0.1% of total nucleated cells (Baum CM et al., 1992; Hao QL et al., 1995). During the differentiation process of HSCs into more committed progenitor cells and finally into mature cells of a defined lineage, the ability of self-renewal is lost. Over the last years, lots of effort was put into the identification of HSC surface markers in mouse and human that would allow a highly purified enrichment of HSCs. So far, the expression pattern of human HSCs includes $CD34^+$ $CD133^{high}$, $CD90^+$, $CD38^{-/low}$ and $CD45RA^-$ (Civin CI et al., 1984; Terstappen et al., 1991; Baum CM et al., 1992; Miraglia et al., 1997; Yin et al., 1997; Majeti et al., 2007). The expression of these surface proteins changes during the differentiation process (Figure 3) and facilitates the distinction of different hematopoietic cell subsets. The surface expression pattern defining HSC in mouse and human differs. For murine HSCs $CD105$ is a well-established marker (Chen et al., 2002; Chen et al., 2003; Roques et al., 2012). There are few reports that $CD105$ is also present on a subset of human HSCs demonstrating that $CD34^+CD105^+$ cells show higher long-term culture-initiating cell frequency than the $CD105^-$ population (Pierelli et al., 2000; Pierelli et al., 2001). $CD105$ or endoglin is a component of the transforming growth factor- β (TGF- β) complex (St-Jacques et al., 1994; Warrington et al., 2005) and is involved in the TGF- β signaling pathway, but it is suggested that it has further functions such as being involved in angiogenesis (Li et al., 1999). $CD105$ is mainly expressed on activated endothelial cells, but is also expressed on other cell types such as activated

macrophages, mesenchymal stem cells (Lin et al., 2013) or progenitor endothelial cells (Nassiri et al., 2011). 72% of the sequence and expression profile between mouse and human is conserved (Letamendía et al., 1998) suggesting that CD105 plays an underrated role in the definition of human HSCs.

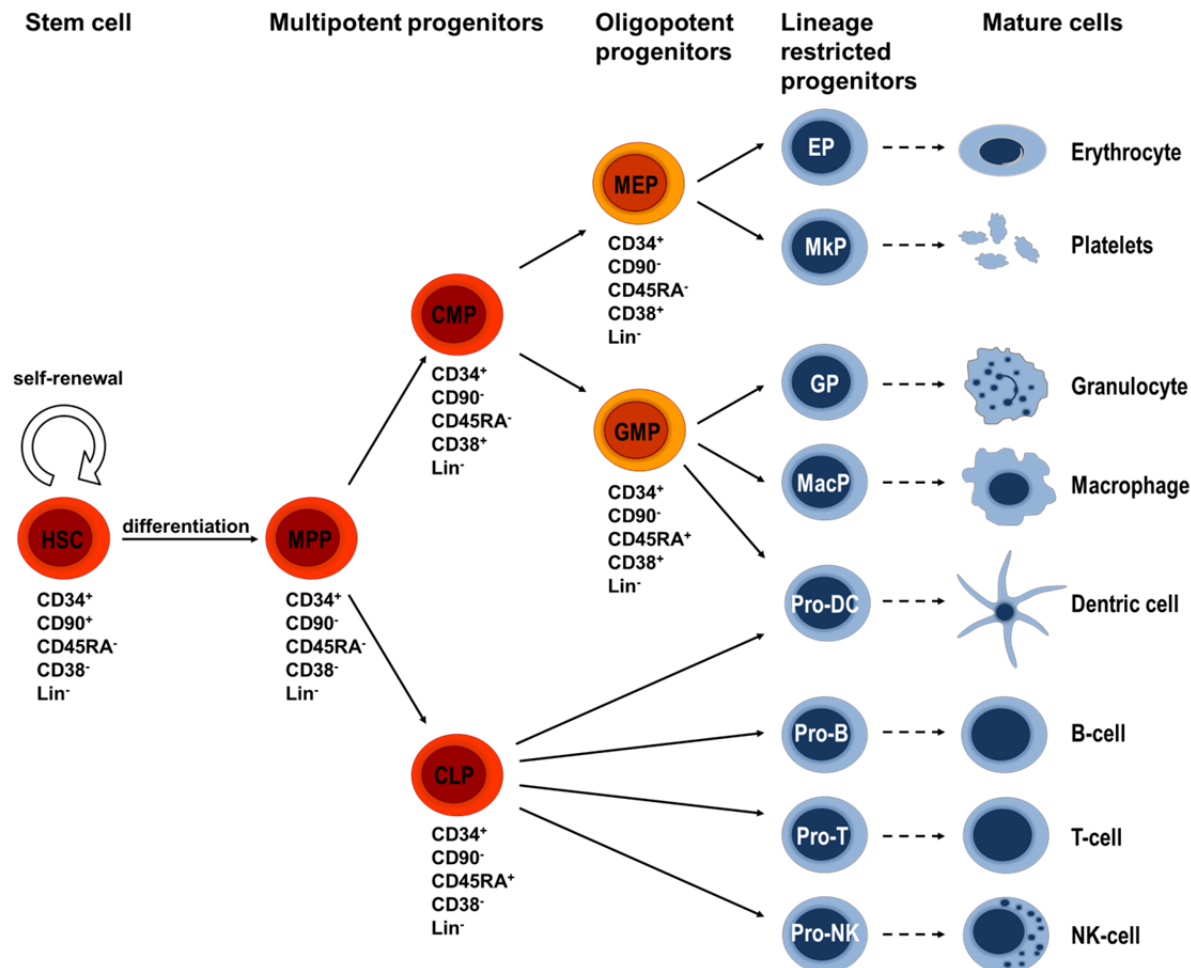


Figure 3: Hematopoietic hierarchy and phenotypic markers associated with HSCs. HSCs are defined by the ability of self-renewal and differentiation capacity. During the differentiation process into multipotent and oligopotent progenitor cells, HSCs lose their potential for self-renewal. The various subpopulations are defined by the expression of the indicated surface proteins. HSC, hematopoietic stem cell; MPP, multipotent progenitor; CLP, common lymphoid progenitor; CMP, common myeloid progenitor; MEP, megakaryocyte/erythrocyte progenitor; GMP, granulocyte/macrophage progenitor; EP, erythrocyte progenitor; MkP, megakaryocyte progenitor; GP, granulocyte progenitor; MacP, macrophage progenitor; Pro-DC, dendritic cell progenitor; Pro-B, B-cell progenitor; Pro-T, T-cell progenitor and Pro-NK, natural killer cell progenitor.

1.7 Objective

Restricting gene delivery to therapeutic relevant cells will take *in vivo* gene therapy one step further. One aim of this thesis was the side by side comparison of LVs and AAV vectors using an identical receptor for cell entry. LV and AAV targeting Her2/neu were chosen, since both vectors present the same targeting ligand on the particle surface, namely the DARPin 9.29, and were well characterized before (Münch et al., 2011; Münch et al., 2013). First, functional and genomic titers of both vector types had to be determined. While functional titers were assessed by transduction of Her2⁺ cells, a qPCR method that allows quantification of genomic titers of both vector types in parallel was established. In a next step, transduction efficiencies of Her2-AAV and Her2-LV were compared *in vitro* and *in vivo*. For the latter, luciferase expression was monitored in a subcutaneous tumor mouse model after systemic administration of either Her2-LV^{luc} or Her2-AAV^{luc} by *in vivo* imaging. In addition, distribution of the targeted vector particles was analyzed in a mouse model at early time points after vector injection. This first side by side comparison between lentiviral and AAV vectors using the identical cell entry receptor provides insight into performance, distribution and applicability of receptor-targeted lentiviral and AAV vectors.

For genetic modification of HSPCs, LVs are mainly used due to their ability to integrate into the host's genome ensuring long-term transgene expression. The second part of this thesis investigated the option to transduce a very primitive long-term repopulating subpopulation of human CD34⁺ cells. Few studies suggested that CD105 is expressed on human HSCs (Pierelli et al., 2000; Pierelli et al., 2001). Therefore, the applicability of CD105 as a potential HSC marker was investigated. Expression levels of CD105 on HSCs were analyzed and the subpopulation expressing CD105 was defined in more detail. With the receptor-targeted CD105-LV that was previously shown to transduce specifically CD105 expressing endothelial cells the ability for gene transfer into unstimulated and stimulated CD34⁺ cells was investigated. Long-term transgene expression and differentiation capacity of CD105-LV transduced cells was determined *in vitro* as well as *in vivo* and eventually compared to the commonly used VSVG-LV in a competitive setting.

In summary, this thesis demonstrates the potential and possible applications of receptor-targeted gene transfer.

2. MATERIAL AND METHODS

2.1 Material

2.1.1 Equipment

Name	Model	Manufacturer
Bacteria incubator shaker	Innova™ 4200	New Brunswick Scientific
Cell incubator	BBD6220	Heraeus, Thermo Scientific
Cell separator	autoMACS® Pro Separator	Miltenyi Biotec
Cell sorter	BD FACSAria™ III	Becton Dickinson
Centrifuge	Multifuge X3, Multifuge 3	Heraeus, Thermo Scientific
Flowcytometer	MACSQuant Analyzer	Miltenyi Biotec
Flowcytometer	LSRII	Becton Dickinson
Fluorescence microscope	Axiovert 200	Zeiss
Gel electrophoresis system	n/a	Bio-Rad
Gel electrophoresis system	Model B3	Owl Separation Systems
Homogenizer	FastPrep®-24 Instrument	MP Biomedicals
HPLC system	Smartline	Knauer
<i>in vivo</i> imaging system	IVIS Spectrum	PerkinElmer
Laminar Flow Cabinet Class II	SteriGARD® III	The Baker Company
Light microscope	Axiovert 25	Zeiss
LightCycler	LightCycler®	Roche
Micropipettes	Research plus®	Eppendorf
Microplate reader	THERMOmax	Molecular Devices
Multichannel pipettes	Finnpipette F2	Thermo Scientific

Pipetboy	Accu-jet®	Brand
Spectrophotometer	NanoDrop 2000c	Thermo Scientific
Table-top processor	Curix 60™	Agfa
Thermo cycler	PTC 200	MJ Research
Ultracentrifuge	Optima™ L-70k	Beckman Coulter

2.1.2 Kits

Name	Supplier
DNeasy Blood and Tissue Kit	Qiagen
96-DNeasy Blood and Tissue Kit	Qiagen
RNeasy Mini Kit	Qiagen
MAXIscript Kit	Invitrogen
Transcriptor First Strand cDNA Synthesis Kit	Roche
CD34 MicroBead Kit, human	Miltenyi Biotec
CD105 MicroBead Kit, human	Miltenyi Biotec
CD34 MultiSort Kit, human	Miltenyi Biotec
FastStart DNA Master ^{PLUS} SYBR Green I	Roche Diagnostics
ABsolute QPCR ROX Mix	Thermo Scientific
GeneJET Gel Extraction Kit	Thermo Scientific
EndoFree Plasmid Maxi Kit	Qiagen
Jetstar 2.0 Maxi Kit	Genomed
Jetstar 2.0 Giga Kit	Genomed
JETStar NoEndo Jetfilter Giga Kit	Genomed
RETROtek HIV-1 p24 Antigen ELISA	ZeptoMetrix
pGEM®-T Easy Vector System	Promega

2.1.3 Buffers and chemicals

Name	Composition/Supplier
AAV lysis buffer	50 mM Tris-HCl, 150 mM NaCl in PBS
BTPE	10 mM PIPES, 30 mM Bis-Tris, 10 mM EDTA, pH 6,5
DEPC H ₂ O	0.1 % DEPC in H ₂ O, Paul-Ehrlich-Institut
D-Luciferin	Perkin Elmer
DNA loading buffer 6x	Thermo Scientific
ELISA blocking buffer	PBS, 0.05% Tween-20, 3% BSA, 5% sucrose
ELISA washing buffer	PBS, 0.05% Tween-20
FACS washing buffer	2% FCS in PBS
FACS fix buffer	1% formaldehyde in PBS
FACS sorting buffer	10 mM HEPES, 2% FCS, 0.5 mM EDTA in PBS
Freezing medium	90% FCS, 10% DMSO
Glyoxal mix	6 ml DMSO, 2 ml 6 M glyoxal, 1.2 ml 10x BTPE, 0.6 ml 80% glycerine, 0.2 ml ethidium bromide (10 mg/ml)
Histopaque®-1077	Sigma-Aldrich
OptiPrep™	Sigma-Aldrich
PBS	Lonza
PBS M/K	2.5 mM KCl, 1 mM MgCl ₂ in PBS
PEI	18 mM polyethylenimine in H ₂ O
SDS running buffer	25 mM Tris, 192 mM Glycine, 1% SDS
StemSpan™ CC100	Stem cell technologies
TAE	40 mM Tris, 20 mM Acetic acid, 1 mM EDTA
TBS-T	10 mM Tris pH 8.0, 150 mM NaCl, 0.1% Tween-20
Thrombopoietin (TPO)	Peptrotech
TMB liquid substrate	Sigma-Aldrich

TNE	25 mM Tris pH 7.4, 150 mM NaCl, 5 mM EDTA
Transfer buffer	48 mM Tris, 39 mM Glycine, 20% Methanol
Triton X-100	Sigma-Aldrich
Trypsin solution	PBS, 2 mM EDTA, 0.25% Trypsin-Melnick
Tween-20	Sigma-Aldrich

2.1.4 Antibodies

Name	Application	Dilution	Supplier
α-AAV intact particle, mouse (A20)	ELISA	1:4	Progen
α-mouse-biotin, donkey	ELISA	1:25,000	Jackson ImmunoResearch
Streptavidin-HRP	ELISA	1:500	Jackson ImmunoResearch
α-Her2/neu-PE, mouse	FC	1:20	BD Pharmingen
α-CD105-APC	FC	1:10	Invitrogen
α-CD34-FITC	FC	1:10	Miltenyi Biotec
α-CD34-PE	FC	1:10	Miltenyi Biotec
α-CD133-PE	FC	1:10	Miltenyi Biotec
α-CD90-PEVio770	FC	1:10	Miltenyi Biotec
α-mCD45-PE	FC	1:10	Miltenyi Biotec
α-hCD45-APC	FC	1:10	Miltenyi Biotec
α-CD3-PE	FC	1:10	Miltenyi Biotec
α-C19-PE	FC	1:10	DAKO
α-CD33-PE	FC	1:10	BD Pharmingen
α-CD38-FITC	FC	1:10	Miltenyi Biotec
FcR blocking reagent, human	FC	1:10	Miltenyi Biotec

FC, flow cytometry; ELISA, enzyme-linked immunosorbent assay.

2.1.5 Oligonucleotides

Name	Sequence (5' – 3')
GFP-for	GCTACCCCGACCACATGAAG
GFP-rev	GTCCATGCCGAGAGTGATCC
luc2-for	TTCGGCTGGCAGAAGCTATG
luc2-rev	GCTCGCGCTCGTTGTAGATG
luc3-fw	GTGGTGTGCAGCGAGAATAG
luc3-rv	CGCTCGTTGTAGATGTCGTTAG
luc3 probe	[6FAM]TTGCAGTTCTTCATGCCCGTGTG[BHQ1]
ivtr_GFP fw	CGTGACCACCCCTGACCTAC
ivtr_GFP rv	GCCGTCGTCCTTGAAGAAAGATG
ivtr_luc fw	CTTCGAGATGAGCGTCGGCTG
ivtr_luc rv	CCATGCTGTCAGCAGCTCG

2.1.6 Plasmids

Name	Description	Source
pCMVΔR8.91	HIV-1 packaging plasmid	U. Blömer (Zufferey et al, 1998)
pSEW	HIV-1 transfer vector encoding GFP under control of the SFFV promoter	M. Grez (Demaison et al, 2002)
pSEW-BFP	HIV-1 transfer vector encoding BFP under control of the SFFV promoter	T. Abel
pS-luc2-W	HIV-1 transfer vector encoding luciferase under control of the SFFV promoter	(Abel et al, 2013)
pMD2.G	Encodes the VSV glycoprotein	D. Trono

pCG-H _{mut} -	encodes MV H _{mut} 18 fused to the	(Anliker et al. 2010)
αCD105	αCD105-scAb	
pCG-FΔ30	Encodes MV F with a truncated cytoplasmic tail of 30 aa under control of the CMV promoter	(Funke et al, 2008)
pCG-H _{mut} Δ18-	Encodes MV H _{mut} 18 fused to the	(Münch et al, 2011)
DARPin-9.29	Her2/neu-specific DARPin 9.29	
pXX6-80	Adenoviral helper plasmid encoding E2A, E4 and VA	H. Büning
pscGFP-SFFV	Self-complementary AAV transfer vector encoding GFP under control of the SFFV promoter	(Münch et al, 2013)
pscluc2-SFFV	Self-complementary AAV transfer vector encoding luciferase under control of the SFFV promoter	(Münch et al, 2013)
pRC-VP2 _{KO} -	Encodes the AAV2 rep and cap proteins	H. Büning
HSGP _{mut}	with mutated VP2 start codon and the point mutations R585A and R588A	
pDARPin-9.29-VP2	Encodes the Her2/neu-specific DARPin 9.29 fused to the N-terminus of the AAV2 VP2 protein containing the point mutations R585A and R588A	(Münch et al, 2013)
pGEM-T7-GFP	Encodes part of the <i>egfp</i> sequence under the control of the T7 promoter	This thesis
pGEM-T7-luc	Encodes part of the <i>luc</i> sequence under the control of the T7 promoter	This thesis

2.1.7 Bacterial strains and mammalian cells

Name	Description	Source
<i>E. coli</i>	Chemically competent bacterial strain	Life
Top10		Technologies
<i>E. coli</i>	Chemically competent bacterial strain (Stop Unwanted Rearrangement Events)	Stratagene
HEK-293T	Human embryonic kidney cell line, genetically engineered to express the SV40 T antigen	ATCC CRL-11268
SK-OV-3	Human ovarian carcinoma cell line	ATCC HTB-77

2.1.8 Culture media

Name	Description	Source
Luria-Bertani (LB) broth	1% tryptone, 0.5% yeast extract, 1% NaCl in H ₂ O pH 7.2	Paul-Ehrlich-Institut
S.O.C. medium	2% Tryptone, 0.5% yeast extract, 10 mM NaCl, 2.5 mM KCl, 10 mM MgCl ₂ , 10 mM MgSO ₄ , 20 mM glucose in H ₂ O	Invitrogen
Dulbecco's modified Eagle medium (DMEM)	Supplemented with 10% FCS and 2 mM L-glutamine as culture medium for HEK-293T	Lonza
McCoy's medium	Supplemented with 10% FCS and 2 mM L-glutamine as culture medium for SK-OV-3 cells	Sigma-Aldrich
StemSpan™ Serum-Free Expansion Medium (SFEM)	Supplemented with 2 mM L-glutamine and 0.5% Penicillin-Streptomycin-Fungizone mix as culture medium for human CD34 ⁺ cells	Stem cell technologies

MethoCult GF	Supplemented with 2 mM L-glutamine and	Stem cell
H4434 medium	0.5% Penicillin-Streptomycin-Fungizone mix as culture medium for human CD34 ⁺ cells in colony forming assays	technologies

2.2 Methods of molecular biology

2.2.1 Transformation of chemically competent bacteria

Chemically competent E. coli Top10 or SURE bacteria were thawed on ice and 50 ng DNA or 2 µl of ligation reaction were added. After 30 min incubation on ice, bacteria were heated to 42°C for 45 sec and then immediately cooled on ice. 500 µl S.O.C medium was added. Bacteria were incubated for 30 min at 37°C and 600 rpm. Subsequently, bacteria were plated onto LB agar plates supplemented with the corresponding antibiotic and incubated overnight at 37°C or for 3 days at 25°C.

2.2.2 Plasmid preparation

Plasmid DNA from transformed bacteria was purified using the GeneJET Plasmid Miniprep Kit, EndoFree Plasmid Maxi Kit or JETStar NoEndo Jetfilter Giga Kit according to the manufacturer's protocol. 4 ml, 250 ml or 2400 ml LB medium supplemented with the corresponding antibiotics were inoculated with a single bacterial clone and incubated overnight at 37°C. Cells were pelleted by centrifugation at 13,000 rpm (Miniprep, Multifuge 3) or 6,000 rpm (Maxiprep, Sorvall Rc26 plus) for 15 min or at 4,500 rpm for 1 hour (Gigaprep, Multifuge 3). The concentration of purified DNA was measured photometrically by NanoDrop 2000c. Plasmid preparations were analyzed by agarose gel electrophoresis (2.2.4) after enzymatic control digest (2.2.3).

2.2.3 Restriction of DNA

All DNA restrictions were performed using restriction endonucleases from New England Biolabs according to the manufacturer's instructions. 10 µg DNA were mixed with 10 U of the respective restriction enzyme under the required buffer conditions and incubated for 3 hours. For double digestions with enzymes requiring different buffer conditions, the optimal buffer for both enzymes was chosen. For digestions with different incubation temperatures, the restriction reactions were performed sequentially. Restriction samples were applied to agarose gel electrophoresis. If required, the desired DNA fragment was purified from the gel using the GeneJET Gel Extraction Kit (Thermo Scientific).

2.2.4 Agarose gel electrophoresis

Agarose gel electrophoresis allows the separation of DNA or RNA fragments according to their size. For the analysis of DNA, agarose powder was dissolved in TAE buffer by heating. 50 µg/ml ethidium bromide that intercalates into DNA strands was added to the agarose solution. After polymerization on a gel tray, DNA samples were mixed with 6x loading buffer and transferred into the gel pockets. Electrophoresis was performed at 80-100 V in a Bio-Rad WIDE MINI-SUB chamber. Separation of DNA fragments was analyzed under UV light and compared to a 2-log ladder (New England Biolabs).

For visualization of RNA, agarose powder was dissolved in BTPE to a final concentration of 1.5%. Polymerization took place on a gel try. 2 µl of RNA were mixed with 10 µl of glyoxal mix containing ethidium bromide. RNA samples as well as the RibuRuler High Range RNA ladder (Life Technologies) were incubated at 55°C for 30 min and then cooled on ice for 5 min. 5x loading buffer was added and the samples loaded into the gel pockets. Electrophoresis was performed at 120 V for 2 hours in a Owl Separation Systems chamber with buffer recirculation. RNA fragments were visualized under UV light.

2.2.5 Isolation of DNA from agarose gels

Gel pieces containing the DNA fragments of interest were cut out of the agarose gel and DNA was isolated using the GeneJET Gel Extraction Kit (Thermo Scientific) according to the company's protocol.

2.2.6 Isolation of genomic DNA

Genomic DNA from AAV vector stocks was isolated using the DNeasy Blood and Tissue Kit (Qiagen), total DNA from tissue was purified using the 96-DNeasy Blood and Tissue Kit (Qiagen) according to the manufacturer's instructions. For quantification of AAV genomic titers 10 µl of the AAV vector stocks were diluted with 190 µl PBS and applied to isolation followed by qPCR. 10 mg of spleen and 20 mg of other tissue was used for DNA isolation. Purification of total DNA included treatment of the samples with RNase.

2.2.7 Isolation of total RNA

RNA from lentiviral vector stocks and tissue was isolated using the RNeasy Mini Kit (Qiagen) according to the company's protocol. 10 µl of LV were used for subsequent quantification of genomic titers. 10 mg of homogenized spleen and 20 mg of other homogenized tissue were applied to RNA purification. An on-column DNase I digest was included into both isolation procedures.

2.2.8 Generation of RNA standard

For the generation of the RNA standard for qPCR, sequences of the transgenes *luc* or *egfp* were amplified by polymerase chain reaction and ligated into the pGEM[®]-T Easy vector (Promega) to introduce a T7 promoter upstream of the gene of interest according to the manufacturer's instruction. The resulting plasmids were linearized by a single cut after the gene of interest. The linearized plasmid served as template for the *in vitro* transcription of RNA. RNA was generated using the MAXIscript Kit (Invitrogen) according to manufacturer's instructions including a DNase I digestion. Then, RNA was purified by two rounds of phenol-chloroform extraction and one

chloroform extraction, followed by two sodium acetate/ethanol precipitations. The purified RNA pellet was resuspended in DPEC H₂O and analyzed by agarose gel electrophoresis. The RNA concentration was determined photometrically by NanoDrop 2000c and adjusted to 1x10¹¹ RNA molecules/μl.

2.2.9 Reverse transcription

In vitro transcribed RNA and RNA from lentiviral vector stocks or tissue was reverse transcribed using the Transcriptor First Strand cDNA Synthesis Kit (Roche) according to the manufacturer's protocol. 1 μl of RNA standard, 3 μl of LV RNA and maximum amounts (up to 5 μg) of total RNA from tissue were incubated with specific primers for 10 min at 65°C to denature secondary RNA structures. The samples were cooled on ice, before reverse transcriptase buffer, enzymes and deoxynucleotide mix were added. After 30 min at 55°C, the reverse transcriptase was inactivated by heating to 85°C for 5 min. The samples were placed on ice and applied to qPCR within 2 hours or stored at -20°C.

2.2.10 Quantitative real-time PCR

Quantitative real-time PCR (qPCR) allows the amplification and quantification of a specific DNA sequence by the use of a fluorescence dye. qPCR was used to determine genomic titers of lentiviral and AAV vector stocks as well as vector amounts in tissue. For the quantification of genomic titers of lentiviral and AAV vector stocks, the SYBR Green containing PCR mix FastStart DNA Master^{PLUS} SYBR Green I (Roche) was used. SYBR Green intercalates into double stranded DNA fragments. For quantification of vector genomes in tissues, a primer/probe set specific for the transgene was used in combination with the ABsolute QPCR ROX Mix (Thermo Scientific) to enhance the signal specificity. At the end of each amplification cycle the fluorescence was measured, whereby an increased fluorescence signal correlated with an increase of the PCR product. Comparison of the crossing points obtained from unknown samples with that of a standard of known concentration, allowed absolute quantification of vector genome content in the samples. As standard for quantification of AAV genomes, a 10-fold serial dilution of the AAV transfer plasmid was used. 10-fold serial dilutions of the RNA standard which was obtained by *in vitro*

transcription were reverse transcribed. The cDNA served as standard to determine the amount of lentiviral RNA in samples. qPCR was performed in either the LightCycler 1.2 or the LightCycler 480 using the conditions specified below.

Table 1: qPCR reaction using SYBR Green

Component	Volume
H ₂ O, nuclease free	14 µl
Primer for (20 pmol/µl)	0.5 µl
Primer rev (20 pmol/µl)	0.5 µl
FastStart DNA Master ^{PLUS} SYBR Green I (1a+1b)	4 µl
Template DNA or cDNA (isolated from AAV or lentiviral vectors)	1 µl

Table 2: qPCR program using SYBR Green

Initial denaturation	95°C	10 min
Quantification (40 cycles)	95°C	10 sec
	64°C	4 s*, 5 s [#]
	72°C	7 s*, 10 s [#]
Melting curve	95°C	0 s
	67°C	10 s
	95°C	0 s

*egfp transferring vectors, [#]luc transferring vectors

Table 3: qPCR reaction using primer/probe set

Component	Volume
H ₂ O, nuclease free	6-10 µl
Primer for (20 pmol/µl)	0.5 µl
Primer rev (20 pmol/µl)	0.5 µl
Probe	0.5 µl
Absolute QPCR ROX Mix (2x)	12.5 µl
Template DNA or cDNA	1-5 µl

Table 4: qPCR program using primer/probe set

Initial denaturation	95°C	15 min
Quantification (40 cycles)	95°C	15 sec
	64°C	30 s
	72°C	30 s

2.2.11 Polymerase chain reaction

To amplify parts of the sequences of either *gfp* or *luc* and introduce specific restriction sites to the corresponding DNA fragments, PCR was performed using the primers ivtr_GFP fw and ivtr_GFP rv or ivtr_luc fw and ivtr_luc rv and the Taq DNA polymerase (5 Prime) according to the manufacturer's protocol. Thereby, adenine overhangs at the 3' ends of the PCR products are introduced for efficient ligation into the pGEM®-T Easy (Promega) vector. The cycling details are specified below.

Table 5: PCR program

Initial denaturation	95°C	2 min
Amplification (20 cycles)	95°C	30 s
	62°C	30 s
	68°C	12 s
Final extension time	68°C	10 min

2.2.12 Enzyme-linked immunosorbent assay (ELISA)

Numbers of physical particles within lentiviral and AAV vectors stocks were determined by ELISA. Quantification of LV particle numbers was based on the amount of p24 protein in lentiviral vector stocks. p24 protein was quantified using the RETROtek HIV p24 antigen ELISA kit (Zeptometrix) according to the company's protocol.

For AAV capsid quantification, Maxisorp immunoplates were coated with serial dilutions of AAV vector stocks over night at 4°C. The following day, plates were washed three times with ELISA washing buffer and blocked with ELISA blocking buffer for 2 hours at room temperature. The α -AAV2-capsid antibody was diluted 1:4 in blocking buffer and added to the bound vector particles for one hour. After three washing steps, the α -mouse Biotin-conjugated secondary antibody was incubated on the samples for one hour at room temperature. The plate was washed again and then incubated with streptavidin-HRP diluted in ELISA blocking buffer. The plate was washed three times with ELISA washing buffer and three times with water. For detection of coated capsids, the TMB liquid substrate system and a microplate reader were used according to the manufacturers' instructions. A previously analyzed vector preparation served as standard.

2.3 Cell culture and virological methods

2.3.1 Cultivation of cell lines

Cells were cultivated in the adequate medium (2.1.8) in a cell culture incubator at 37°C, 5% CO₂ and 90% humidity. Cells were splitted twice a week. Adherent cells were washed with PBS and detached using 0.25% trypsin solution. The adequate fraction of the cell suspension was transferred to a new cell culture flask and fresh medium was added. Cell lines were checked for mycoplasma contamination by PCR regularly.

2.3.2 Freezing and thawing of cultured cells

Adherent cell lines were detached as described in 2.3.1, resuspended in cell culture medium and centrifuged at 800 rpm, 4°C for 4 min. The cell pellet was resuspended in cold freezing medium, aliquoted and frozen at -80°C using a 5100 Cryo Freezing container (Nalgene). The following day, cells were transferred to the gas phase of liquid nitrogen for long-term storage.

Frozen cells were thawed in a 37°C water bath and transferred into pre-warmed culture medium in a fresh cell culture flask. The next day, medium was refreshed.

2.3.3 Production and purification of vector particles

Lentiviral and AAV vector particles were produced by transient transfection of HEK-293T cells by polyethylenimine (PEI). DNA and PEI form positively-charged complexes that bind to the cell surface. DNA/PEI is endocytosed and released into the cell cytoplasm. 1.4x10⁵ HEK-293T cells per cm² cell culture vessels were seeded. The following day, medium was replaced with DMEM supplemented with 15% FCS and 3.2 mM glutamine. 0.2 mg DNA/cm² and 0.8 ml PEI/cm² were diluted in DMEM and vortexed. Both solutions were combined and vortexed thoroughly. The DNA/PEI mixture was incubated for 20 min at room temperature and then added to the cells. After 24 hours, medium was refreshed.

For the production of LVs, lentiviral vector particles were harvested from the supernatant 48 hours post transfection. The supernatant was collected and filtered

through a 0.45 µm PTFE filter. Vector particles were purified and concentrated by centrifugation either at 100,000 x g for 3 hours at 4°C or at 4,400 x g for 24 hours at 4 °C both through a 20% sucrose cushion. LVs were resuspended in PBS, aliquoted and stored at -80°C.

AAV vector producer cells were scraped off the cell culture dish and spun down at 1,000 rpm for 7 min. Cell pellets were resuspended in AAV lysis buffer. After three freeze/thaw cycles, cell lysate was incubated with benzonase at 37°C for 30 min. Cell debris were removed by centrifugation for 20 min at 3700 x g and 4°C. For purification by density centrifugation, vector containing supernatant was diluted with PBS M/K and transferred to a Quick-Seal® ultracentrifugation tube (Beckman Coulter). The supernatant was overlaid consecutively with 9 ml 15%, 6 ml 25%, 5 ml 40% and 6 ml 60% OptiPrep™. After 2 hours centrifugation at 63,000 and 4°C, AAV vectors were recovered from the 40% OptiPrep™ phase, aliquoted and stored at -80°C.

2.3.4 Transduction of adherent cell lines and titration of vectors

The day before transduction, 8x10³ cells were seeded into a single well of a 96-well plate. For titration, vector stocks were diluted in medium (2-fold serial dilutions of AAV vectors, 10-fold serial dilutions of LVs) and added to the cells. The percentage of GFP expressing cells was determined by flow cytometry 72 hours after transduction with LVs and 96 hours after transduction with AAV vectors. For titer calculations fractions between 2 and 20% GFP⁺ cells were considered. In addition, for the quantification of functional AAV titers, the cell proliferation rate was taken into account. For the transduction of cell lines, the required amount of vectors was diluted in medium and added to the cells. Analysis of the percentage of GFP⁺ cells was performed 72, respectively, 96 hours post transduction.

2.3.5 Isolation of human CD34⁺, respectively, CD105⁺ cells from mobilized peripheral blood

G-CSF mobilized peripheral blood was obtained from stem cell donations with written consent of the donors and in accordance with the ethical standards of the responsible committee on human experimentation (IRB permit 329/19). CD34⁺ cells

were isolated by positive selection using α -CD34 microbeads (Miltenyi Biotec) according to manufacturer's instructions. CD34 specific antibodies conjugated to magnetic beads were incubated with the blood at 4°C for 30 min, labeling CD34⁺ cells magnetically. Then, the cells were applied to a column in a magnetic field, retaining the magnetically labeled CD34⁺ cells while unlabeled cells were washed off the column. After releasing the column from the magnetic field, CD34⁺ cells were eluted. Magnetically labeled antibodies remained bound to the cell surface. Cells were pelleted at 1,200 rpm for 5 min and transferred into stem cell culture medium (2.1.8). CD105⁺ cells were purified from mobilized peripheral blood using CD105 microbeads (Miltenyi Biotec) as described for CD34⁺ cells, however, the incubation time at 4°C was 15 min.

For isolation of CD34⁺ cells with subsequent purification of CD105⁺ cells, the CD34 MultiSort Kit (Miltenyi Biotec) was used according to the company's protocol. The principal is the same as for the isolation of CD34⁺ cells from mobilized peripheral blood only, but includes a step for the release of the magnetic beads from the primary antibodies and a second magnetic labeling of the eluted cells from the first purification round. The α -CD34 antibodies that were bound to the cells during the first labeling remained bound to the cells, but only the magnetic beads were released from the cell. The mircobeads conjugated to the α -CD105 antibodies of the second magnetic labeling remained bound to the cell surface as well.

2.3.6 Cultivation and stimulation of HSPCs

Unstimulated CD34⁺ cells were cultured in StemSpan serum free expansion medium (Stemcell Technologies) supplemented with 0.5% Penicillin-Streptomycin-Fungizone Mix (PromoCell) and 2 mM glutamine. 5x10⁴ cells were seeded per well of a 96-well plate. For stimulation of the cells the medium was supplemented with StemSpan CC100 cytokine cocktail (Stemcell Technologies) and 2 μ g/mL thrombopoietin (TPO) (Peprotech). After 24 hours, the cytokine-free medium of unstimulated cells was replaced by cytokine containing medium. CD105⁺ cells from mobilized peripheral blood were cultivated in the same way.

2.3.7 Transduction of HSPCs

5×10^4 CD34⁺ cells/well were transduced in 96-well plates by spinfection at 1,200 rpm and 32°C for 90 min. CD34⁺ cells for animal experiments were transduced in 24- or 12-well plates in the correlating cell density. Transduction of cells took place either immediately after isolation (unstimulated) or after overnight incubation in cytokine containing medium (stimulated). LVs were diluted in the corresponding medium and added to the cells. The final transduction volume was filled up to 250µl/well of a 96-well plate. Seventy-two hours post transduction, GFP expression was analyzed by flow cytometry.

2.3.8 Colony forming assay

The colony forming assay (CFA) is used to enumerate and assess colonies derived from myeloid multipotential progenitors and committed progenitors of the erythroid, monocyte and granulocyte lineages. Hematopoietic progenitor cells are applied to semi-solid methylcellulose medium supplemented with growth factors and cytokines that allows the progenitors to proliferate and differentiate into colonies of mature cells (Pereira et al., 2007). 1.5×10^3 transduced or untransduced primary human CD34⁺ cells were transferred into 3 ml MethoCult GF H4434 medium (Stemcell Technologies, Cologne, Germany) and plated in triplicates. After 10 days at 37°C and 95°C humidity, total and GFP⁺ colonies were counted and morphologically classified by fluorescence microscopy.

2.3.9 Analysis of cells by flow cytometry and fluorescence activated cell sorting

Flow cytometry is a laser-based technique that allows, based on scattered and emitted light, the characterization of cells on the basis of their size, morphology and fluorescence intensity. Additionally, expression of specific proteins can be assessed by binding of fluorophore labeled antibodies. Adherent cells were detached by incubation with PBS-Trypsin (PBS, 100mM EDTA, 0.25% Trypsin-Melnick). Cells were washed once with FACS washing buffer by centrifugation at 800 rpm for 4 min. Then, cells were either fixed immediately using FACS fix buffer or stained with

antibodies (2.1.4). After antibody staining, cells were washed once and fixed using FACS fix buffer. Primary human or murine cells were washed once with FACS washing buffer by centrifugation at 1,200 rpm for 4 min. Afterwards, cells were stained (2.1.4) or fixed with FACS fix buffer. Samples were measured using either the BD LSR II SORP (Becton-Dickinson) or the MACSQuant® Analyzer 10 (Miltenyi Biotec) and analyzed using the FCS Express V4 software (De Novo software).

For fluorescence activated cell sorting (FACS) of CD105⁺ cells, cells from mobilized peripheral blood were washed with PBS, stained with α -CD105-APC antibody and washed again. CD105 high expressing cells were collected in sorting buffer, washed once and resuspended in StemSpan serum free expansion medium supplemented with 0.5% Penicillin-Streptomycin-Fungizone Mix and 2 mM glutamine.

2.3.10 Annexin V/propidium iodide staining

For determination of apoptotic and necrotic cells, cells were stained with annexin V and propidium iodide (PI). Annexin V binds to phosphatidylserine that translocates to the extracellular cell membrane upon apoptosis induction. The cell membrane of late apoptotic and necrotic cells becomes permeable which enables PI to intercalate into the DNA. Thereby, early and late apoptotic/necrotic cells can be distinguished. CD34⁺ cells transduced with either CD105-LV^{GFP} or VSVG-LV^{GFP} were washed once with annexin binding buffer and then resuspended in annexin binding buffer. Cells were mixed with annexin V-APC (BD Bioscience) and incubated for 15 min at room temperature in the dark. After another washing step, cells were resuspended in annexin binding buffer. PI (Miltenyi Biotec) was added to the samples immediately before cells were analyzed by flow cytometry.

2.3.11 Competition assay

For the competition of CD105-LV with soluble CD105 protein, vector particles were incubated with increasing amounts of the extracellular domain of CD105 protein (sCD105) at 37°C for 30 min. Then, CD34⁺ cells were transduced with the vector-protein mixtures by spinfection. Seventy-two hours post transduction, GFP expression was determined by flow cytometry.

2.3.12 Serum stability assay

Serum from mice was collected and pooled. One part of the serum was heat-inactivated by incubation at 56°C for 30 min and then cooled on ice briefly. Heat-inactivated and non-heat-inactivated serum was added to Her2-LV^{GFP} and Her2-AAV^{GFP} in increasing concentrations and incubated at 37°C for 30 min. Afterwards, SK-OV-3 cells were transduced with the serum-vector mixtures. Ninety-six hours post transduction, GFP expression was determined by flow cytometry.

2.3.13 Expression of soluble CD105 protein

Soluble CD105 (sCD105) protein was used for a competition assay with CD105-LV. The recombinant protein was expressed in HEK-293T cells, following PEI transfection of cells with the plasmid encoding the extracellular domain of CD105, fused to a Fc-tag (kindly provided by Irene Schneider and Gundula Braun). After 24 hours, the transfection medium was replaced with Panserin A medium. Forty-eight and 72 hours post transfection sCD105 containing supernatant was collected, filtered through a 0.45 mm filter and stored at 4°C. sCD105 was purified from the supernatant by HPLC purification by binding of the Fc-tag to protein A. Purified protein was dialyzed against PBS at 4°C for 8 hours and additional 12 hours.

2.3.14 Isolation of blood, BM and spleen cells from mice

For the isolation of BM cells, tissue was removed from femur and tibia. The bones were disinfected with 70% ethanol and the joints on both ends were cut off. The BM was flushed out of the bones using PBS, a 5 ml syringe and a 27G cannula. BM cells were resuspended in PBS and passed through a 40 µm cell strainer. After centrifugation for 10 min at 1,200 rpm, remaining red blood cells were removed using the BD Pharm Lyse™ lysing solution (BD Bioscience) according to the manufacturer's instructions. Cells were washed once with PBS, resuspended in FACS washing buffer and stained with antibodies for flow cytometry analysis.

For the isolation of splenocytes, the spleen was transferred into a cell culture dish containing PBS and mashed using the plunger of a 5 ml syringe. The cell suspension

was passed through a 40 µm cell strainer. Afterwards, it was continued as for the preparation of BM cells.

Blood collected from mice was washed once with PBS. BD Pharm Lyse™ lysing solution (BD Bioscience) was used for erythrocyte lysis according to the company's protocol. Cells were washed with PBS, resuspended in FACS wash buffer and then stained with antibodies for flow cytometry analysis.

2.4 Experimental mouse work

Animal experiments were performed according to the German animal protection law and are approved by the responsible institutional ethical committee.

2.4.1 Repopulation of NSG mice with human CD34⁺ cells

5-6 week old NOD-scid IL2R $\gamma^{-/-}$ mice were sublethally irradiated at 1.8 or 2 Gy. After 4 hours, 0.5-1.7x10⁶ transduced or untransduced CD34⁺ cells purified from mobilized peripheral blood were injected via the tail vein using a 30G cannula. Seven days before to 7 days after the cell transplantation, mice received 2.5% bytril in their drinking water.

2.4.2 Subcutaneous injection of SK-OV-3 cells

SK-OV-3 cells were cultured and detached as described above and centrifuged at 1,200 rpm for 7 min. Afterwards, cells were washed once with PBS. 1x10⁷ cells were resuspended in 100 µl PBS and aliquoted. 6-7 week old athymic nude Fox mice (Harlan) were anesthetized with 2.5% isofluran using a XGI-8 Gas Anesthesia System (Caliper Life Sciences). Tumor cells were gently vortex before they were injected subcutaneously into the right flank using a 23G cannula. During the procedure mice were kept on a heating plate.

2.4.3 Administration of vector particles

Concentrated and purified lentiviral and AAV vectors were diluted in PBS to the anticipated vector concentration. Vector suspensions were administered by intravenously injection using a 30G cannula.

2.4.4 *In vivo* imaging

In vivo imaging allows visualization of bioluminescence signals in a non-invasive way. Mice were injected intraperitoneally with 150 mg D-Luciferin/kg body weight (Perkin Elmer) using a 30G cannula. After 5 minutes, mice were anesthetized with 2.5% isofloran using a XGI-8 Gas Anesthesia System (Caliper Life Sciences). Then, mice were transferred to the IVIS® Imaging System 200 (Caliper Life Sciences) and imaging signals were analyzed 9 minutes after substrate injection. Analysis of the data was performed using the Living Image 4.2 software (Caliper Life Sciences).

3. RESULTS

This thesis describes in its first part the side by side comparison of Her2/neu-targeted lentiviral and AAV vectors. Quantification of genomic, physical and functional titers of Her2-LV and Her2-AAV revealed that approximately 10-fold more functional particles than genomes are present in the analyzed Her2-AAV vector stocks which was also confirmed *in vitro* and in a xenograft tumor mouse model.

Making use of the lentiviral vector's capability to integrate into the host cell genome, the second part of this thesis describes an approach for targeted gene transfer into human hematopoietic stem cells. Once surface expression of CD105 on HSCs was confirmed, transduction of CD34⁺ cells using the CD105-targeted LV was investigated. Transduced cells showed long-term stable gene expression and superior engraftment potential in NSG mice compared to VSVG-LV transduced cells. Thereby, CD105 was confirmed to serve as phenotypic marker on early HSCs.

3.1 Side by side comparison of receptor targeted lentiviral and AAV vector stocks

Gene delivery by receptor targeted viral vectors restricts gene transfer to specific cell populations. For gene delivery into Her2/neu positive cells, receptor targeted AAV and lentiviral vectors were generated and well characterized (Münch et al., 2011; Münch et al., 2013). Both vectors display the DARPin 9.29, directed against the tumor antigen Her2/neu. Her2/neu is a type 1 receptor tyrosine kinase belonging to the epidermal growth factor family and is over-expressed on various cancer cells such as pancreatic, ovarian and breast cancer cells (Slamon et al., 1987; Slamon et al., 1989; Hall et al., 1990). Since both vectors mediate gene transfer via the same targeting ligand, in particular the DARPin 9.29, Her2-LV and Her2-AAV were compared side by side in regard to titers, transduction efficiencies and biodistribution *in vivo*.

3.1.1 Quantification of titers of lentiviral and AAV vector stocks

First, genomic, physical and functional titers of Her2-LV and Her-AAV were quantified.

3.1.1.1 Genomic titers

To quantify genome copies within vector stocks a suitable quantitative real-time PCR (qPCR) method was established. Sequences within the transgenes, *egfp* or *luciferase (luc)*, were selected as amplification target. This allows determination of genomic titers of LV and AAV vector stocks within one single qPCR run, avoiding run-to-run variabilities. Absolute quantification by qPCR requires internal standards. For determination of AAV vector titers, the DNA standard was generated by serial dilution of the transfer plasmid (Münch et al., 2013) as described previously (Rohr et al., 2002). Genomic titers of LVs were quantified by use of a RNA standard that was generated by *in vitro* transcription and reverse transcribed in parallel with the lentiviral RNA.

3.1.1.1.1 Establishing the qPCR

For quantification of genomic titers of LVs by qPCR, a RNA standard was generated by *in vitro* transcription. As target sequence for amplification by qPCR, sequences within the transgene (*egfp* or *luc*) were chosen since these are present in both Her2-LV and Her2-AAV vectors. By cloning of the adequate DNA fragment from either pSEW (*egfp*) or pS-luc-W (*luc*) into the pGEM-T easy plasmid (Promega), a T7 promoter was introduced upstream of the target sequence that was then used for the generation of the RNA standard by *in vitro* transcription using the MAXIscript Kit (Invitrogen) according to manufacturer's instructions. In a first approach, the generated RNA was purified by DNase I digest only, followed by two rounds of sodium acetate/ethanol precipitation. In the next approach, two rounds of phenol-chloroform and one additional chloroform extraction were included after the DNase I digest. The purity of RNA was confirmed by agarose gel electrophoresis (Figure 4A). The concentration of the RNA standard was adjusted to 10^{11} RNA molecules/ μl . Serial 10-fold dilutions of the RNA standard were applied to reverse transcription

using specific primers. As a control, RNA from each dilution step was applied to the reaction missing the reverse transcriptase (-RT). Afterwards, cDNA of the RNA standard samples +/- RT were amplified by qPCR using SYBR green (Figure 4B).

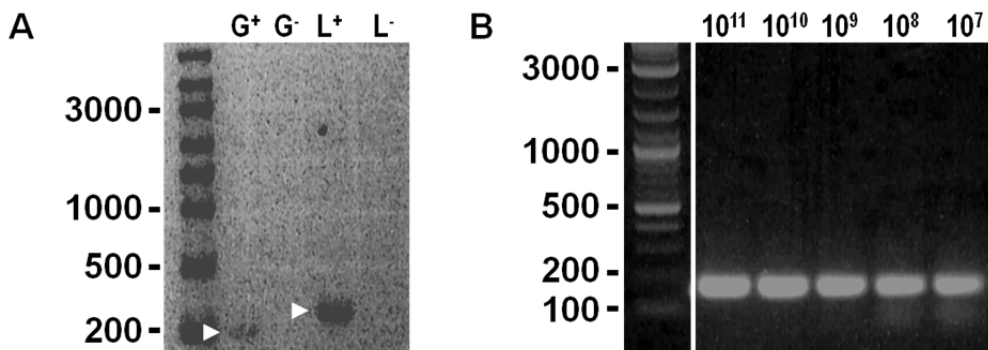


Figure 4: RNA standard for quantification of genomic lentiviral titers generated by *in vitro* transcription. (A) RNA standards after purification on glyoxal-agarose gel. (B) Agarose gel of PCR products of reverse transcribed *luc* RNA standard. G⁺, GFP RNA standard; L⁺, *luc* RNA standard; G⁻, L⁻, RNA standard negative controls: no enzyme present in *in vitro* transcription reaction.

cDNA from 10⁷ to 10¹¹ reverse transcribed RNA molecules showed fluorescence signals in a linear range, whereas less than 10⁷ RNA molecules, which is equivalent to approximately 1pg RNA, led to amplification of unspecific sequences (Figure 5). In addition, only serial 10-fold dilutions from 10¹¹ to 10⁷ molecules led to differences between two crossing points that were close by the theoretically expected difference of 3.32, assuming the efficiency of the qPCR is 100%. Furthermore, -RT-samples showed differences to the crossing points of their corresponding +RT-sample from 15 to 19 cycles, when the RNA standard was phenol-chloroform extracted after *in vitro* transcription (Figure 5). This correlates to a negligible residual DNA contamination of 10^{4.5} to 10⁶ DNA molecules, originating from the preparation of the RNA standard. In contrast, without additional phenol-chloroform extraction the differences between +RT and -RT-samples were only about 5 to 11 cycles. Therefore, the linear range from 10¹¹ to 10⁷ RNA molecules allowed reliable quantification for LV RNA using the phenol-chloroform extracted RNA standard.

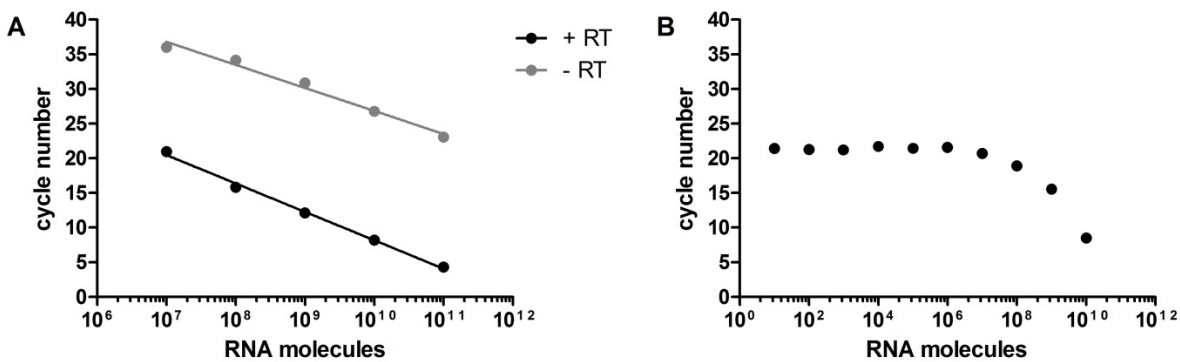


Figure 5: Quantitative real-time PCR of RNA standard. RNA standard was generated by *in vitro* transcription. A serial dilution of the RNA standard molecules was reverse transcribed and analyzed by qPCR. (A) RNA standard which was additionally purified by phenol-chloroform extraction. Reverse transcription took place in the presence (black) or absence (grey) of the reverse transcriptase. (B) RNA standard generated without phenol-chloroform extraction.

3.1.1.1.2 Quantification of genomic titers of by qPCR

Quantification of vector genome copies (gc) within a vector stock does not require transduction of cells, but is assessed by qPCR. cDNA, that was reverse transcribed from LV RNA, as well as DNA, isolated from AAV stocks, were applied to qPCR. As amplification sequence, a sequence which is identical in both vector types is required. Therefore, sequences within the transgene, namely *egfp* or *luc*, were chosen. Using a RNA standard and DNA standard as described in chapter 3.1.1.1 allowed absolute quantification of genomic titers of LV and AAV vector stocks in parallel (Figure 6).

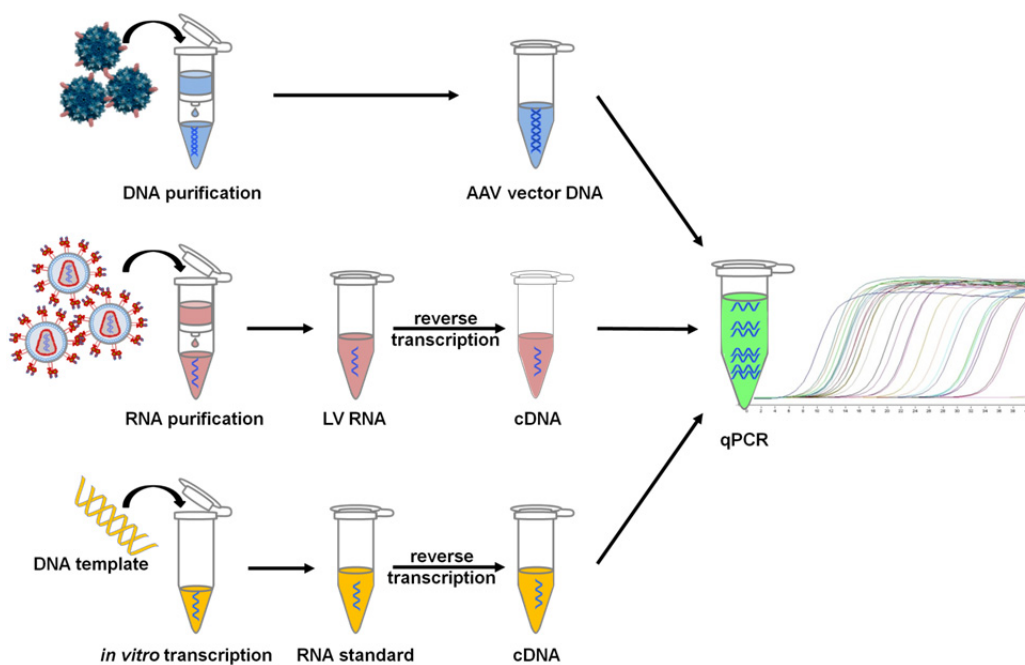


Figure 6: Schematic procedure of quantification of genomic titers. DNA was isolated from AAV, RNA from LV vector stocks. While the standard for the quantification of AAV titers was generated by serial 10-fold dilution of the transfer plasmid, the RNA standard was generated by *in vitro* transcription. The *in vitro* transcribed RNA fragments were reverse transcribed into cDNA in parallel to the isolated RNA from LV stocks. Purified AAV DNA as well as cDNA from LV RNA and the RNA standard were applied to qPCR. Genomic titers of lentiviral and AAV vector stocks were determined by comparison with the respective standards.

On average, Her2-AAV^{GFP} stocks contained 1.46×10^{11} gc/ml ($\pm 8.6 \times 10^{10}$ gc/ml; N=4), whereas genomic titers of Her2-LV^{GFP} stocks were about 10-fold higher showing on average 1.35×10^{12} gc/ml ($\pm 1 \times 10^{12}$ gc/ml; N=3) assuming that each lentiviral particle contains two RNA genome copies. The same 10-fold difference was detected in vector stocks encoding luciferase with 2.25×10^{11} gc/ml ($\pm 3 \times 10^{10}$; N=2) in Her2-AAV^{luc} stocks and 2.2×10^{12} gc/ml ($\pm 2 \times 10^{12}$; N=4) in Her2-LV^{luc} stocks.

Table 6: Genomic titers of Her2-LV or Her2-AAV vector stocks

	Her2-LV ^{GFP} [gc/ml]	Her2-AAV ^{GFP} [gc/ml]	Her2-LV ^{luc} [gc/ml]	Her2-AAV ^{luc} [gc/ml]
vector stock 1	7.3×10^{11}	5.9×10^{10}	2.8×10^{10}	2.5×10^8
vector stock 2	8.1×10^{11}	1.7×10^{11}	1.6×10^{12}	2.0×10^8
vector stock 3	2.5×10^{12}	2.5×10^{11}	2.5×10^{12}	
vector stock 4	7.3×10^{11}	1.0×10^{11}	4.7×10^{12}	

3.1.1.2 Quantification of physical titers

Physical titers define the amount of physically intact particles within a vector stock. Physical titers include functional and non-functional or empty particles without transgene. LV particles were assessed by p24 ELISA which determines the amount of p24 protein per vector stock. Assuming that approximately 2000 p24 proteins are contained within one LV particle (Wilk et al., 2001), the number of particles within a vector stock was calculated. Particles in AAV vector stocks were assessed by capsid ELISA. Comparison with a standard vector with known particle concentration allowed calculation of particle numbers. On average, Her2-LV^{GFP} vector stocks contained 7.0×10^{12} particles/ml ($\pm 6 \times 10^{12}$; N=3), accounting for approximately 10-fold more particles than Her2-AAV^{GFP} vector stocks which comprise 7.8×10^{11} particles/ml ($\pm 6.9 \times 10^{11}$; N=4). No significant difference was observed between GFP or luciferase transgene containing particles (p=0.1932 (LV), p=0.8752 (AAV)). 2.4×10^{12} particles/ml ($\pm 2 \times 10^{12}$; N=4) were detected in Her2-LV^{luc} and 8.8×10^{11} ($\pm 5 \times 10^{11}$; N=2) within Her2-AAV^{luc} vector stocks.

Table 7: Physical titers of Her2-LV and Her2-AAV vector stocks

	Her2-LV ^{GFP} [particles/ml]	Her2-AAV ^{GFP} [particles/ml]	Her2-LV ^{luc} particles/ml]	Her2-AAV ^{luc} [particles/ml]
vector stock 1	3.7×10^{12}	5.3×10^{11}	7.6×10^{11}	1.2×10^{12}
vector stock 2	3.5×10^{12}	2.8×10^{11}	2.6×10^{12}	5.2×10^{11}
vector stock 3	1.4×10^{13}	5.1×10^{11}	4.9×10^{12}	
vector stock 4		1.8×10^{12}	1.4×10^{12}	

3.1.1.3 Quantification of functional titers

Genomic and physical titers include functional and non-functional vector particles. Vector particles encoding fluorescent transgenes allow the determination of functional titers by assessing the fluorescence of transduced cells. 10 to 0.01 µl of concentrated Her2-LV^{GFP} and Her2-AAV^{GFP} vector stocks were added to Her2-positive SK-OV-3 cells. This cell line was selected since it was previously shown to be susceptible to Her2-LV and Her2-AAV *in vitro* as well as *in vivo* (Münch et al.,

2011; Münch et al., 2013) and also to form subcutaneous tumors in nude mice (Goyeneche et al., 2007). Four days post transduction, GFP expression was determined by flow cytometry. On average, the functional titer of Her2-LV^{GFP} was 7.8×10^6 tu/ml (N=3). Her2-AAV^{GFP} stocks contained approximately 2.5 more functional particles resulting in 2×10^7 tu/ml (N=4). As expected, the mean fluorescence intensity for cells transduced with AAV was in general lower than for LV transduced cells (see also Figure 8).

Table 8: Functional titers of Her2-LV and Her2-AAV vector stocks

	Her2-LV ^{GFP} [tu/ml]	Her2-AAV ^{GFP} [tu/ml]
vector stock 1	4.8×10^6	2.3×10^7
vector stock 2	4.7×10^6	3.5×10^7
vector stock 3	1.4×10^7	9.8×10^6
vector stock 4		1.3×10^7

3.1.1.4 Comparison of functional, genomic and physical titers

Having quantified genomic, physical and functional titers of Her2-targeted LV and AAV vector stocks, these titers were compared. This revealed that physical titers of both vector types are higher than functional and genomic titers. Between 2- and 20-fold more AAV capsids than genomes were detected indicating the presence of 50 to 95% empty particles in the individual vector preparations. LV vector stocks contained approximately 5-fold more physical particles than genomes. Genomic and physical titers were about 10-fold higher in LV vector stocks, compared to AAV vector stocks. In contrast, the number of tu/ml was increased in AAV vectors approximately 2.5-fold (Figure 7 A). Therefore, AAV vector stocks that were analyzed here, consist of about 10,000-fold more genomes than transducing units, whereas this excess of non-functional particles in LV vector stocks was even more than 100,000-fold (Figure 7 B).

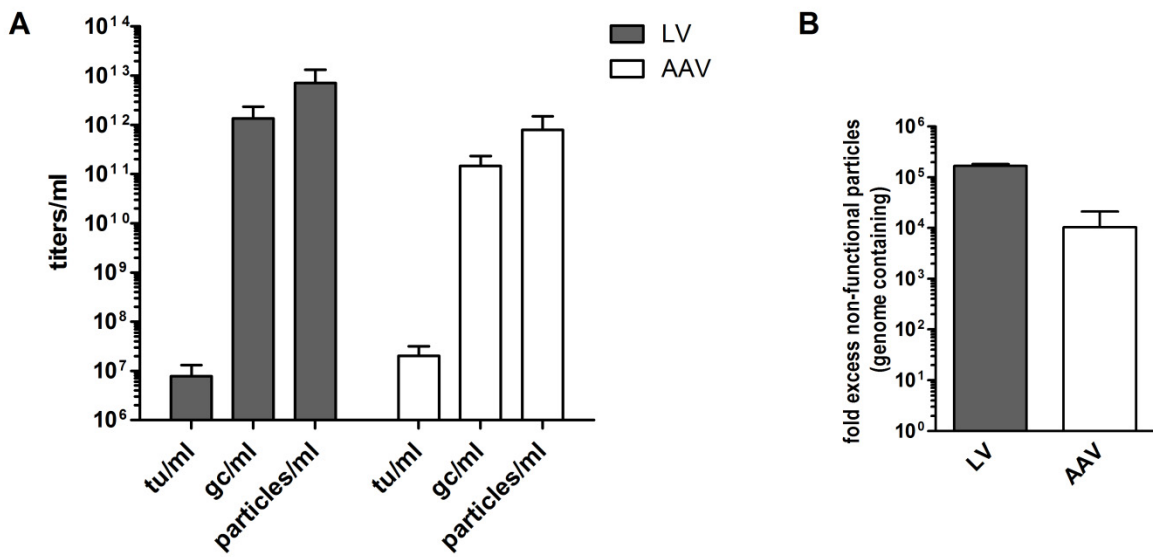


Figure 7: Comparison of functional, genomic and physical titers of Her2-LV^{GFP} and Her2-AAV^{GFP}. Functional titers were determined by transduction of SK-OV-3 cells with Her2-LV^{GFP} or Her2-AAV^{GFP} and subsequent analysis of GFP expressing cells by flow cytometry. Genomic titers were assessed by qPCR of reverse transcribed LV RNA and AAV DNA. Particle numbers per ml were measured by either p24-ELISA or capsid ELISA. (A) Titers of Her2-LV^{GFP} (N=3) and Her2-AAV^{GFP} (N=4) vector stocks. (B) The fold excess of non-functional, but genomes within Her2-LV^{GFP} and Her2-AAV^{GFP} vector stocks. LV N=3; AAV N=4; mean±SD.

3.1.2 Transduction of Her2⁺ SK-OV-3 cells with Her2-AAV^{GFP} and Her2-LV^{GFP} *in vitro*

After quantification of genomic and functional titers, transduction efficiencies of Her2-LV and Her2-AAV were compared *in vitro*. SK-OV-3 cells were transduced with either Her2-AAV^{GFP} or Her2-LV^{GFP} at identical multiplicity of infection (MOI) or genomic particles per cell (GOI). Ninety-six hours post transduction the expression levels of GFP were determined by flow cytometry. Transduction of cells by Her2-AAV^{GFP} at a MOI of 1 resulted in 7.3% ($\pm 1.5\%$; N=3) GFP⁺ cells. In contrast, a transduction efficiency of 6.9% (± 0.04 ; N=2) was achieved by transduction of SK-OV-3 cells with Her2-LV^{GFP} at a MOI of 0.1 (Figure 9). As described in chapter 3.1.1.3, the mean fluorescence intensity of AAV^{GFP} vector transduced cells was lower than that of LV^{GFP} transduced cells (Figure 8).

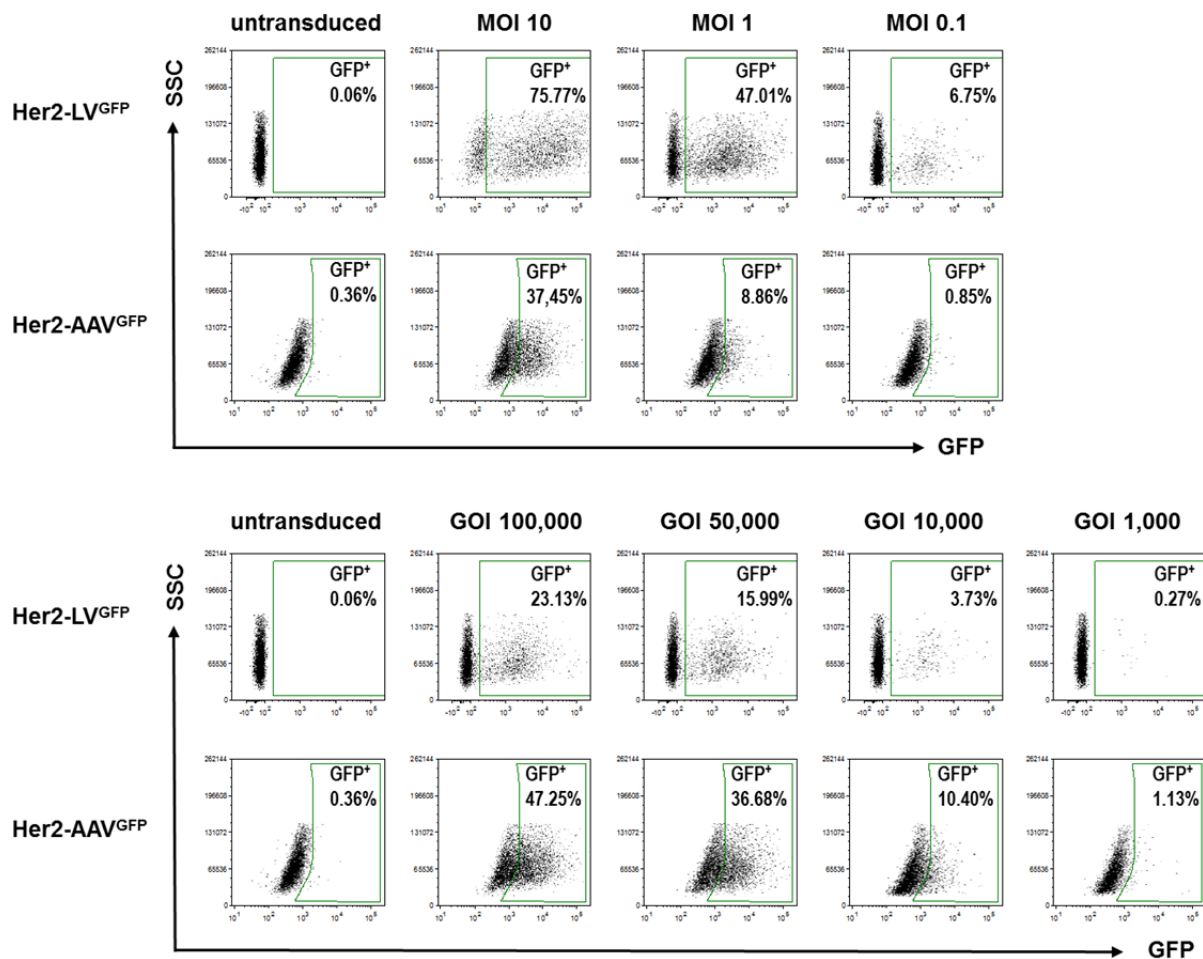


Figure 8: Representative flow cytometry plots of SK-OV-3 cells transduced with Her2-LV^{GFP} or Her2-AAV^{GFP}. SK-OV-3 cells were transduced at matching MOI (A) or GOI (B). Ninety-six hours post transduction; GFP expression was determined by flow cytometry. As it can be seen in the untransduced cells, the GFP signal intensity for cells transduced with Her2-AAV^{GFP} was amplified by applying higher voltage compared to cells transduced with Her2-LV^{GFP}.

On average, AAV vector stocks contained about 10-fold more functional particles within the same amount of genome copies than LV stocks (Figure 7). Therefore, normalizing both vector types to the same genome copies led to higher transduction efficiency in cells transduced with Her2-AAV^{GFP}. Comparing transduction efficiencies of MOI and GOI values, it can be concluded that a MOI of 1 corresponds to 5,000 GOI of Her2-AAV^{GFP}. On the contrary, transduction of SK-OV-3 cells by Her2-LV^{GFP} at a MOI of 1 correlates to 150,000 GOI (Figure 9). These data demonstrate that approximately 3 times more genome copies of Her2-LV are required to match the number of GFP expressing cells obtained with Her2-AAV. Considering this fact, the theoretical amount of functional particles within the number of genome copies used for transduction by either Her2-LV^{GFP} or Her2-AAV^{GFP} was determined. This

calculation confirmed that about 10-fold more transducing AAV than functional LV particles are required to obtain comparable transduction efficiencies.

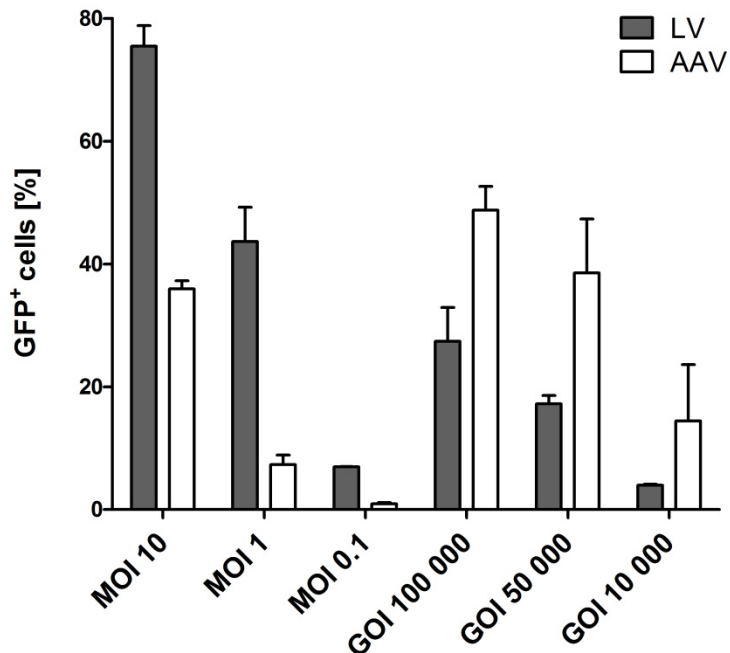


Figure 9: Transduction of SK-OV-3 cells by either Her2-LV^{GFP} or Her2-AAV^{GFP}. SK-OV-3 cells were transduced by Her2-LV^{GFP} or Her2-AAV^{GFP} at different MOI or GOI. Four days post transduction the cells were analyzed by flow cytometry for GFP expression. LV N=2; AAV N=3; mean±SD.

3.1.3 Biodistribution of Her2-LV and Her2-AAV in a subcutaneous tumor mouse model

3.1.3.1 Particle distribution at early time points after vector administration

Having analyzed the transduction efficiencies of Her2-LV and Her2-AAV *in vitro*, the particle distribution at early time points after vector administration, when no transgene expression has occurred yet, was studied *in vivo*. Athymic nude mice were injected with the same gc number (2×10^{10}) per mouse for both vector types, one additional group was implemented receiving 2×10^{11} gc Her2-LV^{luc} (high vector dose). For analysis of the distribution of the vector particles, blood and urine were collected and organs (spleen, liver, lung, heart, kidneys) and tumors were isolated 4, 10 and 24 hours after intravenous vector administration. The distribution of Her2-LV^{luc} in mice within the high vector dose group was analyzed after 4 hours. Total RNA was

isolated from the homogenized organs of LV injected mice using the RNeasy Mini Kit (Qiagen), whereas DNA was isolated using the 96-DNeasy blood and tissue Kit (Qiagen) from tissue of AAV injected mice. RNA was transcribed into cDNA. By qPCR, LV and AAV genomes within the isolated DNA and cDNA were quantified by the use of RNA and DNA standards. In contrast to the determination of AAV and LV titers, quantification of vector genomes from organs was performed by using a luciferase specific, FAM labeled primer/probe set. Since considerable less luciferase DNA was detectable within the organs compared to pure vector stocks, the use of SYBR green resulted in unspecific fluorescence signals as confirmed by melting curve analysis (data not shown). Using the TaqMan-probe-based assay, no false positive signals were measurable.

In tissue isolated from LV injected mice, the highest genome copy number was found in lung at all analyzed time points. In lung and tumor the detectable gc numbers slightly increased after 8 hours, compared to the 4 hour time point, but dropped again after 24 hours. Twenty-four hours post vector administration, the signals in spleen increased, but the gc detectable in heart, kidney and liver decreased below detection limit in the three organs and tumor tissue. Comparable signals were found in tumor and spleen, however, signals in lung were even increased compared to tumor signals. Nevertheless, the differences between the three time points as well as between the various organs remained not significant ($p>0.05$) comparing mice injected with the same gc numbers. No LV gc were detectable in blood and urine at all analyzed time points. When, 10 times more LV gc were injected, signals were approximately 25-fold higher in lung and even 30-fold higher in tumor tissue than in mice injected with 2×10^{10} gc (Figure 10).

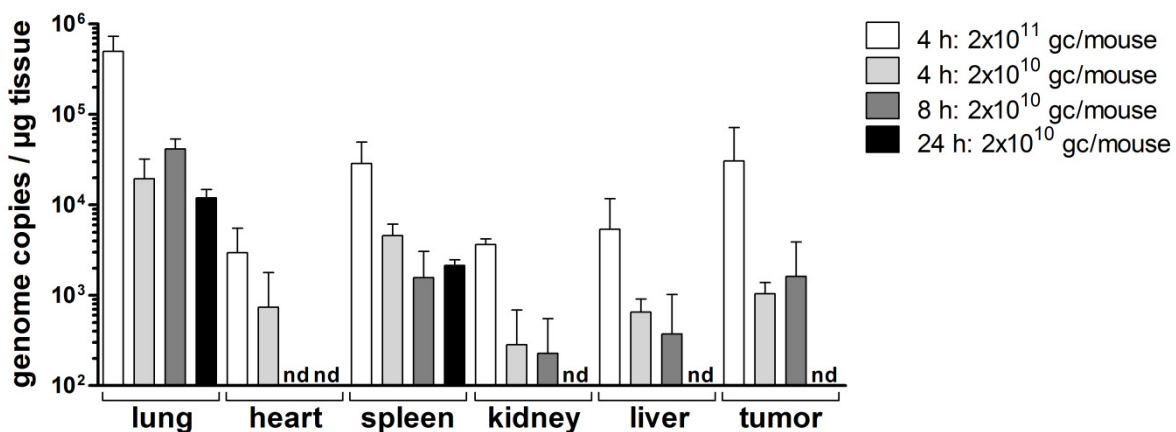


Figure 10: Biodistribution of vector particles after systemic administration of Her2-LV. Mice transplanted with subcutaneous SK-OV-3 tumors were injected with either 2×10^{10} or 2×10^{11} genome copies of Her2-LV^{luc}. After 4, 8 and 24 hours, the mice were sacrificed and blood and urine collected and the indicated organs isolated. The LV genome copies within the organs were determined by qPCR using a luciferase-specific primer/probe set. Absolute genomic copies per μg tissue are shown. No LV genomes were detectable within blood or urine. N=3; mean \pm SD. Nd, not detectable.

In mice injected with Her2-AAV^{luc} significantly more vector genome copies were detected in spleen than in the other organs. The signals obtained for different time points did not significantly differ within the organs except for significant lower gc numbers within spleens 24 hours after vector administration ($p<0.05$). In addition, less vector DNA was recovered in liver 24 hours post vector administration, indicating de-targeting of the natural liver tropism of AAV-2 wild type. While signals from AAV injected mice were mostly comparable with signals from LV injected mice in lung, signals from AAV injected mice were 20-300-fold increased in spleen, kidney or liver. Within tumor tissue approximately 20-fold more AAV DNA was found compared to LV RNA (Figure 10; Figure 11).

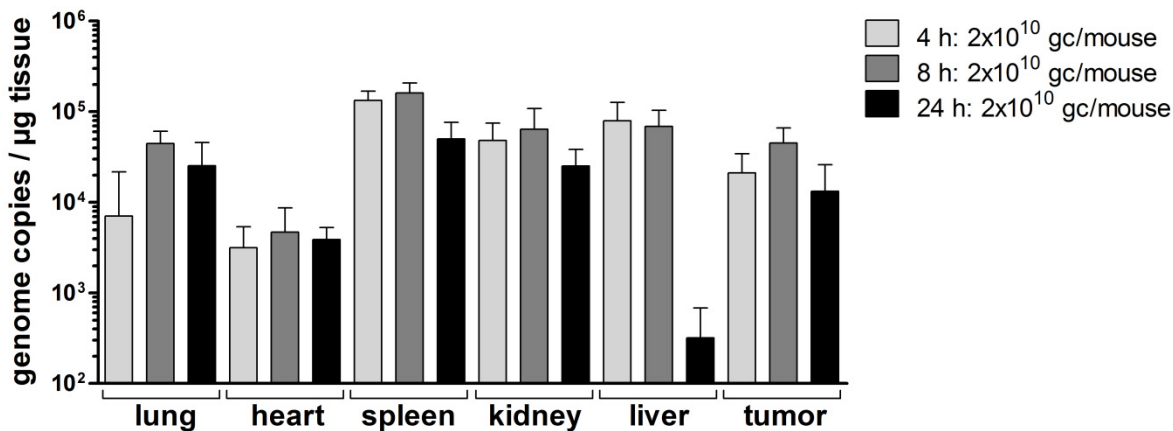


Figure 11: Biodistribution of vector particles after systemic administration of Her2-AAV. Mice transplanted with subcutaneous SK-OV-3 tumors were injected with 2×10^{10} genome copies of Her2-AAV^{luc}. After 4, 8 and 24 hours the mice were sacrificed and blood and urine collected and the indicated organs isolated. The LV genome copies within the organs were determined by qPCR using a luciferase-specific primer probe set. Absolute genome copies per μg tissue are shown. No AAV genomes were detectable within urine. N=3; mean \pm SD.

3.1.3.2 Monitoring the biodistribution of Her2-LV and Her2-AAV by *in vivo* imaging

After investigating the distribution of Her2-LV and Her2-AAV at early time points after vector administration, the transgene expression in mice was analyzed over the period of 12 days by *in vivo* imaging. 2×10^{10} or 2×10^{11} gc Her2-LV^{luc} and 2×10^{10} gc Her2-AAV^{luc} were injected systemically into nude mice bearing subcutaneous SK-OV-3 tumors. Luciferase expression in animals was monitored from day 3 to day 12. On day 12, the strongest luciferase signals were detectable in tumor tissue of two of the three mice that were injected with the high genome copy number (2×10^{11}) of LV. Both mice showed some off-target signals in the spleens. In the third mouse of this group, the luciferase signals were weaker compared to the rest of the mice and therefore they are not visible in Figure 12. Nevertheless, tumor signals in this mouse were measurable from day 3 to day 12 and spleen signals starting from day 6. One mouse showed a dominant signal with the highest signal intensity on the right side of the chest (Figure 12; blue arrow) which was present starting day 6. The source of the strong signal could not be identified, since none of the isolated organs or inner skin parts showed signals after sacrificing the mouse. No tumor cells were detectable at this part of the body. By *in vivo* imaging no luciferase signals were detectable in mice that had received the low genome copy number (2×10^{10}) Her2-LV, which is

comparable to the injected AAV genome copy number. Mice injected with Her2-AAV^{luc} showed tumor specific luciferase expression and in one animal some off-targeting effects in the chest region (Figure 12).

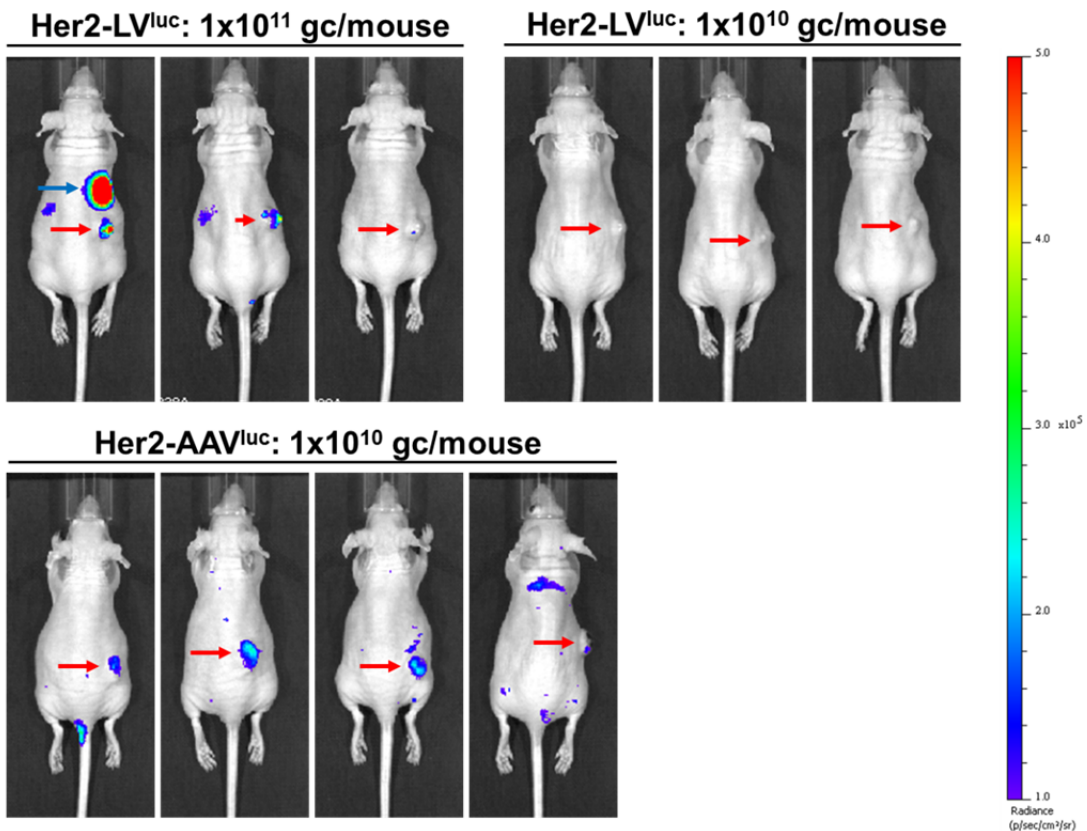


Figure 12: *In vivo* imaging of SK-OV-3 tumor bearing nude mice. SK-OV-3 cells were transplanted subcutaneously into athymic nude mice (red arrows). After tumor vascularization, 2×10^{10} or 2×10^{11} genome copies of Her2-LV^{luc} or 2×10^{10} genome copies of Her2-AAV^{luc} were administered systemically. Twelve days after vector injection, luciferase expression in mice was analyzed by *in vivo* imaging. The luciferase signal intensity is expressed as photons/second/square centimeter/steradian ($\text{p/sec/cm}^2/\text{sr}$). Blue arrow points out the unidentified signal.

Immediately after *in vivo* imaging, mice were sacrificed and luciferase signals in the isolated tumors and organs measured. Imaging of the organs confirmed results from *in vivo* imaging. Strongest luciferase expression was detected in tumors of mice injected with high genome copy number of LV, followed by signals from tumors from AAV injected mice. Increasing the sensitivity for luciferase signals revealed that also in the spleens of mice injected with the low LV dose luciferase was expressed, but to a lower extent than in mice that received the high LV dose. However, in these mice no tumor signals were detectable (Figure 13). Although, in AAV injected mice some off-targeting effects in the chest region were visible during *in vivo* imaging, hardly any

luciferase signals in heart or lung were measurable. In addition, the highest luciferase expression was detected in Her2-positive tumor tissue in mice injected with either AAV or the high LV dose. Based on the luciferase expression in athymic nude mice *in vivo*, these results suggest that AAV is more efficient in transduction compared to LV, when the same amount of genome copies for both vector types is injected per mouse.

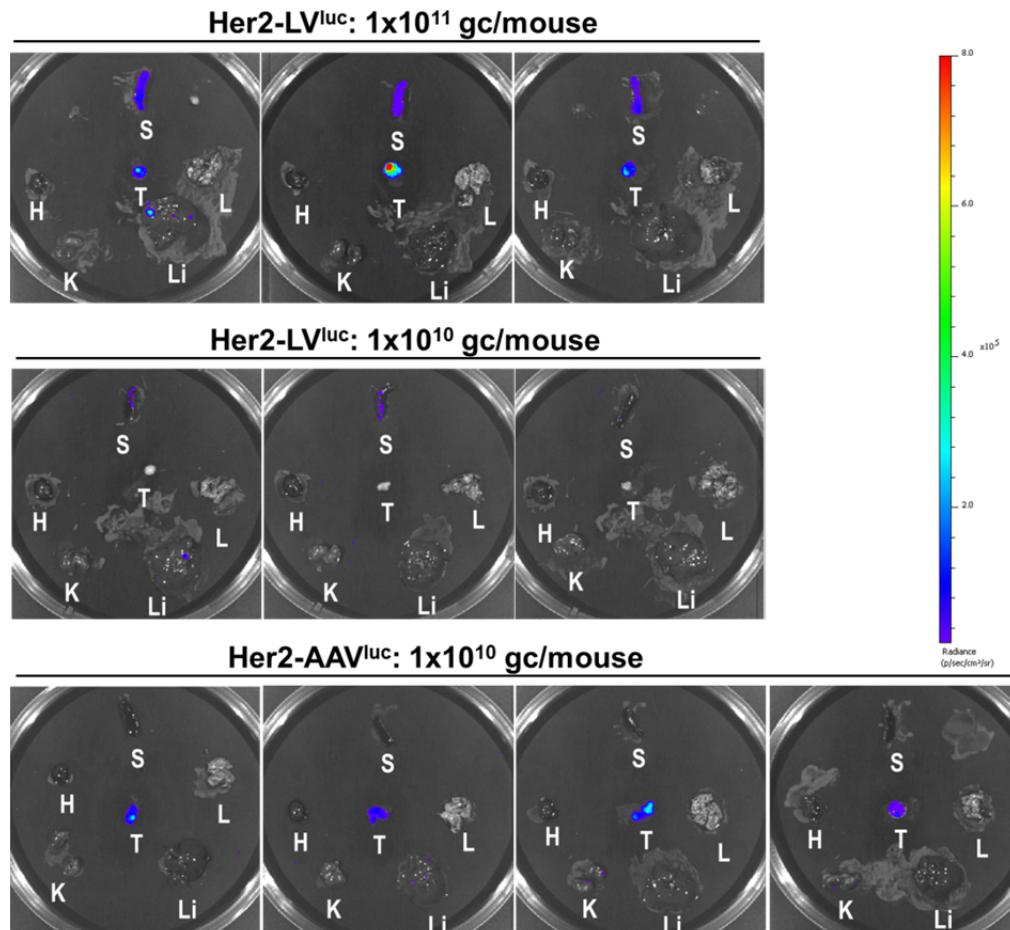


Figure 13: Imaging of organs from SK-OV-3 tumor bearing nude mice. SK-OV-3 cells were transplanted subcutaneously into athymic nude mice. After tumor vascularization, 2×10^{10} or 2×10^{11} genome copies of Her2-LV^{luc} or 2×10^{10} genome copies of Her2-AAV^{luc} were administered systemically. Twelve days after vector injection, luciferase expression in mice was determined by *in vivo* imaging. Afterwards, the luciferase signal in isolated tissues was analyzed. The luciferase signal intensity is expressed as photons/second/square centimeter/steradian ($\text{p/sec}/\text{cm}^2/\text{sr}$). Organs are identified by the capital letter below the tissue. T, tumor; H, heart; S, spleen; L, lung; Li, liver; K, kidney.

3.1.4 Serum stability

To assess, how much the biodistribution of LV or AAV was influenced by sensitivity towards serum, the stability of both vector types was tested. For this purpose, serum from several athymic nude-Foxn1^{nu} mice that had been used for the biodistribution

experiments was collected and pooled. These mice are T-cell deficient but are normal in B-cell function (Harlan Laboratories). The serum was pre-incubated with either Her2-LV^{GFP} or Her2-AAV^{GFP} in cell culture medium in different concentrations at 37°C for 30 min. Then, the serum-vector mixture was added to SK-OV-3 cells. Transduction efficiency was determined by flow cytometry 96 hours later and normalized to the transduction efficiency of vector without serum addition. Furthermore, part of the serum was heat-inactivated prior to incubation with the vectors. Transduction efficiency was reduced to 70-80% by addition of 2.5% serum to the medium for both vector types. Increasing concentrations of serum reduced the transduction efficiencies to approximately 60% for LV as well as for AAV transduced cells. Nevertheless, this reduction was not significant. In addition, no significant difference between both vector types was observed (Figure 14). Heat-inactivation of serum showed comparable results to transduction of cells as in the presence of not heat-inactivated serum (data not shown). However, addition of more than 5% serum to the medium had a negative effect onto the growth of the cells which might affect the transduction of cells. These results demonstrate that the biodistribution of either LV or AAV particles is not significantly influenced by neutralization within the used mouse model.

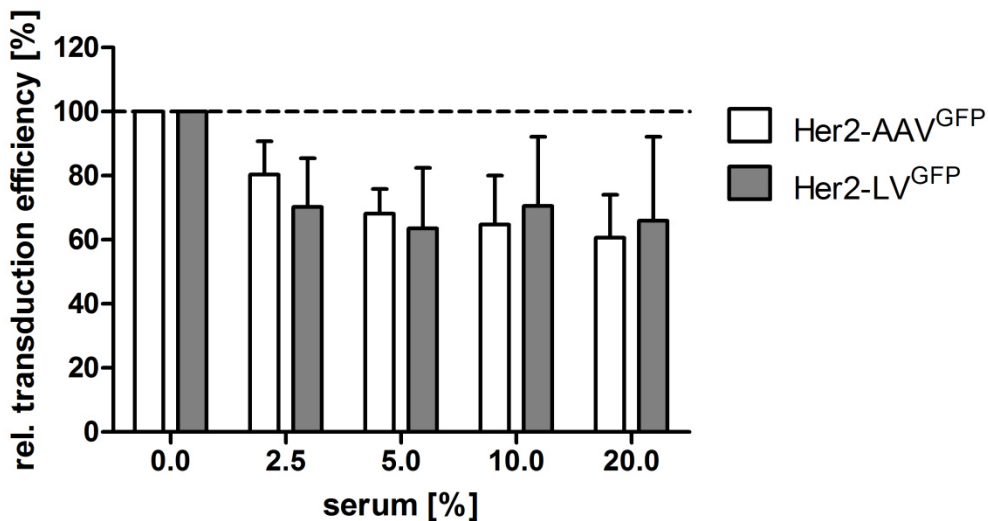


Figure 14: Transduction efficiency of either LV or AAV is not significantly impaired by serum of athymic nude mice. Her2-LV^{GFP} or Her2-AAV^{GFP} were incubated with the indicated concentrations of mouse serum at 37°C for 30 min. Afterwards, the mixtures were added to SK-OV-3. Ninety-six hours later, the number of GFP-positive cells was determined by flow cytometry and transduction efficiencies were calculated in relation to cells transduced in the absence of serum. N=2; mean±SD.

3.2 Targeted gene transfer into human hematopoietic stem cells

Having demonstrated different aspects of targeted gene transfer by lentiviral and AAV vectors the focus of the second part of this thesis is on the selective and stable gene transfer into HSCs by LVs.

Genetic modification of HSCs is commonly achieved by using VSVG-pseudotyped lentiviral or retroviral vectors. Due to its broad tropism while maintaining a low risk for insertional mutagenesis especially VSVG-LV has shown promising results in several clinical studies (Naldini, 2011; Aiuti et al., 2013; Biffi et al., 2013). Nevertheless, efficient transduction of HSCs with VSVG-LV requires extensive stimulation of the cells and high vector dose whereby several days of *ex vivo* cultivation is necessary. Therefore, we investigated whether targeting a receptor specific for early HSCs may represent an alternative transduction approach.

3.2.1 Expression of CD105 on human HSCs

CD105 is a well-established marker on murine HSCs (Chen et al., 2002; Chen et al., 2003; Roques et al., 2012) and Pierelli et al. report that CD105 is also present on subsets of human HSCs (Pierelli et al., 2000; Pierelli et al., 2001). Therefore, CD105 surface expression on unstimulated and stimulated human HSCs was analyzed since *ex vivo* expansion and gene modification of HSCs often requires stimulation with cytokines, by which the duration of *ex vivo* culture is prolonged and which might facilitate proliferation of different HSC subsets. Human CD34⁺ cells were purified using magnetic beads by positive selection from mobilized peripheral blood. CD105 surface expression on unstimulated cells or cells stimulated overnight with cytokines was analyzed by flow cytometry. Donor dependently, CD105 expression varied between 30 – 80% (mean = 60%) in unstimulated cells. The expression levels further increased to 95% after overnight stimulation with cytokines (Figure 15). In addition, frozen BM CD34⁺ cells (Lonza) as well as CD34⁺ isolated from cord blood showed similar results (data not shown). This demonstrates that the common endothelial marker CD105 is also expressed on human HSCs.

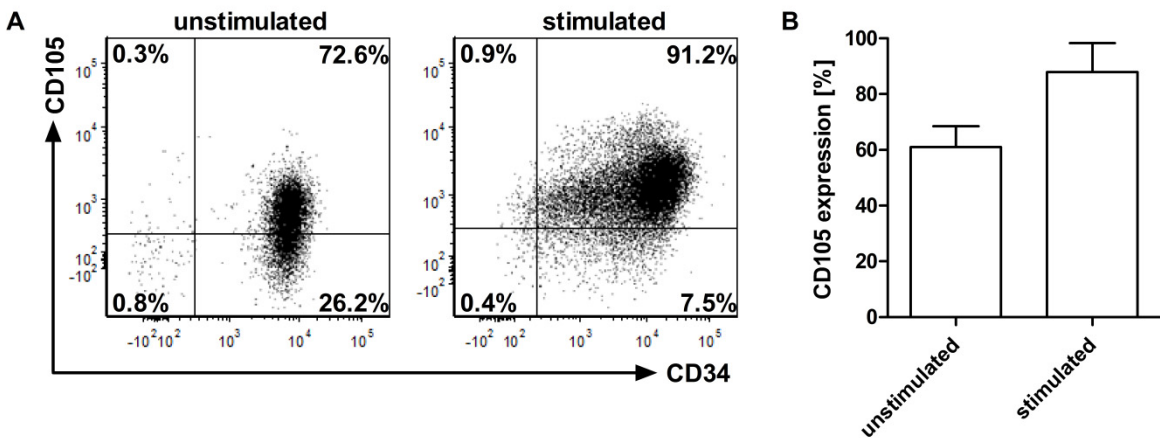


Figure 15: Surface expression of CD105 on human CD34⁺ cells. After purification from G-CSF mobilized peripheral blood using CD34 MACS beads, CD34⁺ cells were analyzed by flow cytometry for their CD105 surface expression either immediately or after stimulation for 24 hours with Flt-3 ligand, stem cell factor, IL-3, IL-6 and TPO. (A) Representative FACS plots of CD34⁺/CD105⁺ cells before and after stimulation. (B) Mean±SD of CD105 expression on CD34⁺ cells from seven individual donors (Kays et al., 2015).

3.2.2 Transduction of HSCs using CD105-LV

3.2.2.1 Transduction of CD34⁺ cells by CD105-LV^{GFP}

In the host laboratory, the CD105-targeted vector CD105-LV has been generated previously and was shown to selectively transduce CD105⁺ endothelial cells in mixed cultures of CD105⁺ and CD105⁻ cells (Anliker et al., 2010). In addition, exclusive gene transfer into CD105-positive liver sinusoidal endothelial cells in mice reconstituted with human liver cells was demonstrated upon systemic administration of CD105-LV (Abel et al., 2013).

Here, the ability of CD105-LV to mediate gene transfer to HSCs was analyzed. CD34⁺ cells were transduced with CD105-LV transferring the marker gene *egfp* (CD105-LV^{GFP}). The vectors were added to the cells either directly after purification from mobilized peripheral blood or after overnight stimulation with cytokines. Seventy-two hours post transduction the expression levels of GFP were determined by flow cytometry. CD105-LV^{GFP} transduced 3 – 5% of unstimulated CD34⁺ cells and up to 20% of stimulated CD34⁺ cells (Figure 16). All of the GFP⁺ cells were also CD105⁺ (Figure 16A) demonstrating specificity of the targeting vector.

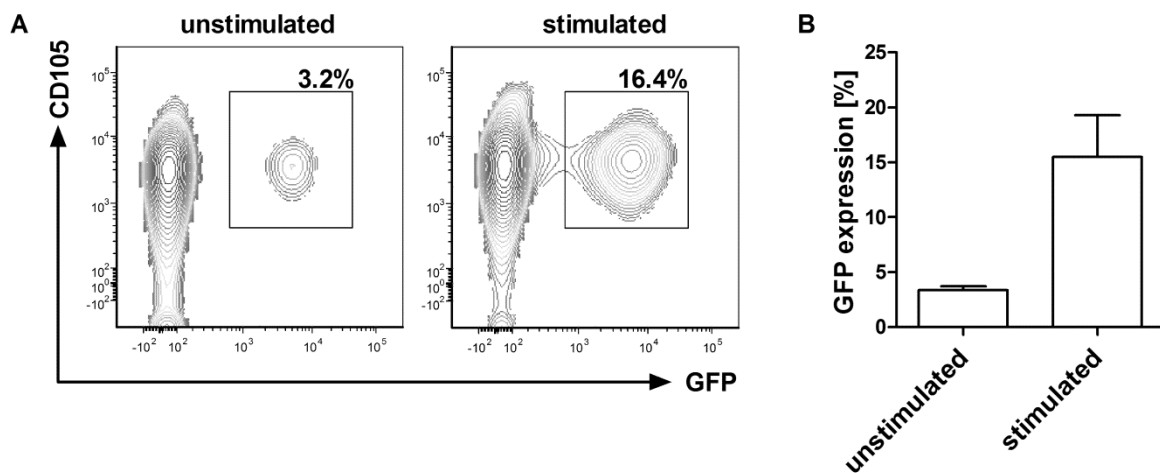


Figure 16: Transduction of unstimulated and stimulated human CD105⁺/CD34⁺ cells by CD105-LV^{GFP}. Unstimulated or stimulated CD34⁺ cells isolated from G-CSF mobilized peripheral blood were transduced by CD105-LV^{GFP} at a multiplicity of infection (MOI) of 1. Seventy-two hours after transduction the cells were analyzed by flow cytometry for expression of GFP and CD105. (A) Representative FACS plots of GFP⁺ cells transduced with or without previous stimulation of cells. (B) Mean±SD of GFP⁺ cells of seven independent experiments (Kays et al., 2015).

To further characterize the transduced cells, the cells were checked for the presence of additional surface markers known to define early HSCs. Approximately 90% of GFP⁺ cells were also positive for the HSC marker CD133 and about 60% for the HSC marker CD90. In addition, the majority (approximately 70%) of transduced cells were CD38⁻ (Figure 17), a surface marker that is present on more committed progenitor cells. These data demonstrate that CD105 is expressed on a more primitive subset of HSCs.

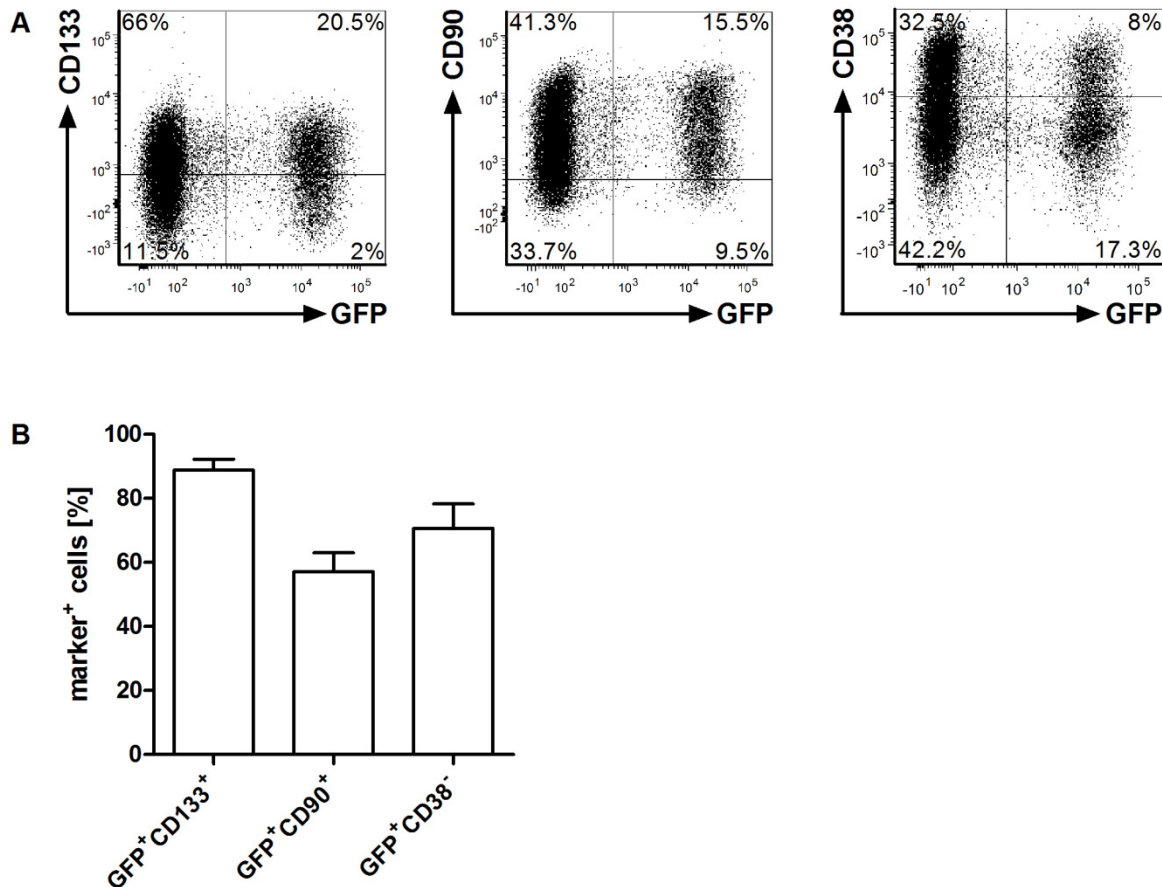


Figure 17: Transduction of stimulated human CD34⁺CD105⁺ cells by CD105-LV^{GFP}. Stimulated CD34⁺ cells isolated from G-CSF mobilized peripheral blood were transduced by CD105-LV^{GFP} at a multiplicity of infection (MOI) of 1. Seventy-two hours after transduction the cells were analyzed by flow cytometry for expression of GFP, CD105 and the surface markers CD133, CD90 and CD38. (A) FACS plots of one representative experiment. (B) Mean values±SD of four biological replicas (Kays et al., 2015).

3.2.2.2 Transduction of CD105 enriched cells by CD105-LV^{GFP}

After confirming that CD105 is expressed on early HSCs it was analyzed if isolation of CD105⁺ cells from mobilized peripheral blood is as effective as purification of CD34⁺ cells.

Enrichment of either CD34⁺ or CD105⁺ cells from mobilized peripheral blood by magnetic activated cell sorting was compared. The CD34⁺ cell population consisted exclusively of cells which showed the typical morphology of HSPCs in subsequent cell culture as determined microscopically. In contrast, the cell population that was only enriched for CD105⁺ was also composed of cells that could morphologically not be assigned to HSPCs (Figure 18). This indicates that CD105 as exclusive marker for

HSC purification from mobilized peripheral blood is not sufficient, but may require additional marker for HSC isolation.

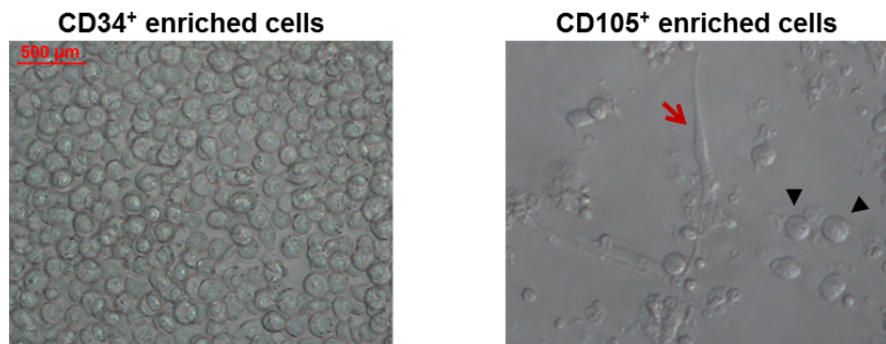


Figure 18: Morphology of CD34⁺ or CD105⁺ purified cells. CD34⁺ or CD105⁺ cells were isolated from mobilized peripheral blood by magnetic activated cell sorting. Black arrow heads designate cells with HSC morphology. Red arrow indicates cell with atypical HSC morphology.

Therefore, enrichment of CD105⁺ cells within the CD34⁺ cell population was investigated. CD34⁺ cells purified from mobilized peripheral blood were either subjected to a second round of purification for CD105 using magnetic activated cell sorting or CD105^{high} expressing cells were isolated from CD34⁺ cells by fluorescence activated cell sorting. Both methods enriched cells with HSPC morphology, however, purification of CD34⁺CD105⁺ cells using the MACS Multisort system led only to marginal enrichment of CD105⁺ cells within the CD34⁺ cell population. In addition, these approaches required binding of anti-CD105 antibodies to the cells. Thereby, subsequent transduction of cells by CD105-LV^{GFP} was inhibited (Figure 19). As a consequence, the approach to further enrich CD105⁺ cells within the CD34⁺ cell population was not followed up further.

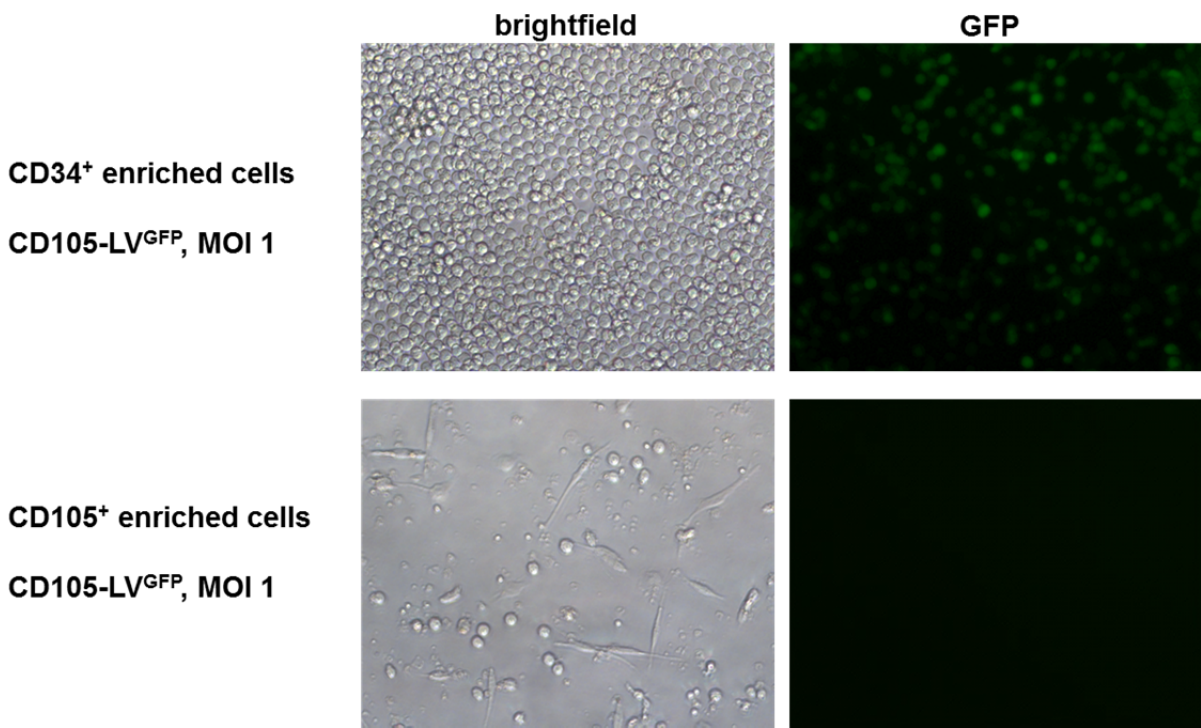


Figure 19: Transduction of either CD34⁺ or CD105⁺ purified cells. CD34⁺ or CD105⁺ cells were isolated from mobilized peripheral blood by magnetic activated cell sorting. Stimulated cells were transduced by CD105-LV^{GFP} at a multiplicity of infection (MOI) of 1. Seventy-two hours after transduction, GFP expression was determined by fluorescence microscopy. 200-fold magnification.

3.2.2.3 Specificity of CD105 dependent transduction

To confirm the specificity of CD105 dependent transduction of CD34⁺ cells we pre-incubated CD105-LV^{GFP} with soluble CD105 protein (sCD105). The extracellular domain of CD105 was fused to an Fc-Tag (plasmid kindly provided by Irene Schneider and Gundula Braun) and expressed in HEK-293T cells. After HPLC purification sCD105 was added in increasing amounts to either CD105-LV^{GFP} or VSVG-LV^{GFP}. In addition, also an Fc tagged control protein (sCD30) was added to CD105-LV^{GFP}. After pre-incubation of vectors and proteins the vector-protein mixture was used for transduction of CD34⁺ cells isolated from mobilized peripheral blood. Pre-incubation of sCD105 with the targeting vector lead to reduced transduction efficiency correlating with the amount of protein used. Incubation with 2 µg of sCD105 resulted in a decrease of transduction of 95%. In contrast, pre-incubation with the control protein sCD30 did not influence the transduction efficiency significantly. Also pre-incubation of sCD105 with VSVG-LV^{GFP} did not reduce the transduction efficiency (Figure 20). Moreover, binding of magnetic or fluorophore labeled anti-CD105 antibodies to CD34-purified cells as described in 3.2.2.2 inhibited

transduction of these cells by CD105-LV^{GFP} (Figure 19). These results clearly demonstrate that binding of CD105-LV to CD105 on the cell surface is necessary for the CD105-LV mediated transduction of CD34⁺ cells.

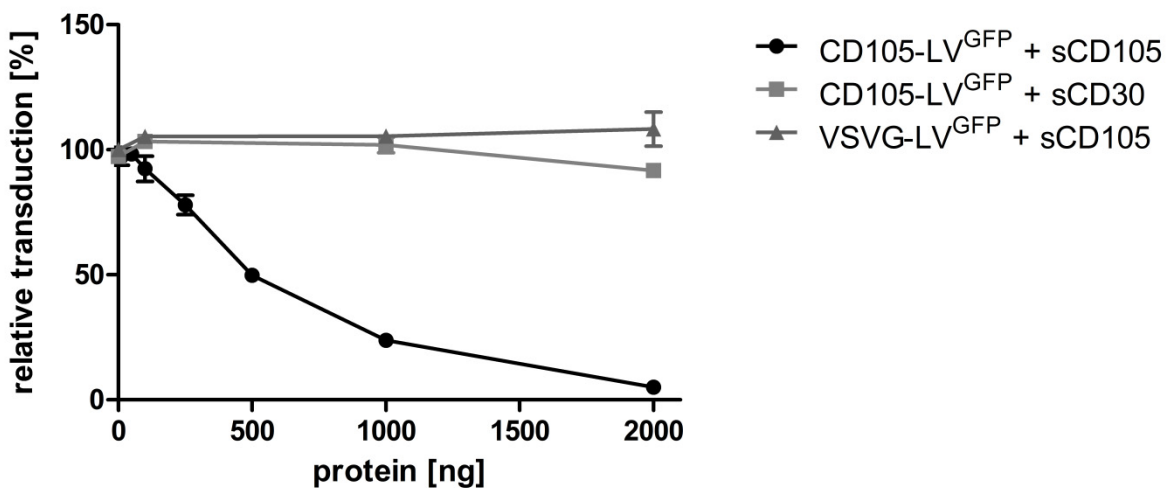


Figure 20: Transduction of CD34-purified cells by CD105-LV^{GFP} is blocked by soluble CD105. The Fc-tagged extracellular part of CD105 (sCD105) or that of CD30 were added to CD105-LV^{GFP} or VSVG-LV^{GFP} in the indicated amounts. After 30 min incubation at 37 °C the vector-protein mixtures were added to primary human CD34-purified cells at a multiplicity of infection (MOI) of 1 for CD105-LV^{GFP} and an MOI of 5 for VSVG-LV^{GFP}. Seventy-two hours later, the number of GFP-positive cells was determined by flow cytometry and the transduction efficiencies were calculated in relation to those obtained in absence of the soluble proteins. N = 2; mean±SD (Kays et al., 2015).

3.2.3 Stable transgene expression *in vitro*

To achieve long-lasting gene therapy it is essential that transduction of cells is stable and does not influence the self-renewal and differentiation capacity of HSC. Therefore, we analyzed the long-term gene expression and the multi-lineage potential of CD105-LV^{GFP} transduced cells *in vitro* and *in vivo*.

The colony forming cell assay (CFA) is a validated tool to determine changes in the proliferation or differentiation capacity of hematopoietic progenitor cells *in vitro*. Hematopoietic progenitor cells are applied to semi-solid methylcellulose medium supplemented with cytokines and growth factors that enable the progenitors to proliferate and differentiate into colonies of mature cells. Thus, myeloid multipotential progenitors and committed progenitors of the erythroid, monocyte, and granulocyte lineages can be enumerated and assessed according to their morphology (Pereira et

al., 2007). Therefore, CFA with CD34⁺ cells transduced either with CD105-LV^{GFP} or VSVG-LV^{GFP} was performed. CD34⁺ were purified from mobilized peripheral blood and transduced with either CD105-LV^{GFP} or VSVG-LV^{GFP}. Seventy-two hours post transduction the fractions of GFP⁺ cells were determined by flow cytometry and cells applied to the CFA. After 10 days, the numbers of GFP⁺ colonies and the type of colony were determined microscopically. All hematopoietic lineages that can be assessed with that assay were detected after colony formation. No significant difference was observed in the differentiation of cells derived from mock, VSVG-LV^{GFP} and CD105-LV^{GFP} transduced cells indicating that the transduction with none of the vectors led to an altered differentiation capacity *in vitro* (Figure 21).

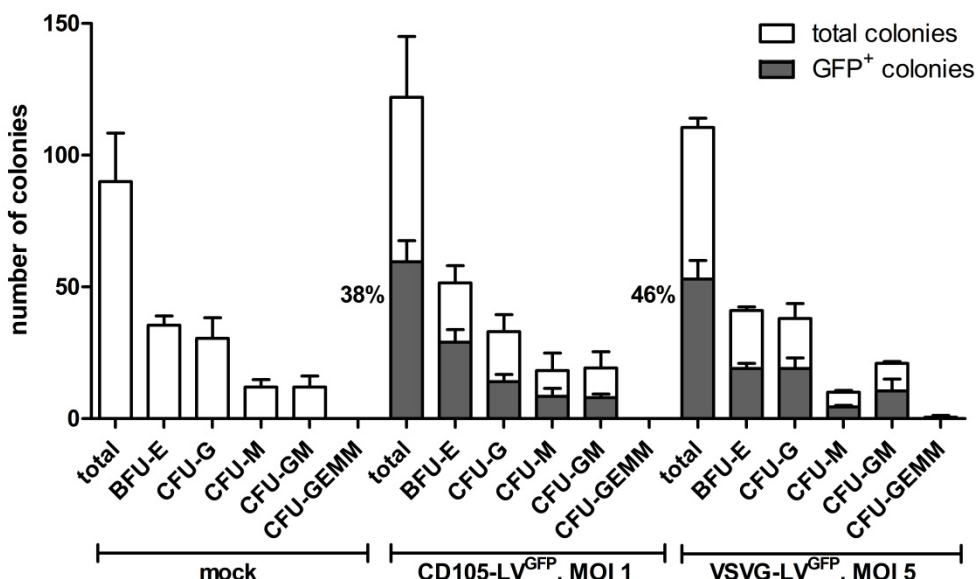


Figure 21: Long-term expression of the transgene in CD105-LV^{GFP} transduced human HSCs *in vitro*. A colony forming assay was performed with CD34⁺ cells purified from G-CSF mobilized peripheral blood that were either transduced with CD105-LV^{GFP} (MOI 1), VSVG-LV^{GFP} (MOI 5) or medium (mock). After 10 days incubation, the percentages of the indicated hematopoietic lineages were determined by fluorescence microscopy. Mean distribution±SD of all colonies is shown in white, mean distribution ± SD of GFP⁺ colonies is shown in grey. Also the percentages of GFP⁺ colonies in relation to the total colonies are indicated. One representative experiment out of three is shown. BFU-E = burst-forming unit-erythroid; CFU-G = colony-forming unit-granulocyte; CFU-M = colony-forming unit-macrophage; CFU-GM = colony-forming unit-granulocyte, erythroid, macrophage, megakaryocyte; MOI = multiplicity of infection (Kays et al., 2015).

Interestingly, the percentage of GFP⁺ colonies was higher than the percentage of GFP⁺ cells before CFA. This was especially pronounced for cells transduced with

CD105-LV^{GFP} which showed an average increase of 89.7% (N=3; SD ± 14.6) compared to 29.3% (N=3; SD ± 13.5) for cells transduced with VSVG-LV^{GFP} (Figure 22).

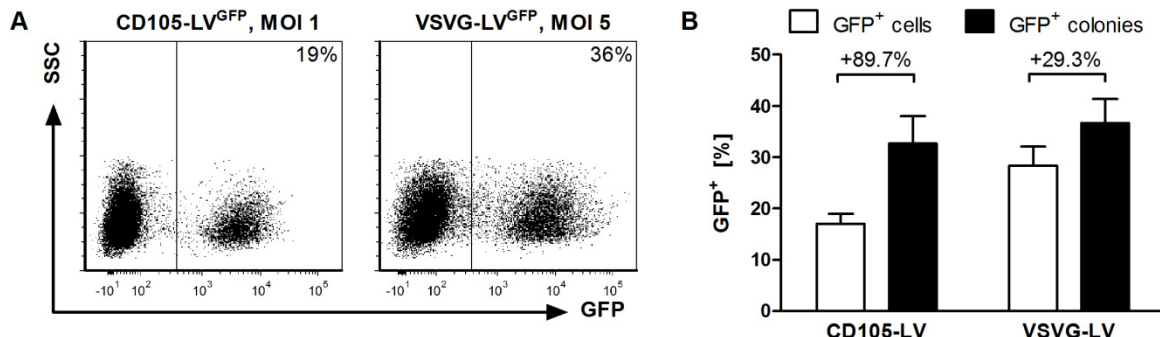


Figure 22: GFP expression of CD105-LV^{GFP} or CD105-LV^{GFP} transduced CD34⁺ cells and their derived colonies. CD34⁺ cells purified from G-CSF mobilized peripheral blood were transduced with either CD105-LV^{GFP} (MOI 1) or VSVG-LV^{GFP} (MOI 5). Seventy-two hours after transduction the percentage of GFP⁺ cells was determined by flow cytometry before the cells were applied to a colony forming assay. MOI = multiplicity of infection. (A) FACS plots of transduced cells corresponding to the colony forming assay shown in Figure 21 (Kays et al., 2015). (B) Percentages of GFP expressing cells and colonies. Difference between fractions is indicated. N=3; mean±SD.

These data show that CD105-LV^{GFP} targets a HSC population with extensive proliferative and multipotent colony forming capacities.

3.2.4 Stable transduction of CD105-LV transduced cells in repopulated NSG mice

The majority of cells giving raise to colonies in colony forming assays consists of more committed progenitor cells whereby not all hematopoietic lineages as well as primitive hematopoietic stem cells can be assessed in that short-time assay. Long-term replicating hematopoietic stem cells are typically identified by repopulation of conditioned mice with human cells. The murine hematopoietic system is usually destroyed by irradiation followed by transplantation of human HSCs. Then, true HSCs that are capable of self-renewal allow restoring of the hematopoietic system over months.

Therefore, it was next investigated in close collaboration with Kerstin B. Kaufmann and Manuel Grez (Georg-Speyer-Haus, Frankfurt) whether CD34⁺ cells transduced

with CD105-LV^{GFP} are able to repopulate NSG mice. The expression of GFP within transduced cells allows not only the detection of gene modified cells after several months but also detailed analysis of the lineage distribution of transduced cells. Thereby, it can be also checked if transduction with CD105-LV alters the self-renewal as well as differentiation capacity of gene marked cells.

Fresh CD34⁺ cells were isolated from human mobilized peripheral blood. After overnight stimulation with cytokines cells were transduced with CD105-LV at a MOI of 1. The following day, cells were washed with PBS once and injected intravenously into sublethally irradiated NOD-scid IL2R $\gamma^{-/-}$ mice. Some of the cells were kept for *in vitro* culture to determine the fraction of GFP⁺ cells by flow cytometry 72 hours post transduction. 7-18 weeks after transplantation, blood, spleen and bone marrow cells were isolated from mice and analyzed by flow cytometry. Engraftment of human cells varied from 13 to 69% in BM and spleen and between 5 and 25% in blood within the individual animals (Figure 23A). Human CD45⁺ cells were further analyzed in regard to lineage distribution and GFP expression. As expected from this humanized mouse model the majority of human cells were CD19⁺, but also CD3⁺ and CD33⁺ cells were detected in BM (Figure 23B) and spleen (Figure 23C). In addition, 10 – 15% of human cells in the bone marrow expressed the common HSC marker CD34 (Figure 23B) indicating self-renewal capacity of the engrafted cells.

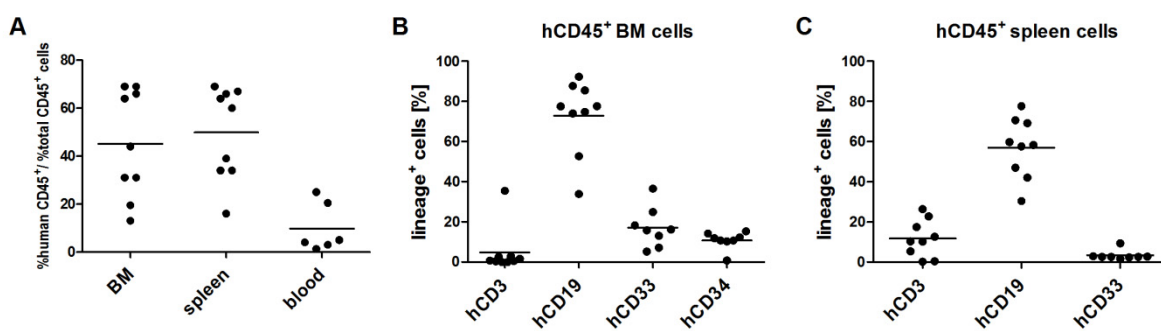


Figure 23: Stable engraftment and repopulation of CD105-LV^{GFP} transduced human HSCs *in vivo*. Six weeks old NSG mice ($N = 9$) were irradiated at 1.8 or 2 Gy. Four hours after conditioning 1.2 - 1.7×10^6 CD105-LV^{GFP} transduced human CD34⁺ cells that were isolated from G-CSF mobilized peripheral blood were transplanted intravenously. 7 - 18 weeks post transplantation cells were isolated from BM, spleen und blood and analyzed by flow cytometry. (A) Percentage of human CD45⁺ cells in relation to all CD45⁺ cells. (B) Lineage distribution of human CD45⁺ cells in BM and (C) spleen (Kays et al., 2015).

The percentages of GFP⁺ cells ranged between 5 and 22% in BM, spleen and blood (Figure 24A) and reflected the fractions of GFP expressing cells initially transplanted into mice (Figure 24B). These data demonstrate that the transgene expression remained stable up to 18 weeks and that the transduced cells engrafted efficiently in mice. Moreover, cells from all hematopoietic lineages were detected within the GFP⁺ cells from BM (Figure 24C) and spleen (Figure 24D). Unfortunately, the numbers of human cells that were recovered from murine blood were too low for further reliable lineage analysis. Notable, there were no significant differences in the fractions of GFP expressing cells in each hematopoietic lineage in BM (Figure 24C) and spleen (Figure 24D) indicating that transduced cells preserved the ability to differentiate into the different lineages. This argues for the fact that CD105-LV transduces not progenitor cells but indeed HSCs.

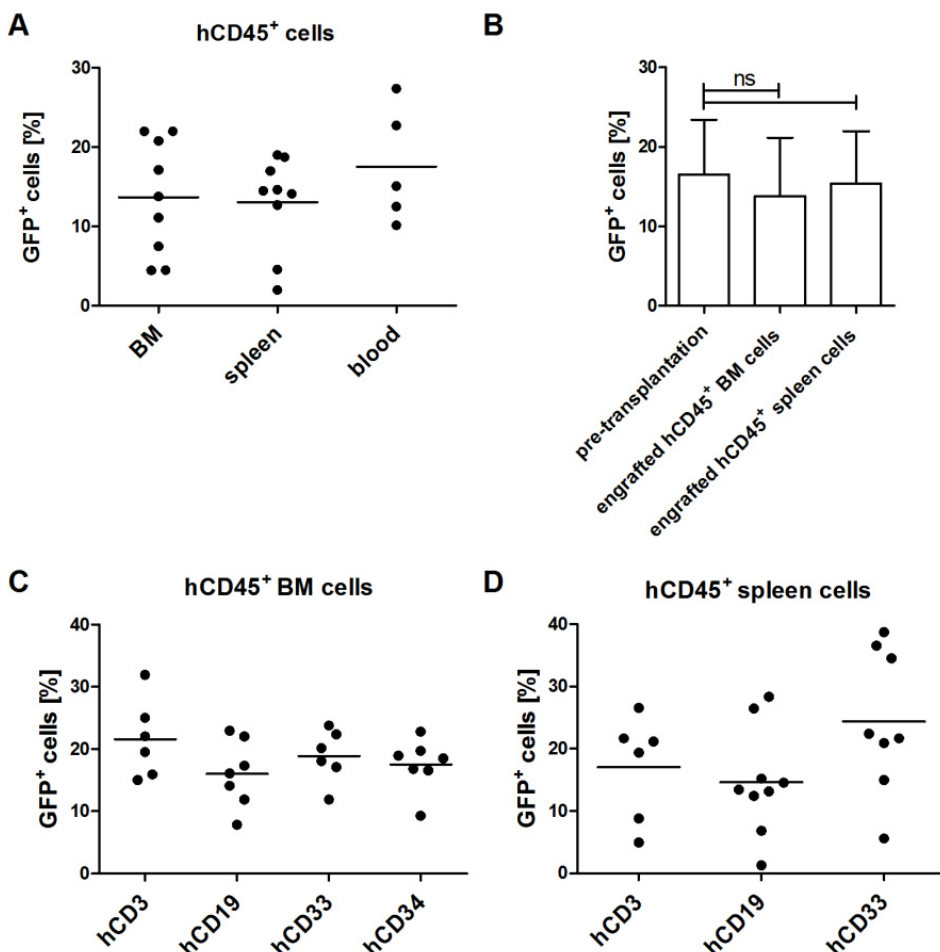


Figure 24: Stable engraftment and repopulation of CD105-LV^{GFP} transduced human HSCs *in vivo*. Six weeks old NSG mice ($N = 9$) were irradiated at 1.8 or 2 Gy. Four hours after conditioning $1.2 - 1.7 \times 10^6$ CD105-LV^{GFP} transduced human CD34⁺ cells that were isolated from G-CSF mobilized peripheral blood were transplanted intravenously. 7 - 18 weeks post transplantation cells were isolated from BM, spleen und blood and analyzed by flow cytometry. (A) Percentages of GFP⁺ cells within the engrafted human CD45⁺ cell population in BM, spleen and blood. (B) GFP expression in human CD34-purified cells 72 h post-transduction (pre-transplantation) and in engrafted human CD45⁺ cells (7 - 18 weeks post-transplantation) in BM and spleen; ns = not significant. Comparable percentages of GFP⁺ cells in each lineage in human CD45⁺ engrafted (C) BM and (D) spleen cells; differences not significant according to 1-way ANOVA analysis: p=0.2752 (BM), p=0.1254 (spleen). BM = bone marrow; h = human (Kays et al., 2015).

3.2.5 Competitive repopulation of CD105-LV or VSVG-LV transduced HSCs in NSG mice

Next, the repopulation capacities of CD34⁺ cells transduced with either CD105-LV or VSVG-LV were compared in a competitive setting *in vitro* and *in vivo*. CD105 or VSVG pseudotyped vector particles transferring either GFP or BFP were generated, resulting in four different vector types: CD105-LV^{GFP}, CD105-LV^{BFP}, VSVG-LV^{GFP} and

VSVG-LV^{BFP}. By having both pseudotypes with both transgenes one can exclude that expression of one of the transgene causes more cell stress than the other. Then, CD34⁺ cells were transduced with one of the vectors without pre-stimulation but in the presence of cytokines aiming to obtain matching transduction efficiencies of around 5% transduced cells. On the next day, CD105-LV^{GFP} and VSVG-LV^{BFP} as well as CD105-LV^{BFP} and VSVG-LV^{GFP} transduced cells were mixed in a 1:1 ratio resulting in two different cell pools each consisting of GFP⁺, BFP⁺ and untransduced cell populations. From these cell pools aliquots were taken for a prolonged *in vitro* culture, whereas the majority of cells were transplanted into sublethally irradiated NOD-scid IL2R $\gamma^{-/-}$ mice (0.5 to 1.0x10⁶ mobilized CD34⁺ cells per mouse, N = 7). 48 h post transduction the marker gene expression was analyzed by flow cytometry (Figure 25).

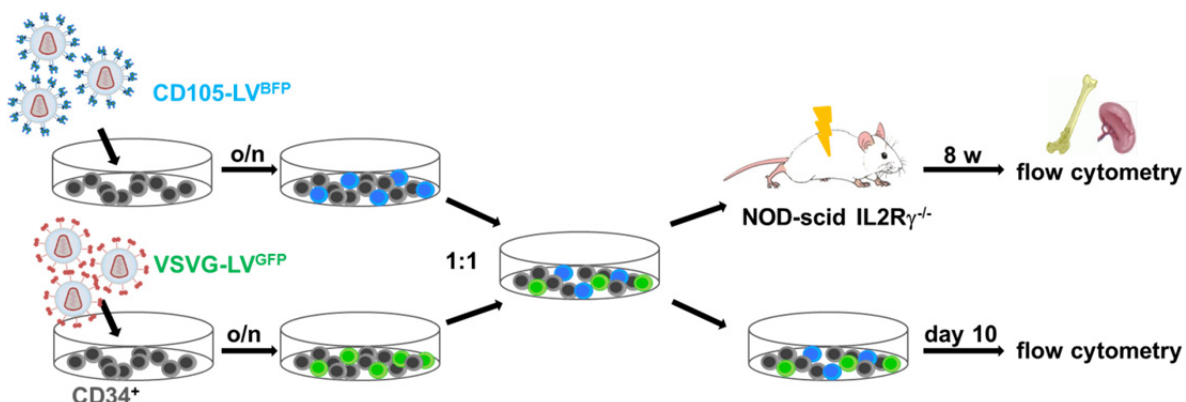


Figure 25: Experimental setting of competitive repopulation experiment. CD34⁺ cells were isolated from mobilized peripheral blood and transduced with either CD105-LV^{BFP} or VSVG-LV^{GFP} (or vice versa) in the presence of cytokines. On the next day, cells were pooled in a 1:1 ratio and either cultured further *in vitro* or transplanted into sublethally irradiated NSG mice. Levels of marker gene expression in cells of the prolonged *in vitro* culture were determined by flow cytometry. Expression of marker genes as well as various cell surface markers from cells isolated from engrafted mice were analyzed by flow cytometry 8 weeks post transplantation.

Corresponding with the anticipated transduction efficiency of 5% we detected for both vectors approximately 2.5 – 3% of marker positive cells (Figure 26 A). In both combinations a slightly higher percentage of gene marking was observed for cells transduced by VSVG-LV as indicated by ratios of 1.3 and 1.1 (%VSVG-LV transduced cells/%CD105-LV transduced cells). From day 2 to day 10 every other day samples from the pooled cell populations were analyzed for marker gene

expression by flow cytometry. GFP/BFP expression mediated by CD105-LV was maintained to a similar percentage throughout the prolonged cell culture, whereas a loss of 60% of marker gene positive cells was detected for VSVG-LV transduced cells (Figure 26B). This demonstrates that CD105-LV provides transduction of cells that are maintained and/or proliferate throughout prolonged cell culture.

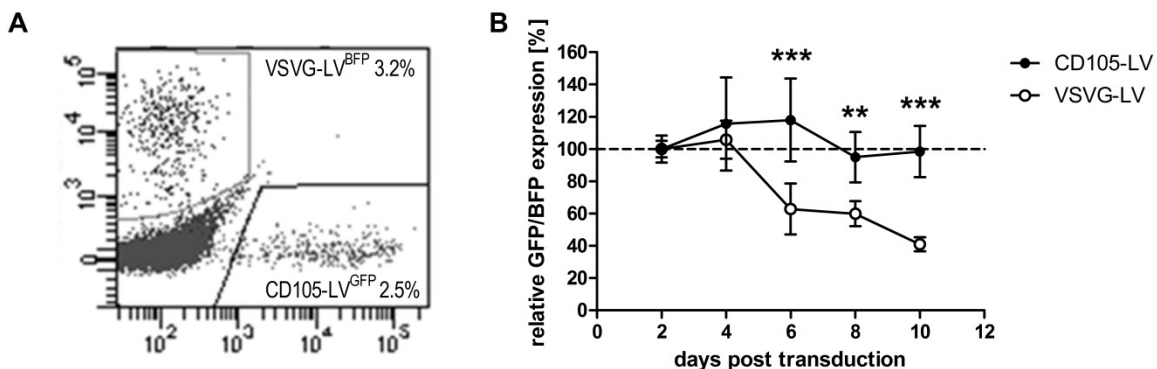


Figure 26: Competitive repopulating capacity of CD105-LV vs. VSVG-LV transduced HSCs *in vitro*. CD34⁺ cells purified from G-CSF mobilized peripheral blood were transduced either with CD105-LV^{GFP}, CD105-LV^{BFP}, VSVG-LV^{GFP} or VSVG-LV^{BFP}. The next day VSVG-LV^{BFP} and CD105-LV^{GFP} and vice versa transduced cells were mixed to equal parts. (A) Representative FACS plot after pooling of the cells 48 h post transduction. (B) *In vitro* monitoring of transgene expression in triplicates of both pseudotype and transgene combinations normalized to the percentage of transduced cells 48 h post transduction; mean±SD; differences are significant on day 6 ($p=0.004$), day 8 ($p=0.0024$) and day 10 ($p=0.0004$). GFP = green fluorescent protein; BFP = blue fluorescent protein (Kays et al., 2015).

Eight weeks after transplantation bone marrow and spleen cells were isolated from the humanized mice. All animals showed moderate to high levels of human cell engraftment (%humanCD45⁺/%totalCD45⁺: $41.1\pm11.8\%$ (BM); $30.0\pm6.6\%$ (spleen)) (Figure 27A). Further analysis revealed that similar to the repopulation experiment described in 3.2.4 the majority of human CD45⁺ cells were CD19⁺ (Figure 27B, C). Cells transduced with CD105-LV showed transgene expression in all hematopoietic lineages without significant differences (mean values of 2-4%) correlating or even exceeding the initial percentage of marker positive cells that were transplanted. In contrast, cells transduced with VSVG-LV showed less than 2% of marker gene expression cells meaning a loss compared to the initial input. The only exception was CD33⁺ splenocytes maintaining the fraction of marker gene positive cells (Figure 27D - F).

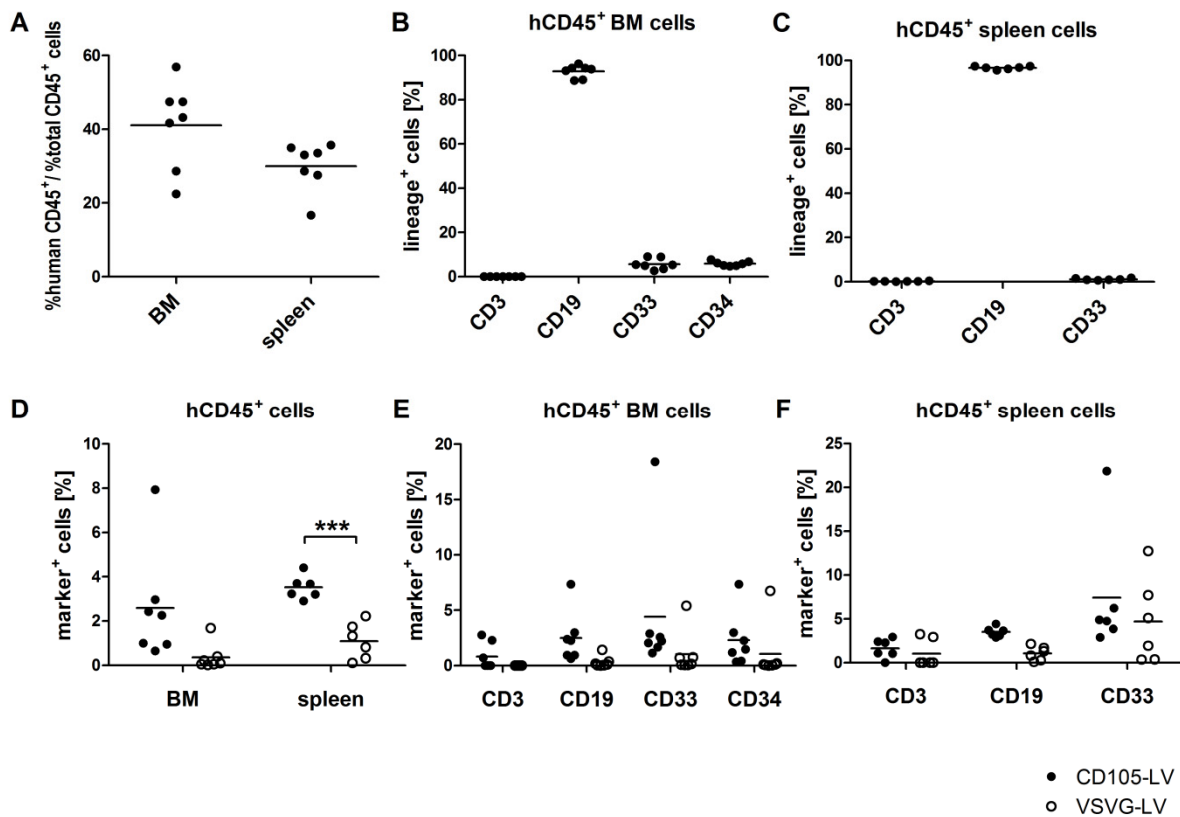


Figure 27: Engraftment and lineage distribution of human cells in NSG mice in competitive repopulation experiments. CD34⁺ cells purified from G-CSF mobilized peripheral blood were transduced either with CD105-LV^{GFP}, CD105-LV^{BFP}, VSVG-LV^{GFP} or VSVG-LV^{BFP}. The next day VSVG-LV^{BFP} and CD105-LV^{GFP} and vice versa transduced cells were mixed to equal parts. 0.5 - 0.6 x 10⁶ cells/mouse were injected intravenously. Eight weeks post transplantation cells were isolated from BM and spleen and analyzed by flow cytometry for human and murine CD45 expression as well as for expression of human lineage markers and transgene expression (GFP⁺ or BFP⁺ = marker⁺) in the hCD45⁺ population; filled circles = CD105-LV; open circles = VSVG-LV. (A) Engraftment of human cells in BM and spleen. Lineage distribution of human CD45⁺ engrafted BM (B) and spleen (C) cells. (D) Engraftment of CD105-LV transduced cells is significantly enhanced in spleen ($p=0.009$) compared to VSVG-LV transduced cells; no significant differences in the distribution of marker-positive cells in each lineage of human CD45⁺ engrafted BM (D) and spleen (F) cells (one-way ANOVA analysis: $p=0.3326$ (BM, CD105-LV), 0.5484 (BM, VSVG-LV), $p=0.0816$ (spleen, CD105-LV), $p=0.0871$ (spleen, VSVG-LV)). GFP = green fluorescent protein; BFP = blue fluorescent protein; BM = bone marrow; h = human (Kays et al., 2015).

Comparing the ratios of gene-marking retrieved *in vivo* (post-transplantation) to marker positive cells pre-transplantation resulted in ratios of approximately 1 in BM and spleen upon transduction with CD105-LV while ratios for VSVG-LV were significantly lower (Figure 28A). To further demonstrate the difference in performance between both vector types the ratio of CD105-LV to VSVG-LV transduced cells within each individual animal was determined and set in proportion to the corresponding input cell population. Thus, values above 1 indicate a repopulation advantage of cells

transduced by CD105-LV. This revealed in BM a 29-fold and in spleen a 9-fold superior engraftment of cells transduced by CD105-LV compared to cells transduced with VSVG-LV demonstrating that CD105-LV facilitates transduction of unstimulated CD34⁺ HSCs that are able to repopulate NSG mice at sustained levels (Figure 28B). These results suggest CD34⁺/CD105⁺ cells have a high repopulating capacity in NSG mice and confirm that CD105 can serve as a phenotypic marker of early human HSCs.

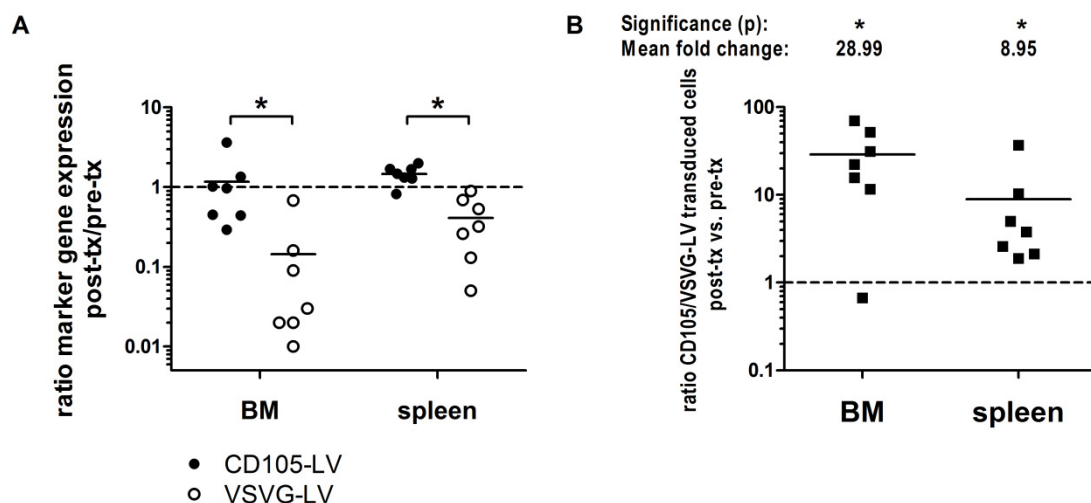


Figure 28: Competitive repopulating capacity of CD105-LV vs. VSVG-LV transduced HSCs *in vivo*. (A) Cells transduced with CD105-LV showed stable expression of the transgene reflected by the ratio of gene-marked cells at final analysis compared to the initial transduction efficiency. The respective ratios for VSVG-LV were significantly lower as analyzed with the Wilcoxon matched-pairs signed rank test; * = p<0.05 [p=0.0313 (BM); p=0.0156 (spleen)]. (B) The relative ratio was obtained by dividing the ratio of the different pseudotype transduced cells (CD105-LV/VSVG-LV) within one individual animal (*in vivo*) by the corresponding ratio obtained 48 h post transduction (*in vitro*). Values above 1 indicate superior performance of CD105-LV compared to VSVG-LV. Mean fold change in BM and spleen are specified. Significance according to Wilcoxon matched-pairs signed rank test; * = p<0.05 [p=0.0313 (BM); p=0.0156 (spleen)] is shown. BM = bone marrow; tx = transplantation; h = human (Kays et al., 2015).

3.2.6 Vector mediated toxicity on CD34⁺ cells

Lentiviral transduction might lead to some cell stress or toxicity. To address this issue vector mediated cell toxicity was investigated. CD34⁺ cells were transduced with either CD105-LV^{GFP} or VSVG-LV^{GFP} aiming to obtain the same transduction efficiencies with both vectors. Forty-eight hours after transduction we analyzed the fractions of early apoptotic and late apoptotic/necrotic cells by annexin V/PI staining. Annexin V binds to phosphatidylserine that translocates to the extracellular cell

membrane upon apoptosis induction. Cells undergoing early apoptosis are only stained with annexin V, whereas late apoptotic or necrotic cells are stained for both annexin V and PI. Cells transduced with CD105-LV showed significantly more apoptotic cells (mean: $11.2 \pm 1.9\%$) than the mock transduced cells (mean: $5.3 \pm 1.4\%$) (Figure 29). However, more than 80% of the CD105-LV transduced apoptotic cells were in the early apoptotic phase and some of these might recover and not enter the late apoptotic status. No significant differences were detected between VSVG-LV and mock transduced cells as well as between CD105-LV and VSVG-LV transduced cells. Therefore, it can be excluded that the superior engraftment potential of CD105-LV transduced cells that was observed in chapter 3.2.6 was due to a more toxic effect of VSVG-LV on the cells, but rather that CD105-LV transduces a more primitive subset of $CD34^+$ cells.

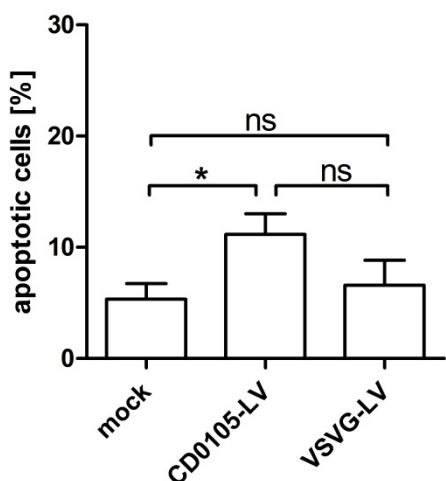


Figure 29: Apoptosis induction upon transduction. $CD34^+$ cells purified from G-CSF mobilized peripheral blood were transduced either with $CD105-LV^{GFP}$ or $VSVG-LV^{GFP}$ resulting in similar transduction efficiencies of 11-18%. After 48 h the fractions of early and late apoptotic/necrotic cells were determined by annexin V/PI staining. Early and late apoptotic cells as well as necrotic cells were included into analysis of vector mediated toxicity. According to one-way ANOVA no significant differences were observed between both mock and VSVG-LV transduced cells and between CD105-LV and VSVG-LV transduced cells. CD105-LV transduced cells showed significantly more apoptotic cells ($p<0.05$) compared to the mock control (Kays et al., 2015).

4. DISCUSSION

4.1 Side by side comparison of lentiviral and AAV vectors

The comparison between two different vector types for their gene transfer activities is not at all trivial, since lentiviral and AAV vector constructs differ in many aspects such as their structural organization, mode of gene expression and entry receptors used. Additionally, LVs integrate the transgene into the host cell's genome allowing stable transgene expression, while AAV vectors are present in the cell episomally. Therefore, the normalization of lentiviral and AAV vector particles for a convincing side by side comparison is critical. Normalization can be based on physical, genomic or functional titers. Genomic titers include vector particles containing vector genomes, but comprise also non-functional particles that contain genetic information, but are not able to transduce target cells or lead to transgene expression. Quantification of genomic titers is performed by quantitative real-time PCR. While the DNA from AAV vectors can be isolated and used for qPCR directly, LV RNA has to be reverse transcribed into cDNA for qPCR first. Physical titers can be determined by ELISA and include empty and non-functional particles. Functional titers are determined by transduction of cells expressing the entry receptor of the respective vector. Thus, comparing different vectors that do not use the identical entry receptor bias the quantification of functional titers. While VSVG-pseudotyped LVs can transduce a variety of cells, since the VSV receptor is expressed on most of the mammalian cells, the transduction ability of recombinant AAV vectors depends on the natural tropism of the AAV serotype used for capsid formation. Therefore, comparison of different AAV vector serotypes is already challenging. Comparing different vector types, such as lentiviral and AAV vectors, is even more difficult. Nevertheless, several studies previously compared the performance of lentiviral and AAV vectors in various gene transfer approaches in terms of efficacy, safety and biodistribution.

One of these studies describes the *in vitro* identification of the best vector for the transduction of various lung cancer cells for a potential anti-cancer treatment. Five recombinant AAV vectors generated from the AAV2 backbone combined with the capsid proteins of the AAV1, AAV4, AAV5 or AAV8 serotypes were compared to VSVG-LV and normalized to identical MOIs. The AAV vectors transduced 6 out of 11

cell lines, while VSVG-LV was able to transduce 10 different cell lines efficiently at low vector doses. This was attributed to the natural tropism of the AAV serotypes. In addition, transduction with AAV vectors required the use of higher vector doses. The vector doses were adjusted to functional particles, however, the functional titers for both vector types were determined by the transduction of different cell lines (Chen et al., 2013). Thereby, normalization based on functional titers is precarious. Altering the natural tropism of vectors circumvents the titer variability based on different cell tropism. This can be achieved by using receptor-targeted vectors that bind to the same cell entry receptor. Quantification of functional titers of lentiviral and AAV vectors by transduction of the same cell line was demonstrated in this thesis.

In another study, aiming at identifying the best vector for gene therapy of hemophilia B, Vandendriessche et al. generated AAV8, AAV9 and lentiviral vectors transferring *factor IX* (FIX) from the same hepatocyte-specific expression cassette. Normalized to genome copies, lentiviral gene transfer into FIX-deficient mice resulted in stable transgene expression at low therapeutic levels, while the use of AAV serotypes 8 and 9 led to supraphysiological FIX expression levels. LV-based FIX expression did evoke a short-term proinflammatory cytokine induction, while this was not observed in AAV vector injected mice. However, AAV9 vector resulted in unexpectedly high transgene expression in the heart, emphasizing the adequate choice of capsid serotype of AAV vectors (Vandendriessche et al., 2007). By the use of receptor-targeted vectors using the same entry receptor, the natural tropism of vectors is altered and gene transfer is restricted to specific cell types. *In vivo* application is therefore not biased by different cell tropism of vectors. This allows the comparison of different vector types in terms of distribution, transgene expression or potential immune responses.

So far, studies comparing lentiviral and AAV vectors have focused mainly on the comparison of the performance of lentiviral and AAV vectors in specific gene therapeutic applications (Harvey et al., 2002; Ahmed et al., 2004; Vandendriessche et al., 2007; Vande Velde et al., 2011; Wang et al., 2012; Chen et al., 2013; Joyeux et al., 2014). All of the LVs included in these studies were pseudotyped with VSVG, whereas binding of the AAV vectors to cells was achieved by the natural tropism of the capsid AAV serotypes. In this thesis, receptor-targeted lentiviral and AAV vectors presenting the same targeting ligand, namely the DARPin 9.29, on the particle

surface, were compared. Her2-LV and Her2-AAV use the same entry receptor, Her2/neu, for selective transduction of cells, allowing for the first time a side by side comparison of lentiviral and AAV vectors. Functional titers were determined by transduction of Her2/neu expressing SK-OV-3 cells (3.1.1.3). Genomic titers of Her2-LV and Her2-AAV were quantified by qPCR using the same amplification target (3.1.1.1.2). This minimizes the variability in quantification of titers and thereby allows a more reliable normalization of Her2-LV and Her2-AAV. Since transduction of both vectors is mediated by binding of the DARPin 9.29 to the cell entry receptor Her2/neu, the distribution of both vector types can be analyzed *in vivo* independently from their natural receptor usage, that have influenced comparative studies so far.

4.2 Side by side comparison of Her2-LV and Her2-AAV

Lentiviral and AAV vectors are the preferred tools in current gene therapeutic approaches. Depending on the desired application, one system may be preferable over the other. In this thesis, receptor-targeted lentiviral and AAVs using the same receptor for cell entry were compared side by side for the first time. Lentiviral and AAV vectors expressing the same targeting ligand on the particle surface, namely the DARPin 9.29, which mediates gene delivery into Her2/neu-positive cells, had been generated and characterized before (Münch et al., 2011; Münch et al., 2013). In this thesis, genomic, physical and functional titers of several Her2-LV and Her2-AAV vector stocks were analyzed and both vector types compared *in vitro* and *in vivo*.

The quantification of genomic titers was based on a qPCR method using an amplification target sequence within the transgene to allow titer determination of both Her2-LV and Her2-AAV within one single qPCR run. On average, Her2-AAV^{GFP} vector stocks contained 1.46×10^{11} gc/ml. Hence, the genomic titers are similar to that of AAV2 wild-type vectors and correspond to those of previous Her2-AAV vector preparations (Münch, 2013). The average genomic titer of Her2-LV^{GFP} vector stocks was 1.35×10^{12} gc/ml, thus, approximately 10-fold more genomes were present than in Her2-AAV^{GFP} vector stocks. However, an amplification target within the transgene was selected for the qPCR, so, it cannot be excluded that contaminating mRNA transcripts from the producer cells had been packaged into the vector particles or co-concentrated, resulting in an overestimation of the true genomic titers of Her2-LV

vector stocks. One can circumvent that by selecting an amplification target within the LTRs (Geraerts et al., 2006). Since the LTR sequences are not present within the AAV vector genome, it was decided against this option. As an alternative amplification sequence during qPCR, sequences within the promoter gene are conceivable, since, no mRNA transcripts would influence the quantification of genomic titers. While the genomic titers of Her2-LV vector stocks might have been overestimated, it is very unlikely that mRNA transcripts or contaminating plasmid DNA from the AAV vector production contributed to the genomic titers of Her2-AAV vector stocks. The purification of AAV vector stocks included benzonase treatment and density gradient centrifugation, while the produced LVs were purified only by centrifugation through a sucrose cushion. Additionally, RNase digestion was implemented during DNA isolation of AAV genomes. Potential contaminating plasmid DNA was removed from LV particles by DNase I digest. However, total RNA was purified from LV vector stocks, which might have led to the co-isolation of lentiviral RNA and mRNA transcripts.

Physical particles of Her2-LV and Her2-AAV vector stocks were determined by ELISA. Based on the assumption that one lentiviral particle contains approximately 2000 p24 proteins (Wilk et al., 2001), the number of physical particles within Her2-LV^{GFP} vector stocks was calculated and accounted on average for 7.0×10^{12} particles/ml. This is consistent with previous data on stocks of receptor-targeted LVs (Anliker et al., 2010). Her2-AAV^{GFP} vector stocks contained 7.8×10^{11} particles/ml which corresponds to previously obtained particle numbers (Münch et al., 2013).

The particle numbers of both Her2-LV and Her2-AAV exceeded the number of genomes (Figure 7A). Comparing physical particles to numbers of genomes revealed that both LV and AAV vector stocks comprised approximately 80% empty particles. The ratios of total to genome containing particles within Her2-AAV vector stocks were similar to previous observations (Münch et al., 2013). In addition, a ratio equal or below 50 had been determined to be wild-type AAV vector phenotype (Grimm et al., 1999). With a ratio of approximately 5, Her2-AAV^{GFP} was clearly within the expected range. It was also previously shown that physical particle numbers of VSVG-LV usually exceed the numbers of genomes (Geraerts et al., 2006).

For the quantification of functional titers, SK-OV-3 cells were transduced with serial dilutions of Her2-LV^{GFP} and Her2-AAV^{GFP} and the transduction efficiencies were

determined by flow cytometry. On average, the functional titer of Her2-LV^{GFP} accounted for 7.8×10^6 tu/ml, while Her2-AAV^{GFP} vector stocks contained about 2×10^7 tu/ml. Comparing the numbers of functional particles and genomes revealed that genomic titers exceeded the functional particles of Her2-AAV about 10,000-fold and that of Her2-LV by about 100,000-fold (Figure 7B). While it cannot be excluded that the true genome copies within LV vector stocks were overestimated, it was demonstrated by several groups that RNA-based titration methods led to 10-10,000-fold more genomes than functional VSVG-LV particles (Scherr et al., 2001; Sastry et al., 2002; Lizée et al., 2003; Geraerts et al., 2006). These data are in line with the results obtained here, considering that the yield of functional particles of receptor-targeted LVs is about 35-fold decreased compared to VSVG-LVs (Anliker et al., 2010).

The amount of functional particles within the Her2-AAV vector stocks was about 10-fold higher than in lentiviral vector stocks, but Her2-LV vector stocks contained about 10-fold more genomes (Figure 7A). Thus, Her2-LV compensates for the lower amount of functional particles. However, normalizing vectors to the same genome copy number resulted in higher transduction efficiencies in AAV-transduced cells, since more functional particles were present in the transduction mix. In contrast, normalizing to functional particles required an approximately 10-fold higher MOI of Her2-AAV than Her2-LV (Figure 9). This was attributed to the ability of LVs to integrate their transgenes into the host's genome, while AAV vectors remain episomally in the target cells. As a result, AAV vectors are diluted out and finally lost during proliferation of the cells.

SK-OV-3 cells transduced with Her2-LV^{GFP} resulted in higher mean fluorescence intensity (MFI) of GFP expression than in cells transduced with Her2-AAV^{GFP} (Figure 8). This indicates that the protein expression per cell is higher in LV transduced cells compared to AAV transduced cells. This was also previously observed in a study comparing VSVG-LV, a non-integrating lentiviral vector (NILV) and AAV vector in terms of transgene expression. The three vectors contained the identical expression cassette consisting of the SFFV promoter, *egfp* and the *wPRE* sequence. The MFIs of the GFP expression of episomal NILV and AAV vectors were lower than that of VSVG-LV. It was further determined that the expression per copy of DNA delivered by VSVG-LV was 3-5 fold higher compared to DILV and AAV vector. Apolonia

suggested that transgene expression mediated by VSVG-LV is higher than that of episomally present NILV, because LVs tend to integrate their genome into transcriptionally active genome sites (Schröder et al., 2002; Mitchell et al., 2004). Another explanation could be that episomally present genomic information is not as easily accessed by the transcription machinery than that of the integrated LV (Apolonia, 2009).

As Her2/neu is overexpressed in several tumor cells, a subcutaneous tumor mouse model was used to analyze the distribution of the Her2-targeted vectors *in vivo*. The same amount of genome copies of Her2-LV^{luc} and Her2-AAV^{luc} were administered via the tail vein. Shortly after vector administration (4, 8 and 24 hours) LV RNA, respectively, AAV vector DNA was isolated from different tissues. In mice injected with Her2-LV, RNA was detectable in spleen up to 24 hours post vector administration. In all other organs, the LV RNA levels decreased 4 hours after vector injection and were not detectable anymore 24 hours post vector administration (Figure 10). This was confirmed by the results obtained from *in vivo* imaging that showed only minor luciferase signals in the spleens of mice injected with Her2-LV (Figure 12; Figure 13). By isolation of RNA from tissue followed by transgene specific qPCR, it was not possible to distinguish between RNA derived from LV particles and *luc* mRNA produced by transcription of integrated LV genomes. However, the data obtained here are consistent with observations demonstrating that the amount of RNA detectable in organs decreased during the first 24 hours after VSVG-LV injection in mice. The RNA levels then increased 72 hours after vector administration indicating vector mediated transcription (Brown et al., 2007). Others showed that DNA integration of HIV-based vectors is detectable earliest 12 hours post transduction (p.t.) and reaches a plateau around 48 hours p.t. (Butler et al., 2001; van Maele et al., 2003).

The fact that no luciferase expression was detected 12 days after LV administration *in vivo* was attributed to the lower amount of functional particles injected into mice compared to Her2-AAV. Corresponding to the data obtained *in vitro*, a 10-fold higher Her2-LV vector dose led to detectable luciferase expression in the tumor and some off-target signals in the spleen (Figure 12; Figure 13). This amount of receptor-targeted LV corresponds to vector doses that were administered systemically before (Münch et al., 2011; Abel et al., 2013).

Analysis of AAV DNA isolated from organs shortly after vector administration revealed that during the first 24 hours, the distribution of Her2-AAV did not significantly differ between the organs except for a reduced spleen signal 24 hours post vector injection (Figure 11). While the AAV vector DNA was not predominant in tumor tissue 24 hours post vector administration, the highest luciferase expression signals were detected in tumors by *in vivo* imaging (Figure 12; Figure 13). Therefore, it can be concluded that vector particle accumulation in tumor tissue by Her2-AAV does not occur within the first 24 hours after vector administration. Organs were not perfused prior to isolation of DNA to remove remaining blood cells. It is therefore possible that Her2-AAV was not present in tissue but was rather still present in the blood of the organs. Perfusion of the organs prior to DNA isolation should then result in lower vector amounts within the tissues. Additionally, time points later than 24 hours post vector administration are required to confirm that Her2-AAV circulates stably for a prolonged time period *in vivo* compared to Her2-LV.

Based on the ratios of functional to genomic titers as well as luciferase expression in athymic nude mice *in vivo*, these results suggest that AAV is more efficient in transduction compared to LV, when the same amount of genome copies for both vector types is injected per mouse.

4.3 Hematopoietic stem cell-targeted lentiviral vectors

Today's standard procedure for gene delivery into HSCs is *ex vivo* transduction using VSVG-pseudotyped LVs. Since quiescent HSCs lack the VSV entry receptor LDL-R (Amirache et al., 2014), efficient transduction of CD34⁺ cells by VSVG-LV requires cytokine stimulation of the cells. This method has been successful in clinical applications (Cartier et al., 2009; Aiuti et al., 2013; Biffi et al., 2013). While unstimulated cells show higher long-term engraftment potential, stimulation facilitates cell cycle transit from quiescent cells resulting in impaired long-term repopulation capacities (Kittler et al., 1997; Glimm et al., 2000). Therefore, several additional LV-based approaches for efficient transduction of primitive HSCs have been investigated.

This thesis investigates the use of receptor-targeted LVs. For the rational design of LVs targeted to primitive HSCs, receptors expressed on long-term repopulating cells

have to be identified. Pierelli et al. showed that human CD34⁺CD105⁺ sorted cells represent an immature cell population containing primitive hematopoietic precursor cells that are significantly more enriched in long-term culture-initiating cells (LTC-IC) compared to CD34⁺CD105⁻ cells (Pierelli et al., 2000). However, the time period for this *in vitro* analysis was limited to 5 weeks and *in vivo* experiments that allow an assessment of the long-term repopulation capacity of cells were missing. By oligonucleotide microarray analysis of the mouse BM side-population (SP) enriched in HSC activity, mouse CD105 was identified as functional marker of long-term repopulating murine HSCs. These findings were confirmed by a competitive repopulation experiment. Transplantation of SP CD105⁺ cells resulted in an increase of donor cells whereas a decreased reconstitution contribution of SP CD105⁻ donor cells was observed (Chen et al., 2002).

CD105 is a component of the TGF- β receptor complex (St-Jacques et al., 1994; Warrington et al., 2005). The role of CD105 in maintaining the primitive state of HSCs is still not fully understood. It is suggested that CD105 as well as CD34 are positively regulated by TGF- β 1 in hematopoietic cells and that TGF- β 1 is the main soluble factor that inhibits the cell cycle progression of primitive precursor cells, thereby preserving their proliferative capacity (Hatzfeld et al., 1991; Pierelli et al., 2001). In this thesis, the long-term repopulating capacity of human CD105⁺ cells was evaluated using receptor-targeted LV.

CD34-purified cells were transduced with CD105-LV^{GFP} and then engrafted into NSG mice. After 7-18 weeks, similar fractions of gene marked human cells were detected in blood, BM and spleen compared to the percentages of GFP⁺ cells that were initially transplanted (Figure 24). This demonstrates the long-term stability of transgene expression and efficient engraftment of transduced cells into mice. Interestingly, similar percentages of gene marked cells in the analyzed lineages were obtained suggesting that multipotent HSCs, rather than more differentiated and hence lineage-restricted progenitors, had been transduced. This is in accordance with results found *in vitro* by CFA (Figure 21). The specificity of CD105-LV was proven by blocking the transduction of CD34⁺ cells through incubation of CD105-LV with soluble CD105 protein (Figure 20). In addition, off-target transduction was not observed in mixed cultures of CD105⁺ endothelial cells and CD105⁻ peripheral blood mononuclear cells, or after systemic vector administration in mice transplanted with human CD105⁺ cells

(Anliker et al., 2010; Abel et al., 2013). Therefore, it can be concluded that the gene marked cells in mice or colonies must have been derived from CD105⁺ HSCs. Additionally, the long-term repopulation potential of either CD105-LV or VSVG-LV transduced cells was compared *in vivo*. VSVG-LV and CD105-LV were labeled with different fluorescent reporter genes and CD34⁺ cells were transduced with one of the vector types. This allowed transplantation and tracking of either CD105-LV or VSVG-LV transduced cells within the same animal. The fractions of CD105-LV transduced cells remained stable or even increased *in vitro* as well as *in vivo* whereas the percentage of VSVG-LV transduced cells decreased over time (Figure 26A; Figure 28A). This resulted in a 29-fold superior engraftment of CD105-LV transduced cells in BM and 9-fold superior engraftment in spleen than cells transduced with VSVG-LV (Figure 28B) demonstrating that CD105-LV is capable of transducing long-term repopulating cells.

Certainly, the transduction conditions that were used for the competition assay favor CD105-LV, since cells were transduced with a low vector dose to gain comparable transduction efficiencies. The high amount of VSVG-LV that is usually used for transduction of CD34⁺ cells in clinical settings most likely facilitates the transduction of the relatively small HSC population capable of self-renewal. In these experiments, VSVG-LV probably transduced the vast excess of multilineage progenitor cells with short-term engraftment properties as well as more differentiated lineage-restricted progenitors with low or no engraftment potential. In addition, cells were transduced without pre-stimulation. While quiescent CD34⁺ cells lack the VSV entry receptor LDL-R, CD105-LV transduced unstimulated CD34⁺ cells. This resulted in sustained transduction levels in repopulated NSG mice. These data suggest that CD34⁺CD105⁺ cells represent an early stem cell population with high repopulating capacity and confirm that CD105 is a marker on primitive human HSCs.

Further evidence for this could be obtained by mixing limiting dilutions of either CD105-LV or VSVG-LV transduced cells with non-gene marked cells and transplant these cells into mice. The lowest number of gene-marked cells necessary for successful contribution for reconstitution of a human hematopoietic system could therefore be determined. Then, the frequency of long-term repopulating cells within the gene marked cell population could be calculated. According to the results presented in this thesis, one can assume that the frequency of long-term

repopulating HSCs is higher in the CD105-LV transduced cell population than in the VSVG-LV gene marked cell population.

As demonstrated in this thesis, CD105-LV is able to transduce unstimulated CD34⁺ cells more efficiently than VSVG-LV. Also other approaches have been investigated to improve transduction of quiescent cells. Verhoeven et al. generated VSVG-pseudotyped LVs displaying “early-acting-cytokines”, namely thrombopoietin (TPO) and stem cell factor (SCF). CD34⁺ cells were not pre-stimulated by adding cytokines to the medium, but cells were only stimulated during vector particle entry. Using this transient stimulation, the transduction efficiency was enhanced while maintaining the stem cell capabilities of the transduced cells. This resulted in selective transduction of long-term repopulating cells (Verhoeven et al., 2005). This cytokine displaying vector was improved by replacing the VSVG with RDTR, a chimeric envelope protein consisting of the extracellular and transmembrane domains of the feline leukemia virus RD114 and the cytoplasmic tail of the murine leukemia virus amphotropic envelope (MLV-A) (Di Nunzio et al., 2007). This newly generated vector RDTR/SCFHA-LV was able to obtain higher transduction rates of CD34⁺ cells in unfractionated blood of patients suffering from Fanconi anemia, compared to RDTR-LV, VSVG/SCFHA-LV or VSVG-LV. In addition, the vector preferentially transduced CD34⁺ cells in mice reconstituted with human HSCs after intrafemoral vector administration (Frecha et al., 2012).

Another vector that was rationally generated to transduce primitive and unstimulated HSCs is the CD133-targeted LV. CD34 and CD133 expression on HSCs correlates well, but HSCs include a subpopulation of CD34⁻CD133⁺ cells that can be converted to CD34⁺CD133⁺ cells, indicating that CD34⁻CD133⁺ cells represent a more primitive HSC population, and that CD133 is a marker for long-term repopulating HSCs (Gallacher et al., 2000). Brendel et al. produced CD133-targeted LV (CD133-LV) using vectors pseudotyped with the measles H and F protein. After transduction of unstimulated CD34⁺ cells, CD133-LV outperformed VSVG-LV in repopulation experiments in first and second transplantation of gene marked CD34⁺ cells in NSG mice (Brendel et al., 2015). Recently, Girard-Gagnepain et al. showed up to 30% of GFP⁺ cells following gene transfer into unstimulated CD34⁺ cells with BaEVgp-LVs (Girard-Gagnepain et al., 2014). These LVs were pseudotyped with a chimeric glycoprotein consisting of the cytoplasmic tail of MLV-A and the glycoprotein of the

baboon endogenous retrovirus (BaEV). BaEV recognizes the receptors neutral amino acid transporter 1 (ASCT-1) and ASCT-2 (Rasko et al., 1999; Marin et al., 2000) that are present on CD34⁺ cells. In contrast to these observations, transduction efficiencies of unstimulated CD34⁺ cells did not exceed 10% using CD133-LV (Brendel et al., 2015). However, a 10-fold higher vector dose (MOI 10) was used for BaEVgp-LV mediated gene delivery. In addition, these high transduction efficiencies were only achieved in the presence of the transduction enhancer retronectin (Girard-Gagnepain et al., 2014), whereas transduction of CD34⁺ cells by CD133-LV was performed in uncoated cell culture plates (Brendel et al., 2015).

While the transduction of CD34⁺ cells with the LVs discussed above in the absence of a transduction enhancer results in relatively low transduction efficiencies, all of the vectors show stable transduction into long-term repopulating cells. Gene transfer into few of these cells, can reconstitute the entire hematopoietic system with cells carrying the corrected gene compensating for initially low transduction events. Others showed that CD133 is expressed on these primitive HSCs (Gallacher et al., 2000), and it could be confirmed for CD105 in this thesis. In contrast, the HSPC subpopulation transduced by BaEVgp-LV or RDTR/SCFHA-LV has not been fully characterized. Depending on the application, it might be favorable to transduce defined subpopulations by receptor-targeted LVs or to deliver a transgene into a broader HSPC population expressing the receptors of RDTR/SCFHA-LV or BaEVgp-LV. To date, only CD105-LV and CD133-LV have been compared with the state of the art vector (VSVG-LV) side by side within the same animal. Thereby, the variability in repopulation experiments, influenced by the culture conditions, donor cells and individual mouse variability to engraft human cells, can be circumvented. Thus, final conclusions about the performance of all the HSC-targeted vectors discussed above should ideally be based on competitive repopulation experiments *in vivo*.

4.4 Potential of receptor-targeted lentiviral vectors

VSVG-LVs have been successfully used in clinical trials for the transduction of HSCs providing benefit to the patients (Cartier et al., 2009; Aiuti et al., 2013; Biffi et al., 2013). The broad tropism of VSVG-LVs enables gene transfer into all mammalian cells including HSPCs, although this requires pre-stimulation of quiescent CD34⁺

cells. In this thesis, selective and efficient gene transfer of the marker gene *egfp* into unstimulated long-term repopulating cells using CD105-LV was demonstrated. The therapeutic applicability of receptor-targeted LVs was shown by Brendel et al. using CD133-LV. Transduction of CD34⁺ cells from a X-CGD patient with CD133-LV transferring *pg91^{phox}* resulted in the expression of the therapeutic gene in human cells for at least 10 weeks after transplantation of the modified cells into NSG mice (Brendel et al., 2015), which demonstrates the potential of receptor-targeted LVs for the use in clinical applications. However, for broad application the production of receptor-targeted LVs, such as CD105-LV, needs to be optimized. Currently, the yield of CD105-LV is 35-fold lower than that of VSVG-LV (Anliker et al., 2010). Nevertheless, a lower vector dose of CD105-LV is required for efficient transduction of long-term repopulating HSCs. Due to the selective transduction of CD105⁺ cells by CD105-LV, the cell population that is genetically modified is smaller compared to VSVG-LV transduced cells that include also CD105⁻ cells. In combination with the lower amount of CD105-LV that is required for transduction, it is conceivable that the risk of multicopy vector integration and insertional mutagenesis is reduced compared to VSVG-LVs mediated gene therapy. However, the vector copy number within CD105-LV transduced cells needs to be analyzed.

By the use of receptor-targeted LVs even *in vivo* gene transfer into HSCs is conceivable. The current standard for HSC-based gene therapy is *ex vivo* modification of CD34⁺ cells using VSVG-LVs (Cartier et al., 2009; Aiuti et al., 2013; Biffi et al., 2013). Ultimately, *in vivo* gene delivery into HSCs is desirable. Thereby, the procedure of harvesting cells from the patients could be prevented. Additionally, primitive CD34⁻ cell populations, such as CD133⁺CD34⁻ (Gallacher et al., 2000) that are currently lost during the purification of CD34⁺ cells from mobilized peripheral blood or BM could be transduced. However, LV-based *in vivo* gene transfer into HSCs faces several challenges. VSVG-pseudotyped LVs are not suitable for *in vivo* application, since systemical gene transfer is difficult to control due to the broad tropism. Furthermore, antibody and complement mediated immune response against the glycoprotein could be induced and cytotoxicity was observed when VSVG-LV was administered at high doses *in vivo* (DePolo et al., 2000; Higashikawa and Chang, 2001; Watson et al., 2002). Moreover, VSVG-LVs poorly transduce unstimulated HSCs (Amirache et al., 2014). Clearly, LVs for *in vivo* HSC gene therapy should restrict gene transfer into specific target cells and result in efficient gene transfer into

unstimulated HSCs. Furthermore, safety issues concerning insertional mutagenesis, ectopic transgene expression, cytotoxic effects of the transgene or induction of an immune response must be clarified.

By the use of receptor-targeted LVs, gene delivery is restricted to specific cells limiting vector integration and transgene expression to target cells. The high specificity of receptor-targeted LVs has been demonstrated in *in vivo* applications (Münch et al., 2011; Zhou et al., 2012; Abel et al., 2013). CD105 is not only expressed on HSCs, but also on activated endothelial cells, activated macrophages, mesenchymal stem cells and progenitor endothelial cells (Nassiri et al., 2011; Lin et al., 2013). This is important to keep in mind when planning *in vivo* studies. *In vivo* selectivity for HSCs could be achieved by local injection into the BM and possible further vector modifications such as cell specific promoters or the integration of microRNA (miRNA) target sequences into the 3'UTR of the transgene. Binding of complementary endogenous miRNA to the transcribed transgene reduces or eliminates the transgene translation, thereby detargeting the transgene expression within specific cell types (Heckl et al., 2011; Chiriaco et al., 2014). Other approaches include the use of integrase-deficient LVs (IDLVs) in combination with a tool allowing site-targeted integration into the host genome such as zinc-finger nucleases (ZFN) (Lombardo et al., 2007; Genovese et al., 2014; Hoban et al., 2015).

Combining the safety mechanisms mentioned above, will enhance the safety of LVs further and will allow gene therapy of HSCs *in vivo* sometime in the near future. However, the risk associated with *in vivo* HSC gene therapy must be considered in relation to the severity of the disease.

Receptor-targeted LVs are not only useful tools for gene therapy, but also for tracking and identification of cells, as demonstrated in this thesis. Cells expressing a specific surface protein can be selectively transduced by receptor-targeted LVs transferring reporter genes. Then, all cells derived from the target-receptor positive cell can be identified by the transferred reporter gene and analyzed in detail at various time points, e.g. regarding specific surface markers by flow cytometry and be assigned to specific cell populations. Thereby, the gene-marked cells can be traced, even if the targeted surface protein is not expressed during or after the differentiation process. The flexibility of the targeting system has been demonstrated by replacing the targeting ligand (Anliker et al., 2010). Thus, the approach shown in this thesis can be

easily transferred to other specific surface markers and will allow the identification of other potential markers on stem or progenitor cell populations.

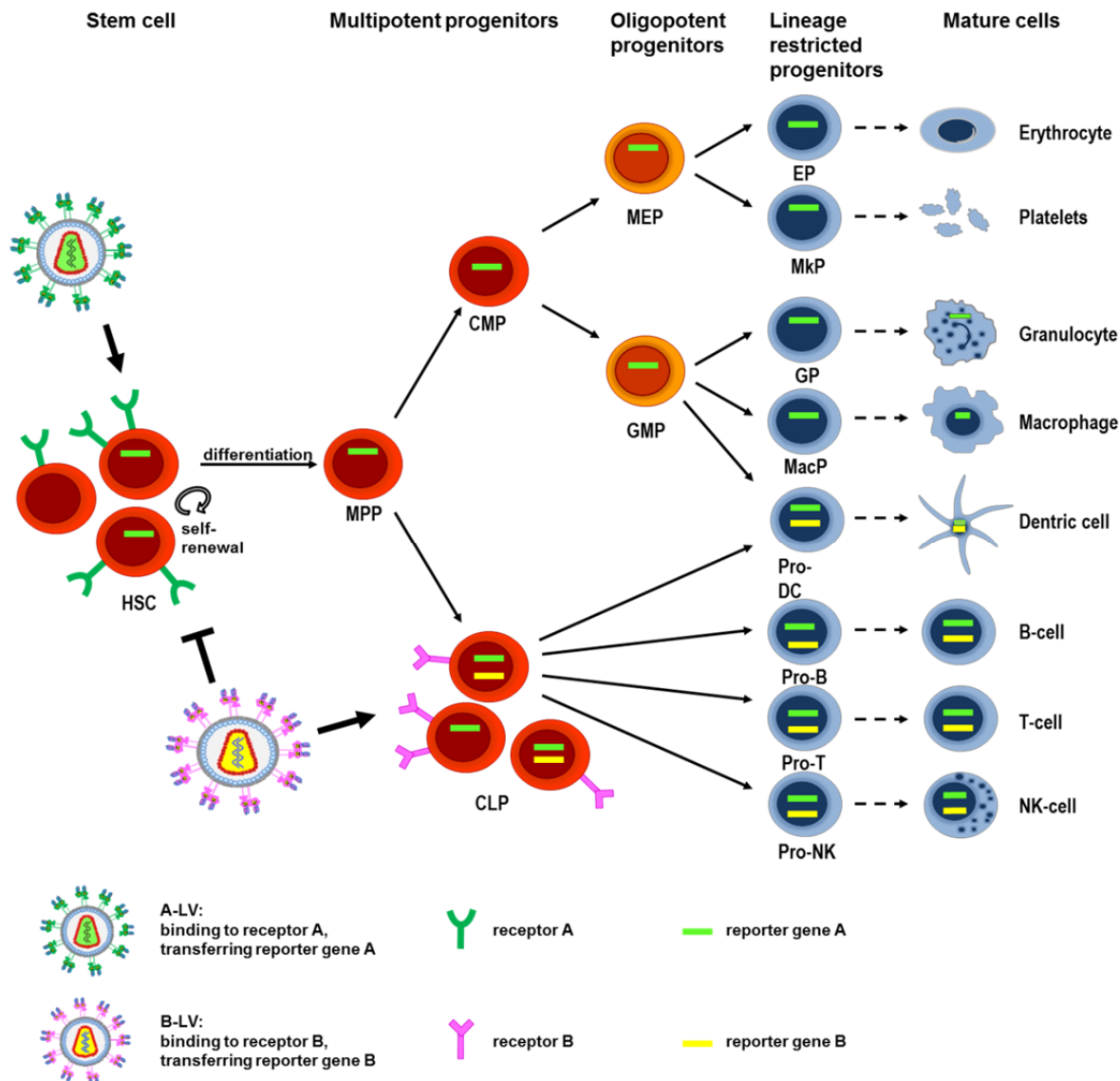


Figure 30: Tracking of gene-marked cells using receptor-targeted LVs. HSCs differentiate into multipotent and oligopotent progenitor cells and then into mature cells of the hematopoietic system. The various subpopulations are defined by the expression of specific surface proteins. Receptor targeted LVs can be used to gene mark cells of a specific subpopulation. By expression of the marker gene, the cells can be tracked during the differentiation process. LV with green surface proteins represents LV binding to receptor A (green), LV with pink surface proteins binds to receptor B (pink). Green bar represents reporter gene A, yellow bar reporter gene B. HSC, hematopoietic stem cell; MPP, multipotent progenitor; CLP, common lymphoid progenitor; CMP, common myeloid progenitor; MEP, megakaryocyte/erythrocyte progenitor; GMP, granulocyte/macrophage progenitor; EP, erythrocyte progenitor; MkP, megakaryocyte progenitor; GP, granulocyte progenitor; MacP, macrophage progenitor; Pro-DC, dendritic cell progenitor; Pro-B, B-cell progenitor; Pro-T, T-cell progenitor and Pro-NK, natural killer cell progenitor.

5. REFERENCES

- Abel, T., El Filali, E., Waern, J., Schneider, I.C., Yuan, Q., Münch, R.C., Hick, M., Warnecke, G., Madrahimov, N., and Kontermann, R.E., et al. (2013). Specific gene delivery to liver sinusoidal and artery endothelial cells. *Blood* 122, 2030-2038.
- Ahmed, B.Y., Chakravarthy, S., Eggers, R., Hermens, Wim T J M C, Zhang, J.Y., Niclou, S.P., Levelt, C., Sablitzky, F., Anderson, P.N., and Lieberman, A.R., et al. (2004). Efficient delivery of Cre-recombinase to neurons in vivo and stable transduction of neurons using adeno-associated and lentiviral vectors. *BMC neuroscience* 5, 4.
- Aiuti, A., Biasco, L., Scaramuzza, S., Ferrua, F., Cicalese, M.P., Baricordi, C., Dionisio, F., Calabria, A., Giannelli, S., and Castiello, M.C., et al. (2013). Lentiviral hematopoietic stem cell gene therapy in patients with Wiskott-Aldrich syndrome. *Science (New York, N.Y.)* 341, 1233151.
- Amirache, F., Lévy, C., Costa, C., Mangeot, P.-E., Torbett, B.E., Wang, C.X., Nègre, D., Cosset, F.-L., and Verhoeven, E. (2014). Mystery solved: VSV-G-LVs do not allow efficient gene transfer into unstimulated T cells, B cells, and HSCs because they lack the LDL receptor. *Blood* 123, 1422-1424.
- Anliker, B., Abel, T., Kneissl, S., Hlavaty, J., Caputi, A., Brynza, J., Schneider, I.C., Münch, R.C., Petznek, H., and Kontermann, R.E., et al. (2010). Specific gene transfer to neurons, endothelial cells and hematopoietic progenitors with lentiviral vectors. *Nature methods* 7, 929-935.
- Apolonia, L. (2009). Development and Application of Non-Integrating Lentiviral Vectors for Gene Therapy. Dissertation (London).
- Bainbridge, James W B, Smith, A.J., Barker, S.S., Robbie, S., Henderson, R., Balaggan, K., Viswanathan, A., Holder, G.E., Stockman, A., and Tyler, N., et al. (2008). Effect of gene therapy on visual function in Leber's congenital amaurosis. *The New England journal of medicine* 358, 2231-2239.
- Baum CM, Weissman IL, Tsukamoto AS, Buckle AM, and Peault B (1992). Isolation of a candidate human hematopoietic stem-cell population. *Proceedings of the National Academy of Sciences of the United States of America*, 2804-2808.

- Berns, K., and Parrish, C.R. (2006). Parvoviridae. In Fields Virology, David M Knipe, Peter M Howley, ed. (Philadelphia: Lippincott Williams & Wilkins).
- Biffi, A., Montini, E., Lorioli, L., Cesani, M., Fumagalli, F., Plati, T., Baldoli, C., Martino, S., Calabria, A., and Canale, S., et al. (2013). Lentiviral hematopoietic stem cell gene therapy benefits metachromatic leukodystrophy. *Science (New York, N.Y.)* 341, 1233158.
- Blaese, R.M., Culver, K.W., Miller, A.D., Carter, C.S., Fleisher, T., Clerici, M., Shearer, G., Chang, L., Chiang, Y., and Tolstoshev, P., et al. (1995). T lymphocyte-directed gene therapy for ADA- SCID: initial trial results after 4 years. *Science (New York, N.Y.)* 270, 475-480.
- Braun, C.J., Boztug, K., Paruzynski, A., Witzel, M., Schwarzer, A., Rothe, M., Modlich, U., Beier, R., Göhring, G., and Steinemann, D., et al. (2014). Gene therapy for Wiskott-Aldrich syndrome--long-term efficacy and genotoxicity. *Science translational medicine* 6, 227ra33.
- Brendel, C., Goebel, B., Daniela, A., Brugman, M., Kneissl, S., Schwäble, J., Kaufmann, K.B., Müller-Kuller, U., Kunkel, H., and Chen-Wichmann, L., et al. (2015). CD133-targeted gene transfer into long-term repopulating hematopoietic stem cells. *Molecular therapy : the journal of the American Society of Gene Therapy* 23, 63-70.
- Brown, B.D., Sitia, G., Annoni, A., Hauben, E., Sergi, L.S., Zingale, A., Roncarolo, M.G., Guidotti, L.G., and Naldini, L. (2007). In vivo administration of lentiviral vectors triggers a type I interferon response that restricts hepatocyte gene transfer and promotes vector clearance. *Blood* 109, 2797-2805.
- Buller, R.M., Janik, J.E., Sebring, E.D., and Rose, J.A. (1981). Herpes simplex virus types 1 and 2 completely help adenovirus-associated virus replication. *Journal of virology* 40, 241-247.
- Butler, S.L., Hansen, M.S., and Bushman, F.D. (2001). A quantitative assay for HIV DNA integration in vivo. *Nature medicine* 7, 631-634.
- Cartier, N., Hacein-Bey-Abina, S., Bartholomae, C.C., Bougnères, P., Schmidt, M., Kalle, C. von, Fischer, A., Cavazzana-Calvo, M., and Aubourg, P. (2012). Lentiviral hematopoietic cell gene therapy for X-linked adrenoleukodystrophy. *Methods in enzymology* 507, 187-198.

- Cartier, N., Hacein-Bey-Abina, S., Bartholomae, C.C., Veres, G., Schmidt, M., Kutschera, I., Vidaud, M., Abel, U., Dal-Cortivo, L., and Caccavelli, L., et al. (2009). Hematopoietic stem cell gene therapy with a lentiviral vector in X-linked adrenoleukodystrophy. *Science (New York, N.Y.)* 326, 818-823.
- Casto, B.C., Atchison, R.W., and Hammon, W.M. (1967). Studies on the relationship between adeno-associated virus type I (AAV-1) and adenoviruses. I. Replication of AAV-1 in certain cell cultures and its effect on helper adenovirus. *Virology* 32, 52-59.
- Cavazzana-Calvo, M., Payen, E., Negre, O., Wang, G., Hehir, K., Fusil, F., Down, J., Denaro, M., Brady, T., and Westerman, K., et al. (2010). Transfusion independence and HMGA2 activation after gene therapy of human [bgr]-thalassaemia. *Nature* 467, 318-322.
- Chen, C., Akerstrom, V., Baus, J., Lan, M.S., and Breslin, M.B. (2013). Comparative analysis of the transduction efficiency of five adeno associated virus serotypes and VSV-G pseudotype lentiviral vector in lung cancer cells. *Virology journal* 10, 86.
- Chen, C.-Z., Li, L., Li, M., and Lodish, H.F. (2003). The endoglin(positive) sca-1(positive) rhodamine(low) phenotype defines a near-homogeneous population of long-term repopulating hematopoietic stem cells. *Immunity* 19, 525-533.
- Chen, C.-Z., Li, M., Graaf, D. de, Monti, S., Göttgens, B., Sanchez, M.-J., Lander, E.S., Golub, T.R., Green, A.R., and Lodish, H.F. (2002). Identification of endoglin as a functional marker that defines long-term repopulating hematopoietic stem cells. *Proceedings of the National Academy of Sciences of the United States of America* 99, 15468-15473.
- Chiriaco, M., Farinelli, G., Capo, V., Zonari, E., Scaramuzza, S., Di Matteo, G., Sergi, L.S., Migliavacca, M., Hernandez, R.J., and Bombelli, F., et al. (2014). Dual-regulated lentiviral vector for gene therapy of X-linked chronic granulomatosis. *Molecular therapy : the journal of the American Society of Gene Therapy* 22, 1472-1483.
- Civin CI, Strauss LC, Brovall C, Fackler MJ, Schwartz JF, and Shaper JH (1984). Antigenic analysis of hematopoiesis. III. A hematopoietic progenitor cell surface antigen defined by a monoclonal antibody raised against KG-1a cells. *Journal of immunology (Baltimore, Md. : 1950)*, 157-165.
- Cronin, J., Zhang, X.-Y., and Reiser, J. (2005). Altering the tropism of lentiviral vectors through pseudotyping. *Current gene therapy* 5, 387-398.

- Deichmann, A., Hacein-Bey-Abina, S., Schmidt, M., Garrigue, A., Brugman, M.H., Hu, J., Glimm, H., Gyapay, G., Prum, B., and Fraser, C.C., et al. (2007). Vector integration is nonrandom and clustered and influences the fate of lymphopoiesis in SCID-X1 gene therapy. *The Journal of clinical investigation* **117**, 2225-2232.
- DePolo, N.J., Reed, J.D., Sheridan, P.L., Townsend, K., Sauter, S.L., Jolly, D.J., and Dubensky, T.W. (2000). VSV-G pseudotyped lentiviral vector particles produced in human cells are inactivated by human serum. *Molecular therapy : the journal of the American Society of Gene Therapy* **2**, 218-222.
- Di Nunzio, F., Piovani, B., Cosset, F.-L., Mavilio, F., and Stornaiuolo, A. (2007). Transduction of human hematopoietic stem cells by lentiviral vectors pseudotyped with the RD114-TR chimeric envelope glycoprotein. *Human gene therapy* **18**, 811-820.
- Ferreira, V., Petry, H., and Salmon, F. (2014). Immune Responses to AAV-Vectors, the Glybera Example from Bench to Bedside. *Frontiers in immunology* **5**, 82.
- Frecha, C., Costa, C., Nègre, D., Amirache, F., Trono, D., Rio, P., Bueren, J., Cosset, F.-L., and Verhoeyen, E. (2012). A novel lentiviral vector targets gene transfer into human hematopoietic stem cells in marrow from patients with bone marrow failure syndrome and in vivo in humanized mice. *Blood* **119**, 1139-1150.
- Frecha, C., Szécsi, J., Cosset, F.-L., and Verhoeyen, E. (2008). Strategies for targeting lentiviral vectors. *Current gene therapy* **8**, 449-460.
- Freed, E.O., and Martin, M.A. (2006). HIVs and Their Replication. In *Fields Virology*, David M Knipe, Peter M Howley, ed. (Philadelphia: Lippincott Williams & Wilkins).
- Friedel, T., Hanisch, L.J., Muth, A., Honegger, A., Abken, H., Plückthun, A., Buchholz, C.J., and Schneider, I.C. (2015). Receptor-targeted lentiviral vectors are exceptionally sensitive toward the biophysical properties of the displayed single-chain Fv. *Protein engineering, design & selection : PEDS*.
- Funke, S., Maisner, A., Mühlebach, M.D., Koehl, U., Grez, M., Cattaneo, R., Cichutek, K., and Buchholz, C.J. (2008). Targeted cell entry of lentiviral vectors. *Molecular therapy : the journal of the American Society of Gene Therapy* **16**, 1427-1436.

- Gallacher, L., Murdoch, B., Wu, D.M., Karanu, F.N., Keeney, M., and Bhatia, M. (2000). Isolation and characterization of human CD34(-)Lin(-) and CD34(+)Lin(-) hematopoietic stem cells using cell surface markers AC133 and CD7. *Blood* 95, 2813-2820.
- Gaudet, D., Méthot, J., and Kastelein, J. (2012). Gene therapy for lipoprotein lipase deficiency. *Current opinion in lipidology* 23, 310-320.
- Genovese, P., Schiroli, G., Escobar, G., Di Tomaso, T., Firrito, C., Calabria, A., Moi, D., Mazzieri, R., Bonini, C., and Holmes, M.C., et al. (2014). Targeted genome editing in human repopulating haematopoietic stem cells. *Nature* 510, 235-240.
- Geraerts, M., Willems, S., Baekelandt, V., Debysyer, Z., and Gijsbers, R. (2006). Comparison of lentiviral vector titration methods. *BMC biotechnology* 6, 34.
- Girard-Gagnepain, A., Amirache, F., Costa, C., Lévy, C., Frecha, C., Fusil, F., Nègre, D., Lavillette, D., Cosset, F.-L., and Verhoeven, E. (2014). Baboon envelope pseudotyped LVs outperform VSV-G-LVs for gene transfer into early-cytokine-stimulated and resting HSCs. *Blood* 124, 1221-1231.
- Glimm, H., Oh, I.H., and Eaves, C.J. (2000). Human hematopoietic stem cells stimulated to proliferate in vitro lose engraftment potential during their S/G(2)/M transit and do not reenter G(0). *Blood* 96, 4185-4193.
- Goyeneche, A.A., Carón, R.W., and Telleria, C.M. (2007). Mifepristone inhibits ovarian cancer cell growth in vitro and in vivo. *Clinical cancer research : an official journal of the American Association for Cancer Research* 13, 3370-3379.
- Grimm, D., Kern, A., Pawlita, M., Ferrari, F., Samulski, R., and Kleinschmidt, J. (1999). Titration of AAV-2 particles via a novel capsid ELISA: packaging of genomes can limit production of recombinant AAV-2. *Gene therapy* 6, 1322-1330.
- Grimm, D., Lee, J.S., Wang, L., Desai, T., Akache, B., Storm, T.A., and Kay, M.A. (2008). In vitro and in vivo gene therapy vector evolution via multispecies interbreeding and retargeting of adeno-associated viruses. *Journal of virology* 82, 5887-5911.
- Hacein-Bey-Abina, S., Kalle, C.v., Schmidt, M., McCormack, M.P., Wulffraat, N., Leboulch, P., Lim, A., Osborne, C.S., Pawliuk, R., and Morillon, E., et al. (2003).

LMO2-associated clonal T cell proliferation in two patients after gene therapy for SCID-X1. *Science (New York, N.Y.)* 302, 415-419.

Hall, P.A., Hughes, C.M., Staddon, S.L., Richman, P.I., Gullick, W.J., and Lemoine, N.R. (1990). The c-erb B-2 proto-oncogene in human pancreatic cancer. *The Journal of pathology* 161, 195-200.

Hao QL, Shah AJ, Thiemann FT, Smogorzewska EM, and Crooks GM (1995). A functional comparison of CD34 + CD38- cells in cord blood and bone marrow. *Blood*, 3745-3753.

Harlan Laboratories.
http://www.harlan.com/products_and_services/research_models_and_services/research_models/athymic_nude_mice/hsdathymic-nude-foxn1nu/the-netherlands.html.
24.03.2015.

Harvey, A.R., Kamphuis, W., Eggers, R., Symons, N.A., Blits, B., Niclou, S., Boer, G.J., and Verhaagen, J. (2002). Intravitreal injection of adeno-associated viral vectors results in the transduction of different types of retinal neurons in neonatal and adult rats: a comparison with lentiviral vectors. *Molecular and cellular neurosciences* 21, 141-157.

Hatzfeld, J., Li, M.L., Brown, E.L., Sookdeo, H., Levesque, J.P., O'Toole, T., Gurney, C., Clark, S.C., and Hatzfeld, A. (1991). Release of early human hematopoietic progenitors from quiescence by antisense transforming growth factor beta 1 or Rb oligonucleotides. *The Journal of experimental medicine* 174, 925-929.

Hauck, B., Chen, L., and Xiao, W. (2003). Generation and characterization of chimeric recombinant AAV vectors. *Molecular therapy : the journal of the American Society of Gene Therapy* 7, 419-425.

Hauck, B., and Xiao, W. (2003). Characterization of tissue tropism determinants of adeno-associated virus type 1. *Journal of virology* 77, 2768-2774.

Hauswirth, W.W., Aleman, T.S., Kaushal, S., Cideciyan, A.V., Schwartz, S.B., Wang, L., Conlon, T.J., Boye, S.L., Flotte, T.R., and Byrne, B.J., et al. (2008). Treatment of leber congenital amaurosis due to RPE65 mutations by ocular subretinal injection of adeno-associated virus gene vector: short-term results of a phase I trial. *Human gene therapy* 19, 979-990.

- Heckl, D., Wicke, D.C., Brugman, M.H., Meyer, J., Schambach, A., Büsche, G., Ballmaier, M., Baum, C., and Modlich, U. (2011). Lentiviral gene transfer regenerates hematopoietic stem cells in a mouse model for Mpl-deficient aplastic anemia. *Blood* 117, 3737-3747.
- Higashikawa, F., and Chang, L. (2001). Kinetic analyses of stability of simple and complex retroviral vectors. *Virology* 280, 124-131.
- Hoban, M.D., Cost, G.J., Mendel, M.C., Romero, Z., Kaufman, M.L., Joglekar, A.V., Ho, M., Lumaquin, D., Gray, D., and Lill, G.R., et al. (2015). Correction of the sickle cell disease mutation in human hematopoietic stem/progenitor cells. *Blood* 125, 2597-2604.
- Howe, S.J., Mansour, M.R., Schwarzwälder, K., Bartholomae, C., Hubank, M., Kempski, H., Brugman, M.H., Pike-Overzet, K., Chatters, S.J., and Ridder, D. de, et al. (2008). Insertional mutagenesis combined with acquired somatic mutations causes leukemogenesis following gene therapy of SCID-X1 patients. *The Journal of clinical investigation* 118, 3143-3150.
- Jacobson, S.G., Cideciyan, A.V., Ratnakaram, R., Heon, E., Schwartz, S.B., Roman, A.J., Peden, M.C., Aleman, T.S., Boye, S.L., and Sumaroka, A., et al. (2012). Gene therapy for leber congenital amaurosis caused by RPE65 mutations: safety and efficacy in 15 children and adults followed up to 3 years. *Archives of ophthalmology* 130, 9-24.
- Joyeux, L., Danzer, E., Limberis, M.P., Zoltick, P.W., Radu, A., Flake, A.W., and Davey, M.G. (2014). In utero lung gene transfer using adeno-associated viral and lentiviral vectors in mice. *Human gene therapy methods* 25, 197-205.
- Kay, M.A., Manno, C.S., Ragni, M.V., Larson, P.J., Couto, L.B., McClelland, A., Glader, B., Chew, A.J., Tai, S.J., and Herzog, R.W., et al. (2000). Evidence for gene transfer and expression of factor IX in haemophilia B patients treated with an AAV vector. *Nature genetics* 24, 257-261.
- Kays, S.-K., Kaufmann, K.B., Abel, T., Brendel, C., Bonig, H., Grez, M., Buchholz, C.J., and Kneissl, S. (2015). CD105 Is a Surface Marker for Receptor-Targeted Gene Transfer into Human Long-Term Repopulating Hematopoietic Stem Cells. *Stem cells and development* 24, 714-723.

- Kern, A., Schmidt, K., Leder, C., Muller, O.J., Wobus, C.E., Bettinger, K., Von der Lieth, C. W., King, J.A., and Kleinschmidt, J.A. (2003). Identification of a Heparin-Binding Motif on Adeno-Associated Virus Type 2 Capsids. *Journal of virology* 77, 11072-11081.
- Kittler, E.L., Peters, S.O., Crittenden, R.B., Debatis, M.E., Ramshaw, H.S., Stewart, F.M., and Quesenberry, P.J. (1997). Cytokine-facilitated transduction leads to low-level engraftment in nonablated hosts. *Blood* 90, 865-872.
- Kotin, R.M., Siniscalco, M., Samulski, R.J., Zhu, X.D., Hunter, L., Laughlin, C.A., McLaughlin, S., Muzyczka, N., Rocchi, M., and Berns, K.I. (1990). Site-specific integration by adeno-associated virus. *Proceedings of the National Academy of Sciences of the United States of America* 87, 2211-2215.
- Kumar, M., Keller, B., Makalou, N., and Sutton, R.E. (2001). Systematic determination of the packaging limit of lentiviral vectors. *Human gene therapy* 12, 1893-1905.
- Landau, N.R., Page, K.A., and Littman, D.R. (1991). Pseudotyping with human T-cell leukemia virus type I broadens the human immunodeficiency virus host range. *Journal of virology* 65, 162-169.
- Letamendía, A., Lastres, P., Almendro, N., Raab, U., Bühring, H.J., Kumar, S., and Bernabéu, C. (1998). Endoglin, a component of the TGF-beta receptor system, is a differentiation marker of human choriocarcinoma cells. *International journal of cancer. Journal international du cancer* 76, 541-546.
- Li, C., Goudy, K., Hirsch, M., Asokan, A., Fan, Y., Alexander, J., Sun, J., Monahan, P., Seiber, D., and Sidney, J., et al. (2009). Cellular immune response to cryptic epitopes during therapeutic gene transfer. *Proceedings of the National Academy of Sciences of the United States of America* 106, 10770-10774.
- Li, D.Y., Sorensen, L.K., Brooke, B.S., Urness, L.D., Davis, E.C., Taylor, D.G., Boak, B.B., and Wendel, D.P. (1999). Defective angiogenesis in mice lacking endoglin. *Science (New York, N.Y.)* 284, 1534-1537.
- Lin, C.-S., Xin, Z.-C., Dai, J., and Lue, T.F. (2013). Commonly Used Mesenchymal Stem Cell Markers and Tracking Labels: Limitations and Challenges. *Histology and histopathology* 28, 1109-1116.

- Lizée, G., Aerts, J.L., Gonzales, M.I., Chinnasamy, N., Morgan, R.A., and Topalian, S.L. (2003). Real-time quantitative reverse transcriptase-polymerase chain reaction as a method for determining lentiviral vector titers and measuring transgene expression. *Human gene therapy* 14, 497-507.
- Lombardo, A., Genovese, P., Beausejour, C.M., Colleoni, S., Lee, Y.-L., Kim, K.A., Ando, D., Urnov, F.D., Galli, C., and Gregory, P.D., et al. (2007). Gene editing in human stem cells using zinc finger nucleases and integrase-defective lentiviral vector delivery. *Nature biotechnology* 25, 1298-1306.
- Maguire, A.M., Simonelli, F., Pierce, E.A., Pugh, E.N., Mingozzi, F., Bennicelli, J., Banfi, S., Marshall, K.A., Testa, F., and Surace, E.M., et al. (2008). Safety and efficacy of gene transfer for Leber's congenital amaurosis. *The New England journal of medicine* 358, 2240-2248.
- Maheshri, N., Koerber, J.T., Kaspar, B.K., and Schaffer, D.V. (2006). Directed evolution of adeno-associated virus yields enhanced gene delivery vectors. *Nature biotechnology* 24, 198-204.
- Majeti, R., Park, C.Y., and Weissman, I.L. (2007). Identification of a Hierarchy of Multipotent Hematopoietic Progenitors in Human Cord Blood. *Cell stem cell* 1, 635-645.
- Manno, C.S., Pierce, G.F., Arruda, V.R., Glader, B., Ragni, M., Rasko, J.J., Rasko, J., Ozelo, M.C., Hoots, K., and Blatt, P., et al. (2006). Successful transduction of liver in hemophilia by AAV-Factor IX and limitations imposed by the host immune response. *Nature medicine* 12, 342-347.
- Marin, M., Tailor, C.S., Nouri, A., and Kabat, D. (2000). Sodium-dependent neutral amino acid transporter type 1 is an auxiliary receptor for baboon endogenous retrovirus. *Journal of virology* 74, 8085-8093.
- Mays, L.E., and Wilson, J.M. (2011). The complex and evolving story of T cell activation to AAV vector-encoded transgene products. *Molecular therapy : the journal of the American Society of Gene Therapy* 19, 16-27.
- McCarty, D.M. (2008). Self-complementary AAV vectors; advances and applications. *Molecular therapy : the journal of the American Society of Gene Therapy* 16, 1648-1656.

- McCarty, D.M., Fu, H., Monahan, P.E., Toulson, C.E., Naik, P., and Samulski, R.J. (2003). Adeno-associated virus terminal repeat (TR) mutant generates self-complementary vectors to overcome the rate-limiting step to transduction in vivo. *Gene therapy* 10, 2112-2118.
- McCarty, D.M., Monahan, P.E., and Samulski, R.J. (2001). Self-complementary recombinant adeno-associated virus (scAAV) vectors promote efficient transduction independently of DNA synthesis. *Gene therapy* 8, 1248-1254.
- McPherson, R.A., Rosenthal, L.J., and Rose, J.A. (1985). Human cytomegalovirus completely helps adeno-associated virus replication. *Virology* 147, 217-222.
- Michelfelder, S., Lee, M.-K., deLima-Hahn, E., Wilmes, T., Kaul, F., Müller, O., Kleinschmidt, J.A., and Trepel, M. (2007). Vectors selected from adeno-associated viral display peptide libraries for leukemia cell-targeted cytotoxic gene therapy. *Experimental hematology* 35, 1766-1776.
- Mingozzi, F., and High, K.A. (2011). Immune responses to AAV in clinical trials. *Current gene therapy* 11, 321-330.
- Mingozzi, F., Meulenberg, J.J., Hui, D.J., Basner-Tschakarjan, E., Hasbrouck, N.C., Edmonson, S.A., Hutnick, N.A., Betts, M.R., Kastelein, J.J., and Stroes, E.S., et al. (2009). AAV-1-mediated gene transfer to skeletal muscle in humans results in dose-dependent activation of capsid-specific T cells. *Blood* 114, 2077-2086.
- Miraglia, S., Godfrey, W., Yin, A.H., Atkins, K., Warnke, R., Holden, J.T., Bray, R.A., Waller, E.K., and Buck, D.W. (1997). A Novel Five-Transmembrane Hematopoietic Stem Cell Antigen: Isolation, Characterization, and Molecular Cloning. *Blood* 90, 5013-5021.
- Mitchell, R.S., Beitzel, B.F., Schroder, Astrid R W, Shinn, P., Chen, H., Berry, C.C., Ecker, J.R., and Bushman, F.D. (2004). Retroviral DNA integration: ASLV, HIV, and MLV show distinct target site preferences. *PLoS biology* 2, E234.
- Miyoshi, H., Blömer, U., Takahashi, M., Gage, F.H., and Verma, I.M. (1998). Development of a self-inactivating lentivirus vector. *Journal of virology* 72, 8150-8157.

- Müller, O.J., Kaul, F., Weitzman, M.D., Pasqualini, R., Arap, W., Kleinschmidt, J.A., and Trepel, M. (2003). Random peptide libraries displayed on adeno-associated virus to select for targeted gene therapy vectors. *Nature biotechnology* 21, 1040-1046.
- Münch, R.C. (2013). A rational approach for targeted cell entry of adeno-associated viral vectors. Dissertation (Heidelberg).
- Münch, R.C., Janicki, H., Völker, I., Rasbach, A., Hallek, M., Büning, H., and Buchholz, C.J. (2013). Displaying high-affinity ligands on adeno-associated viral vectors enables tumor cell-specific and safe gene transfer. *Molecular therapy : the journal of the American Society of Gene Therapy* 21, 109-118.
- Münch, R.C., Mühlbach, M.D., Schaser, T., Kneissl, S., Jost, C., Plückthun, A., Cichutek, K., and Buchholz, C.J. (2011). DARPinS: an efficient targeting domain for lentiviral vectors. *Molecular therapy : the journal of the American Society of Gene Therapy* 19, 686-693.
- Münch, R.C., Muth, A., Muik, A., Friedel, T., Schmatz, J., Dreier, B., Trkola, A., Plückthun, A., Büning, H., and Buchholz, C.J. (2015). Off-target-free gene delivery by affinity-purified receptor-targeted viral vectors. *Nature communications* 6, 6246.
- Naldini, L. (2011). Ex vivo gene transfer and correction for cell-based therapies. *Nature reviews. Genetics* 12, 301-315.
- Nassiri, F., Cusimano, M.D., Scheithauer, B.W., Rotondo, F., Fazio, A., Yousef, G.M., Syro, L.V., Kovacs, K., and Lloyd, R.V. (2011). Endoglin (CD105): a review of its role in angiogenesis and tumor diagnosis, progression and therapy. *Anticancer research* 31, 2283-2290.
- Opie, S.R., Warrington, K.H., Agbandje-McKenna, M., Zolotukhin, S., and Muzyczka, N. (2003). Identification of amino acid residues in the capsid proteins of adeno-associated virus type 2 that contribute to heparan sulfate proteoglycan binding. *Journal of virology* 77, 6995-7006.
- Ott, M.G., Schmidt, M., Schwarzwälder, K., Stein, S., Siler, U., Koehl, U., Glimm, H., Kühlcke, K., Schilz, A., and Kunkel, H., et al. (2006). Correction of X-linked chronic granulomatous disease by gene therapy, augmented by insertional activation of MDS1-EVI1, PRDM16 or SETBP1. *Nature medicine* 12, 401-409.

- Page, K.A., Landau, N.R., and Littman, D.R. (1990). Construction and use of a human immunodeficiency virus vector for analysis of virus infectivity. *J Virol.* 11, 5270-5276.
- Palma, M. de, Montini, E., Santoni de Sio, Francesca R, Benedicenti, F., Gentile, A., Medico, E., and Naldini, L. (2005). Promoter trapping reveals significant differences in integration site selection between MLV and HIV vectors in primary hematopoietic cells. *Blood* 105, 2307-2315.
- Perabo, L., Büning, H., Kofler, D.M., Ried, M.U., Girod, A., Wendtner, C.M., Enssle, J., and Hallek, M. (2003). In vitro selection of viral vectors with modified tropism: the adeno-associated virus display. *Molecular therapy : the journal of the American Society of Gene Therapy* 8, 151-157.
- Perabo, L., Endell, J., King, S., Lux, K., Goldnau, D., Hallek, M., and Büning, H. (2006). Combinatorial engineering of a gene therapy vector: directed evolution of adeno-associated virus. *The journal of gene medicine* 8, 155-162.
- Pereira, C., Clarke, E., and Damen, J. (2007). Hematopoietic colony-forming cell assays. *Methods in molecular biology (Clifton, N.J.)* 407, 177-208.
- Persons, D.A., and Baum, C. (2011). Solving the problem of γ -retroviral vectors containing long terminal repeats. *Molecular therapy : the journal of the American Society of Gene Therapy* 19, 229-231.
- Philpott, N.J., Giraud-Wali, C., Dupuis, C., Gomos, J., Hamilton, H., Berns, K.I., and Falck-Pedersen, E. (2002). Efficient integration of recombinant adeno-associated virus DNA vectors requires a p5-rep sequence in cis. *Journal of virology* 76, 5411-5421.
- Pierelli, L., Bonanno, G., Rutella, S., Marone, M., Scambia, G., and Leone, G. (2001). CD105 (Endoglin) Expression on Hematopoietic Stem/Progenitor Cells. *Leuk Lymphoma* 42, 1195-1206.
- Pierelli, L., Scambia, G., Bonanno, G., Rutella, S., Puggioni, P., Battaglia, A., Mozzetti, S., Marone, M., Menichella, G., and Rumi, C., et al. (2000). CD34+/CD105+ cells are enriched in primitive circulating progenitors residing in the G0 phase of the cell cycle and contain all bone marrow and cord blood CD34+/CD38low/- precursors. *British journal of haematology* 108, 610-620.

- Pluta, K., and Kacprzak, M.M. (2009). Use of HIV as a gene transfer vector. *Acta biochimica Polonica* **56**, 531-595.
- Rasko, J.E., Battini, J.L., Gottschalk, R.J., Mazo, I., and Miller, A.D. (1999). The RD114/simian type D retrovirus receptor is a neutral amino acid transporter. *Proceedings of the National Academy of Sciences of the United States of America* **96**, 2129-2134.
- Ried, M.U., Girod, A., Leike, K., Buning, H., and Hallek, M. (2002). Adeno-Associated Virus Capsids Displaying Immunoglobulin-Binding Domains Permit Antibody-Mediated Vector Retargeting to Specific Cell Surface Receptors. *Journal of virology* **76**, 4559-4566.
- Rohr, U.-P., Wulf, M.-A., Stahn, S., Steidl, U., Haas, R., and Kronenwett, R. (2002). Fast and reliable titration of recombinant adeno-associated virus type-2 using quantitative real-time PCR. *Journal of virological methods* **106**, 81-88.
- Roques, M., Durand, C., Gautier, R., Canto, P.-Y., Petit-Cocault, L., Yvernogeau, L., Dunon, D., Souyri, M., and Jaffredo, T. (2012). Endoglin expression level discriminates long-term hematopoietic from short-term clonogenic progenitor cells in the aorta. *Haematologica* **97**, 975-979.
- Samulski, R.J., Zhu, X., Xiao, X., Brook, J.D., Housman, D.E., Epstein, N., and Hunter, L.A. (1991). Targeted integration of adeno-associated virus (AAV) into human chromosome 19. *The EMBO journal* **10**, 3941-3950.
- Sandrin, V., Boson, B., Salmon, P., Gay, W., Nègre, D., Le Grand, R., Trono, D., and Cosset, F.-L. (2002). Lentiviral vectors pseudotyped with a modified RD114 envelope glycoprotein show increased stability in sera and augmented transduction of primary lymphocytes and CD34+ cells derived from human and nonhuman primates. *Blood* **100**, 823-832.
- Sastray, L., Johnson, T., Hobson, M.J., Smucker, B., and Cornetta, K. (2002). Titering lentiviral vectors: comparison of DNA, RNA and marker expression methods. *Gene therapy* **9**, 1155-1162.
- Scherr, M., Battmer, K., Blömer, U., Ganser, A., and Grez, M. (2001). Quantitative determination of lentiviral vector particle numbers by real-time PCR. *BioTechniques* **31**, 520, 522, 524, passim.

- Schlehofer, J.R., Ehrbar, M., and Zur Hausen, H. (1986). Vaccinia virus, herpes simplex virus, and carcinogens induce DNA amplification in a human cell line and support replication of a helpervirus dependent parvovirus. *Virology* 152, 110-117.
- Schröder, A.R., Shinn, P., Chen, H., Berry, C., Ecker, J.R., and Bushman, F. (2002). HIV-1 integration in the human genome favors active genes and local hotspots. *Cell* 110, 521-529.
- Slamon, D.J., Clark, G.M., Wong, S.G., Levin, W.J., Ullrich, A., and McGuire, W.L. (1987). Human breast cancer: correlation of relapse and survival with amplification of the HER-2/neu oncogene. *Science (New York, N.Y.)* 235, 177-182.
- Slamon, D.J., Godolphin, W., Jones, L.A., Holt, J.A., Wong, S.G., Keith, D.E., Levin, W.J., Stuart, S.G., Udove, J., and Ullrich, A. (1989). Studies of the HER-2/neu proto-oncogene in human breast and ovarian cancer. *Science (New York, N.Y.)* 244, 707-712.
- Soneoka, Y., Cannon, P.M., Ramsdale, E.E., Griffiths, J.C., Romano, G., Kingsman, S.M., and Kingsman, A.J. (1995). A transient three-plasmid expression system for the production of high titer retroviral vectors. *Nucleic acids research* 23, 628-633.
- St-Jacques, S., Cymerman, U., Pece, N., and Letarte, M. (1994). Molecular characterization and in situ localization of murine endoglin reveal that it is a transforming growth factor-beta binding protein of endothelial and stromal cells. *Endocrinology* 134, 2645-2657.
- Terstappen, L.W., Huang, S., Safford, M., Lansdorp, P.M., and Loken (1991). Sequential generations of hematopoietic colonies derived from single nonlineage-committed CD34+CD38- progenitor cells. *Blood* 77, 1218-1227.
- van Maele, B., Rijck, J. de, Clercq, E. de, and Debyser, Z. (2003). Impact of the central polypurine tract on the kinetics of human immunodeficiency virus type 1 vector transduction. *Journal of virology* 77, 4685-4694.
- Vande Velde, G., Rangarajan, J.R., Toelen, J., Dresselaers, T., Ibrahimi, A., Krylychkina, O., Vreys, R., Van der Linden, A, Maes, F., and Debyser, Z., et al. (2011). Evaluation of the specificity and sensitivity of ferritin as an MRI reporter gene in the mouse brain using lentiviral and adeno-associated viral vectors. *Gene therapy* 18, 594-605.

- Vandendriessche, T., Thorrez, L., Acosta-Sanchez, A., Petrus, I., Wang, L., Ma, L., Waele, L. de, Iwasaki, Y., Gillijns, V., and Wilson, J.M., et al. (2007). Efficacy and safety of adeno-associated viral vectors based on serotype 8 and 9 vs. lentiviral vectors for hemophilia B gene therapy. *Journal of thrombosis and haemostasis : JTH* 5, 16-24.
- Verhoeyen, E., Wiznerowicz, M., Olivier, D., Izac, B., Trono, D., Dubart-Kupperschmitt, A., and Cosset, F.-L. (2005). Novel lentiviral vectors displaying "early-acting cytokines" selectively promote survival and transduction of NOD/SCID repopulating human hematopoietic stem cells. *Blood* 106, 3386-3395.
- Wang, G.P., Levine, B.L., Binder, G.K., Berry, C.C., Malani, N., McGarrity, G., Tebas, P., June, C.H., and Bushman, F.D. (2009). Analysis of lentiviral vector integration in HIV+ study subjects receiving autologous infusions of gene modified CD4+ T cells. *Molecular therapy : the journal of the American Society of Gene Therapy* 17, 844-850.
- Wang, L., Rosenberg, J.B., De, B.P., Ferris, B., Wang, R., Rivella, S., Kaminsky, S.M., and Crystal, R.G. (2012). In vivo gene transfer strategies to achieve partial correction of von Willebrand disease. *Human gene therapy* 23, 576-588.
- Wang, Z., Ma, H.-I., Li, J., Sun, L., Zhang, J., and Xiao, X. (2003). Rapid and highly efficient transduction by double-stranded adeno-associated virus vectors in vitro and in vivo. *Gene therapy* 10, 2105-2111.
- Warrington, K., Hillarby, M.C., Li, C., Letarte, M., and Kumar, S. (2005). Functional role of CD105 in TGF-beta1 signalling in murine and human endothelial cells. *Anticancer research* 25, 1851-1864.
- Watson, D.J., Kobinger, G.P., Passini, M.A., Wilson, J.M., and Wolfe, J.H. (2002). Targeted transduction patterns in the mouse brain by lentivirus vectors pseudotyped with VSV, Ebola, Mokola, LCMV, or MuLV envelope proteins. *Molecular therapy : the journal of the American Society of Gene Therapy* 5, 528-537.
- Wilk, T., Gross, I., Gowen, B.E., Rutten, T., Haas, F. de, Welker, R., Kräusslich, H.G., Boulanger, P., and Fuller, S.D. (2001). Organization of immature human immunodeficiency virus type 1. *Journal of virology* 75, 759-771.
- Wu, P., Xiao, W., Conlon, T., Hughes, J., Agbandje-McKenna, M., Ferkol, T., Flotte, T., and Muzyczka, N. (2000). Mutational analysis of the adeno-associated virus type

- 2 (AAV2) capsid gene and construction of AAV2 vectors with altered tropism. *Journal of virology* 74, 8635-8647.
- Wu, X., Li, Y., Crise, B., and Burgess, S.M. (2003). Transcription start regions in the human genome are favored targets for MLV integration. *Science (New York, N.Y.)* 300, 1749-1751.
- Wu, Z., Asokan, A., and Samulski, R.J. (2006). Adeno-associated virus serotypes: vector toolkit for human gene therapy. *Molecular therapy : the journal of the American Society of Gene Therapy* 14, 316-327.
- Xie, Q., Bu, W., Bhatia, S., Hare, J., Somasundaram, T., Azzi, A., and Chapman, M.S. (2002). The atomic structure of adeno-associated virus (AAV-2), a vector for human gene therapy. *Proceedings of the National Academy of Sciences of the United States of America* 99, 10405-10410.
- Yang, Q., Mamounas, M., Yu, G., Kennedy, S., Leaker, B., Merson, J., Wong-Staal, F., Yu, M., and Barber, J.R. (1998). Development of novel cell surface CD34-targeted recombinant adenoassociated virus vectors for gene therapy. *Human gene therapy* 9, 1929-1937.
- Yin, A.H., Miraglia, S., Zanjani, E.D., Almeida-Porada, G., Ogawa, M., Leary, A.G., Olweus, J., Kearney, J., and Buck, D.W. (1997). AC133, a Novel Marker for Human Hematopoietic Stem and Progenitor Cells. *Blood* 90, 5002-5012.
- Zhou, Q., Schneider, I.C., Edes, I., Honegger, A., Bach, P., Schönfeld, K., Schambach, A., Wels, W.S., Kneissl, S., and Uckert, W., et al. (2012). T-cell receptor gene transfer exclusively to human CD8(+) cells enhances tumor cell killing. *Blood* 120, 4334-4342.
- Zufferey, R., Nagy, D., Mandel, R.J., Naldini, L., and Trono, D. (1997). Multiply attenuated lentiviral vector achieves efficient gene delivery in vivo. *Nat Biotech* 15, 871-875.

6. ABBREVIATIONS

α	anti
°C	degree Celsius
AAV	adeno-associated virus
ADA	adenosine deaminase
ALD	adrenoleukodystrophy
ATCC	American Type Culture Collection
BFP	blue fluorescent protein
BM	bone marrow
bp	base pair
cap	capsid protein
CD	cluster of differentiation
CD	cluster of differentiation
cDNA	complementary DNA
CGD	chronic granulomatous disease
CMV	cytomegalovirus
DARPin	designed ankyrin repeat protein
DEPC	diethyl dicarbonate
DMEM	Dulbecco's modified Eagle medium
DMSO	dimethyl sulfoxide
DNA	deoxyribonucleic acid
E. coli	Escherichia coli
EDTA	ethylenediaminetetraacetic acid
EGFP	enhanced green fluorescent protein
ELISA	enzyme-linked immunosorbent assay
Env	envelope protein
EpCAM	epithelial cell adhesion molecule
et al.	and others
F	fusion protein
FACS	fluorescence-activated cell sorting
FCS	fetal calf serum
for	forward
fw	forward
g	gram
GFP	green fluorescent protein
GM-CSF	granulocyte colony stimulating factor
GOI	genomes per cell
H	hemagglutinin
HEK	human embryonic kidney
Her2/neu	human epidermal growth factor receptor 2
HIV	human immunodeficiency virus
HPLC	high-performance liquid chromatography
HRP	horseradish peroxidase

HSC	hematopoietic stem cell
HSCT	hematopoietic stem cell transplantation
HSPG	heparan sulfate proteoglycan
HSV-TK	herpes simplex virus thymidine kinase
IL2R	Interleukin-2 receptor
ITR	inverted terminal repeat
K	potassium
kDa	kilo Dalton
kg	kilogram
l	liter
LB	Luria-Bertani
LDL-R	low-density lipid receptor
LMO2	LIM domain only 2
LTR	long terminal repeat
luc	luciferase
LV	lentiviral vector
m	milli
Mg	Magnesium
MLD	metachromatic leukodystrophy
MLV	murine leukemia virus
MOI	multiplicity of infection
mRNA	messenger RNA
MV	measles virus
ns	not significant
NSG mice	NOD-scid IL2R $\gamma^{-/-}$ mice
ORF	open reading frame
p.t.	post transduction
PBMC	peripheral blood mononuclear cells
PBS	phosphate buffered saline
PBS M/K	PBS supplemented with Mg/K
PCR	polymerase chain reaction
PEI	polyethylenimine
PID	Primary immune deficiencies
qPCR	quantitative real-time PCR
rep	viral regulatory proteins
rev	reverse
RNA	ribonucleic acid
rpm	rounds per minute
RT	reverse transcription
rv	reverse
sCAAV	AAV vector with self-complementary genome
SCF	stem cell factor
scFv	single chain Fragment variable
SFFV	spleen focus forming virus

SIN-LV	self-inactivating LV
ssAAV	single-stranded AAV
T-ALL	T-cell lymphoblastic leukemia
TPO	thrombopoietin
tu	transducing unit
U	unit
V	volt
VP	viral protein
VSV	vesicular stomatitis virus
VSVG	envelope glycoprotein of VSV
WAS	Wiskott-Aldrich syndrome
Δ	delta
μ	micro
γ	gamma

7. CURRICULUM VITAE

Persönliche Informationen

Name: Sarah-Katharina Kays
Geburtstag: 3. August 1985
Geburtsort: Nürnberg

Ausbildung und Berufserfahrung

Juni 2015	Abgabe der Doktorarbeit am Fachbereich Biologie, TU Darmstadt Titel: Receptor-targeted viral vectors: Tracking of stem cells and side by side comparison of AAV and lentiviral vectors
Seit März 2015	Wissenschaftliche Mitarbeiterin am Paul-Ehrlich-Institut, Langen Arbeitsgruppe von Dr. Veronika von Messling
August 2011 – Februar 2015	Anfertigung der Doktorarbeit am Paul-Ehrlich-Institut, Langen Arbeitsgruppe von Prof. Dr. Christian Buchholz
Oktober 2008 – Oktober 2010	Studium der Biologie an der Technischen Universität München (TUM) Studienabschluss: Master of Science (Note: 1,1)
Oktober 2005 – Oktober 2008	Studium der Biologie an der Technischen Universität München (TUM) Studienabschluss: Bachelor of Science (Note: 2,0)
Juni 2005	Allgemeine Hochschulreife am Ostendorfer Gymnasium, Neumarkt i.d.Opf. (Note: 1,9)

8. DANKSAGUNG

Ich bedanke mich bei Herrn Prof. Dr. Christian J. Buchholz, für die Möglichkeit, meine Doktorarbeit in seiner Arbeitsgruppe am Paul-Ehrlich-Institut durchführen zu können, sowie die freundliche und angenehme Arbeitsatmosphäre. Seine Ratschläge, die sehr gute wissenschaftliche Anleitung und stete Diskussionsbereitschaft haben maßgeblich zum Gelingen dieser Arbeit beigetragen.

Frau Prof. Dr. Beatrix Süß danke ich für die nette und unkomplizierte Betreuung seitens der TU Darmstadt. Des Weiteren bedanke ich mich bei Frau Prof. Dr. Ulrike A. Nuber für ihre Bereitschaft, die Aufgabe der Zweitgutachterin für meine Arbeit zu übernehmen.

Ich bedanke mich bei allen Kooperationspartnern, mit denen ich in den letzten Jahren zusammenarbeiten durfte. Allen voran: Dr. Kerstin B. Kaufmann, Dr. Manuel Grez, Dr. Christian Brendel und Prof. Dr. Halvard Bönig.

Besonderer Dank geht an meine aktuellen und ehemaligen Kollegen Sabrina, Anke, Robert, Ruben, Alex, Theresa, Bevan, Tobi, Thorsten, Johanna, Irene, Qi, Jessi, Gundl, Manu, Ruth, Julia, Anett, Patricia und Dina. Danke für die tolle Arbeitsatmosphäre, die unzähligen Diskussionen, eure ständige Hilfsbereitschaft und die Zeit, die wir auch nach der Arbeit gemeinsam verbracht haben. Mit keiner anderen Gruppe hätte ich die Zeit der Promotion verbringen wollen.

Ein großes Dankeschön geht an meine Freunde für ihre Unterstützung und das Verständnis, das sie mir während der ganzen Arbeit entgegengebracht haben.

Besonders bedanke ich mich bei meinen Eltern, meiner Schwester und meiner besten Freundin. Danke für eure bedingungslose und uneingeschränkte Unterstützung in allen Lebenslagen! Danke, dass ihr mir diesen Weg ermöglicht habt!

9. EHRENWÖRTLICHE ERKLÄRUNG

Ich erkläre hiermit ehrenwörtlich, dass ich die vorliegende Arbeit entsprechend den Regeln guter wissenschaftlicher Praxis selbstständig und ohne unzulässige Hilfe Dritter angefertigt habe.

Sämtliche aus fremden Quellen direkt oder indirekt übernommenen Gedanken sowie sämtliche von Anderen direkt oder indirekt übernommenen Daten, Techniken und Materialien sind als solche kenntlich gemacht. Die Arbeit wurde bisher bei keiner anderen Hochschule zu Prüfungszwecken eingereicht.

Darmstadt, den 09. Juni 2015

.....
Sarah-Katharina Kays